JOURNAL OF
THE ASIATIC SOCIETY OF BANGLADESH
SCIENCE

ISSN 1016-6947

Vol. 51 **No. 1** **June 2025**

THE ASIATIC SOCIETY OF BANGLADESH

THE ASIATIC SOCIETY OF BANGLADESH

Journal of the Asiatic Society of Bangladesh (Science)

Journal of the Asiatic Society of Bangladesh, Science is published twice a year (June and December comprising one volume) in English. Original research papers dealing with all branches of science with special reference to Asiatic studies by the members of the Society are published. Any non-member of the Society may publish a research paper if it is communicated by a member of the Society.

SUBSCRIPTION

Annual per volume:		Single issue:	
Inland	Tk. 500.00	Inland	Tk. 250.00
Foreign	US$ 40.00	Foreign	US$ 20.00

CORRESPONDENCE

All correspondence should be addressed to The General Secretary, The Asiatic Society of Bangladesh, 5 Old Secretariat Road (Nimtali), Ramna, Dhaka-1000, Bangladesh.
Phone: 2226640753, E-mail : asbpublication@gmail.com, www.asiaticsociety.org.bd

PRINTED BY

SRL Printing Press
8/12 Babupura, Nilkhet, Dhaka-1205

JOURNAL OF
THE ASIATIC SOCIETY OF BANGLADESH
SCIENCE

Volume **51**, Issue 1, June 2025
ISSN **1016-6947** eISSN **2408-8676**
Available at: https://www.asiaticsociety.org.bd/journals
https://www.banglajol.info/index.php/JASBS

Journal of the Asiatic Society of Bangladesh, Science
is indexed in the following online scholarly database:

JOURNAL OF
THE ASIATIC SOCIETY OF BANGLADESH
SCIENCE

(J. Asiat. Soc. Bangladesh, Sci.)

Vol. 51 **No. 1** **June 2025**

CONTENTS

THE ASIATIC SOCIETY OF BANGLADESH
Council 2024 & 2025

President	:	Professor Dr. Harun-or-Rashid
Vice-Presidents	:	Professor Dr. Hafiza Khatun Professor Dr. Sajahan Miah Professor Dr. Yearul Kabir
Treasurer	:	Dr. Muhammad Abdul Mazid
General Secretary	:	Professor Dr. Mohammad Siddiqur Rahman Khan
Secretary	:	Professor Dr. Md. Abdur Rahim
Members	:	Professor Dr. Syed Anwar Husain (Fellow) Barrister Shafique Ahmed (Fellow) Professor Dr. A K M Golam Rabbani Professor Dr. Mahbuba Nasreen Professor Md. Lutfor Rahaman Professor Dr. Sadeka Halim Professor Dr. Asha Islam Nayeem Professor Dr. Abdul Bashir Professor Dr. Najma Khan Majlis Professor Dr. Md. Abdul Karim Professor Dr. Shuchita Sharmin Professor Dr. Sabbir Ahmed

Guidelines to authors

The Journal of the Asiatic Society of Bangladesh publishes original research papers related to any field of sciences from anywhere in the world.

All manuscripts written in English and typed on one side of a good quality paper (A4) with one and a half space and 2.54 cm margins on all sides should be submitted in duplicate (one copy without identity of the authors) to the Editor. However, authors from overseas countries may submit soft copy of the paper. Regarding publication of the paper after review, the decision of the Editorial Board shall be final. All papers accepted by the Editorial Board are subjected to editorial modifications.

The manuscript of a full paper, preferably be limited within 12 typed pages (A4) including tables, figures, graphs, references, etc. For short communication it should not exceed five pages.

The manuscript should contain the following sub-titles in sequence: Title, Abstract, Key words, Introduction, Materials and Methods, Results and Discussion, Acknowledgements, if any, and References. In case of **'Short Communication'** no sub-titles are necessary.

Title: It should be brief and specific. The manuscript will have a separate title page giving name of the paper, authors name and address and a running head.

Abstract: It should not exceed 200 words containing the gist of results only.

Key words: Should not exceed 6 words and it should be after Abstract.

Text: The text of the article should be clear and precise. Introduction should be concise, precise and relevant to the study. Methods already published should be indicated by references. In case of modifications of a method give explicit descriptions. Results should be stated concisely and presented logically referring to tables and graphs. The same data should not be used both for the tables and for the graphs and/or figures. Simple data may be presented as a text instead of Tables and Figs. Each result should be followed by discussion or interpretation (in any case the Results and Discussion must not be separated) with appropriate reference(s). Discussion should deal with the obtained results and related results published nationally and internationally. Concluding remarks (without heading) must be given (that tally with the objective) in the last paragraph. The references in the text should be arranged chronologically.

Units: All measurements must be given in SI (International System) or SI-derived units.

Tables, Graphs and Figures: Number of tables, graphs and figures should be minimum. However, these should be typed separately. The graphs and figures should be drawn giving statistical analysis and properly labelled. The figures and graphs should be properly drawn with bold, solid lines so that these could be reduced up to half or less of the original. The photographs should be submitted on glossy papers or in JPEG format. Symbols in the graphs should be distinct and labels should be readable. Coloured photographs are also accepted.

Acknowledgment:

All persons or organizations that contribute substantially to a paper without fulfilling the criteria for authorship should be acknowledged.

Author contributions:

Authorship should be reserved for those and only those who have made significant intellectual contributions to the research. For transparency, we encourage authors to submit an author contribution statement outlining each author's contributions to the paper. The authors should have participated sufficiently to take public responsibility for appropriate portions of the content.

References and Text Citations:

In the text, references should be cited within brackets quoting the first author's surname followed by *et al*. (if necessary) and the year of publication, e.g. (Chowdhury, 2023), Khan *et al*. (2022) or (Khan *et al*., 2023). In the case of two authors, only the surnames are mentioned, e.g., (Khan and Rahman, 2023). A semicolon should separate two or more references when putting them within the same bracket. At the end of the manuscript, references should be listed and arranged alphabetically according to the first author's surname, following the style described below:

(a) Journal article:

In each reference, the names of all authors will have to be given, followed by the year of publication. The year of publication will be followed by the full title of the article and the journal's abbreviated title (in italics). The volume number (issue number) and page ranges will be given next. **Examples:**

Alva, A.K. and D.G. Edwards. 1990. Response of lupin cultivars to concentration of calcium and activity of aluminum in dilute nutrient solutions. *J. Plant Nutr.* **13**(1): 57-76.

Hossen, M.M., M.A. Al Mamun, M.M. Rahman and M.A. Karim. 2023. Exogenous application of potassium fertilizer alleviates the detrimental effect of water logging on soybean. *J. Bangladesh Acad. Sci*. **47**(2): 155-167

(b) Book or Chapter in a Book:

The name and place of the publisher and year of publication will have to be given in addition to the name of the author(s), the title of the book (in italics), edition number (if not first), and the number of pages. In the case of an article or chapter in a book, the author(s) name, the year of publication, and the title of the article or chapter will be followed by the title of the book (in italics), the names of the editors of the book, edition number (if not first), the name and place of the publisher, and page or page numbers of chapter.

Examples:

Book:

Carlson, B.M. 2009. *Human Embryology and Developmental Biology*. 4th ed. St. Louis: Mosby; p. 541.

Cassese, A., G. Acquaviva, M.Fan and A. Whiting. 2011. *International Criminal Law: Cases and Commentary*. Oxford University Press; p. 600.

Chapter in an edited book:

Heylar, K.R. and W.M. Porter. 1989. Soil acidification, its measurement, and the processes involved. In: *Soil Acidity and Plant Growth*, A.D. Robson (ed.), Academic press, San Diego, CA, USA. pp. 61-101.

(c) Proceedings of a Conference:

Harnden, P., J.K. Joffe and W.G. Jones, editors. Germ cell tumours V. Proceedings of the 5th Germ Cell Tumour Conference; 2001 Sep 13-15; Leeds, UK. New York: Springer; 2002.

(d) Reports:

BBS (Bangladesh Bureau of Statistics). 2023. Statistical Yearbook of Bangladesh, 2021-2022. Statistics Division, Ministry of Planning, Govt. of Peoples Republic of Bangladesh, Dhaka, Bangladesh.

FAO. 1988. Land Resource Appraisal of Bangladesh for Agricultural Development UNDP/FAO Project BGD/81/035. Technical Report -2. UNDP/FAO, Rome. p. 570.

Declarations

While submitting a manuscript, the corresponding author will have to make a declaration to the effect that (i) the work reported was carried out by them, and they prepared the manuscript, (ii) they take public responsibility for the contents of the paper, (iii) the paper was not published before or submitted for publication in any other journal and that all the co-authors have given consent for the article to be considered for publication in the Journal of the Asiatic Society of Bangladesh.

The corresponding author must provide a formal conflict of interest statement for all authors disclosing any financial and personal relationships with other people or organizations that could inappropriately influence (bias) their work. If no conflict exists, please state that 'The author(s) declare(s) that they have no conflicts of interest regarding the publication of this article.'

Galley Proof:

Final galley proofs will be sent to the authors. No alternations or additions in the text are desirable at this stage.

J. Asiat. Soc. Bangladesh, Sci. **51**(1): 1-17, June 2025
DOI: http://doi.org/10:3329/jasbs.v51i1.82786

FIRE HAZARD VULNERABILITY ASSESSMENT OF COMMERCIAL HIGH-RISE BUILDINGS OF DHAKA, BANGLADESH

NISHAT TASNIM[1], MD MARUFUR RAHMAN[1]*
AND M. MAKSUDUR RAHMAN[2]
[1]Department of Disaster Science and Climate Resilience, University of Dhaka, Dhaka-1000, Bangladesh
[2]Department of Geography and Environment, University of Dhaka, Dhaka-1000, Bangladesh

Abstract

A detailed building survey was conducted to assess the fire hazard vulnerability of high-rises in the Banani area of Dhaka. Assessments were done by interviewing building management and experts. The buildings were assessed rated based on thirty-three indicators. The study reveals that around 47% of the surveyed buildings are in a high level of vulnerability. The remaining 37% are medium, and around 16% are less vulnerable. All the buildings constructed before 1993 (before the drafting of the BNBC - Bangladesh National Building Code and any act and regulation of fire protection and prevention) are highly vulnerable. The buildings constructed between 1993 and 2006 (the Fire Prevention and Fighting Act - 2003 came into force), before the enactment of the BNBC, 62% were in medium, and the rest (38%) were in high vulnerability level. Those were constructed after the enactment of the Dhaka Building Construction Rules 2008 also enforced); only 12.5% are high, 50% medium, and 37% less vulnerable. We found that safety regulations (BNBC, building construction rules) and properly implementing the fire safety acts/rules can drastically enhance safety standards. Policymakers and other stakeholders can find this research outcome helpful regarding fire safety enforcement.

Key words: Fire hazard, Vulnerabilities, High-rise buildings, Dhaka.

Introduction

Dhaka, the capital of Bangladesh, is expanding spatially and vertically rapidly due to a high urbanization rate and a burgeoning population (Rahman *et al.*, 2020; Rashid *et al.*, 2023). However, the city is growing unplanned, and the concentration of different types of economic activities and diverse land use patterns (mixed use of land for commercial, residential, and industrial purposes) sometimes flout safety regulations, making fire safety a complex riddle to solve. Moreover, the storage of chemicals in residential areas

*Corresponding author: maruf.dsm@du.ac.bd

without proper safety measures (Sahebi *et al.*, 2020) and more than 35000 slums (Nazem and Sultana, 2021) exacerbated the risk of fire incidents. The nature of the fire incident in Dhaka is diverse. Dhaka's fire incidents' occurrence ranges from factories, garments, industries, residential buildings, high-rise buildings, chemical storage-originated fires, and fires in slums to fires in marketplaces. There is only a small number of research on fire incidents in Dhaka. Alam and Barai (2004) categorize fire hazards and identify several zones as the most hazardous for fire incidents. Islam and Adri (2008) studied public perception and policy issues related to fire hazards in Dhaka. Wadud *et al.* (2014) assesses fire risk in ready-made garments by developing a fire risk index. Jahan *et al.* (2015) identified the fire risk of chemical warehouse and residential unit areas in Dhaka. Rahman *et al.* (2015) have done vulnerability mapping to illustrate the fire vulnerability of Dhaka. Azad *et al.* (2018) researched the fire risk of industries in Gazipur and Dhaka. Islam and Hossain's (2018) study were on the mitigation perspective of fire hazards in Dhaka. Sahebi *et al.* (2020) evaluated the fire risk in the Nimtoli area, where a devastating fire incident occurred in 2010. Tishi and Islam (2019) studied the distribution pattern of fire incidents in different land use and infrastructure. Chisty and Rahman (2020) explore the coping capacity of fire disasters in old Dhaka. Rahman *et al.* (2022) studied individual-level fire hazard preparedness of Dhaka dwellers. Huda's (2022) research was on user-level fire hazard awareness of high rises in the Mohakhali area. Our literature review reveals inadequate research focus on fire hazards in Dhaka. However, fire is the most frequently occurring urban hazard in Dhaka (Huda, 2022).

For this reason, this research has been done to determine the vulnerabilities of high-rise buildings to fire incidents. The building vulnerability is assessed based on several indicators related to fire safety standards. The chosen area for the study is the neighbourhood of Kemal Ataturk Avenue in the Banani-Gulshan area, as there is a previous history of devastating fire incidents in high-rise buildings, and many commercial multistorey buildings are located there.

Study area: On 28 March 2019, FR Tower, located in the Kemal Ataturk Avenue of Banani of Dhaka, experienced a devastating fire incident, resulting in the tragic death of 26 people (Huda, 2022). That incident underscored the critical shortcomings of fire safety, such as faulty construction, inadequate fire-fighting equipment, poor emergency management measures, and insufficient knowledge of the operation of existing equipment. In response to that tragedy, this research was carried out on 19 high-rise commercial buildings in the vicinity of FR Tower, along the Kemal Ataturk Avenue, between 2019 and 2020 (Fig. 1). The Bangladesh National Building Code (BNBC) 2006 categorizes buildings over 20 meters as high-rise buildings; however, within the BNBC

2020, the definition of high-rise is updated, and over ten storeys/ 33 meters are now considered high-rise buildings (Huda, 2022; MoHPW, 2024a; MoHPW, 2024b). According to the Fire Protection and Prevention Law 2003, buildings more than six storeys are considered as high-rise (Huda, 2022). We considered the previous definition of high rise and included 7-26 storeys building in our research. We have followed two steps in our building selection process. The first step was a census (all buildings close to the vicinity of the FR tower were taken into consideration), followed by purposive sampling. During the census (done during the reconnaissance survey), we identified the building based on a few criteria for the detailed survey. The criteria are as follows: The building must be a high-rise, fully or partially used for commercial purposes, and close to FR Tower. We could not access all the buildings, and the building management was not interested in participating in the survey. As a result, in the second step, we selected 19 buildings using purposive sampling (see Tongco, 2007) methods from the selected building in the first step.

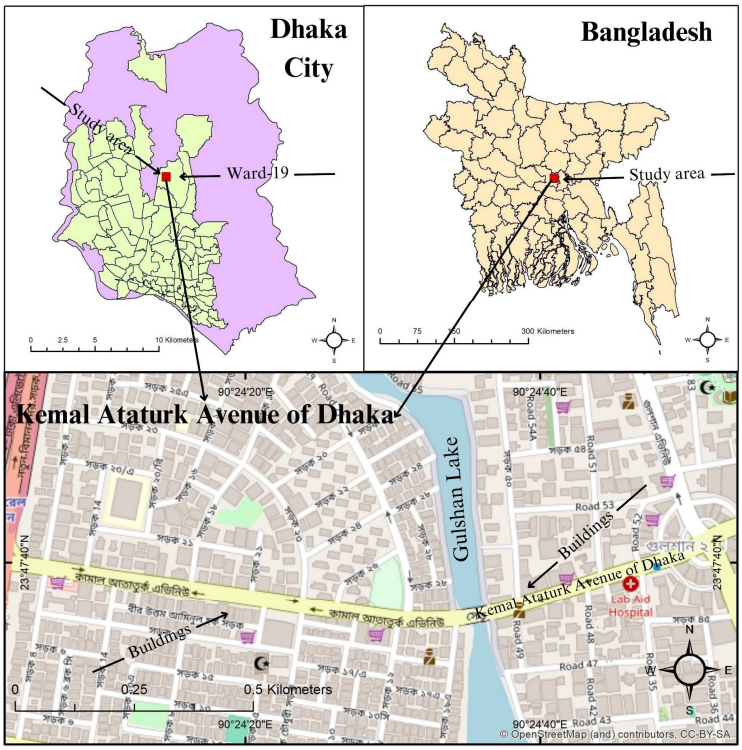

Fig. 1. Location of the study area.

Materials and Methods

Vulnerability is defined as the susceptibility of individuals, communities, assets, or a system to the impact of a hazard, which is determined by a group of conditions, including physical, social, economic, and environmental (UNDDR, 2024). We emphasise the assessment of physical vulnerability (the ability of the built environment- building road and other infrastructure to withstand the impact of any hazard) (Woodruff *et al.*, 2018) of buildings and user-level susceptibility to fire hazards. A total number of 19 high-rise buildings (7-26 storeys) have been evaluated in this research. The building was chosen during a reconnaissance survey. Expert opinion was taken, and the Department of Fire Service and Civil Defence (DoFSCD) checklist was considered to develop the building's indicator-based fire safety framework. From 2019 to 2020, the lead author conducted a detailed building survey. The lead researcher interviewed the management of all surveyed buildings and maintained a field notebook during the survey. Weighing and grading the indicators was done by averaging the scores of five experts. A composite vulnerability score was derived for each building from the weighted and graded parameters. Previous studies by Wadud *et al.,* 2014, Rahman *et al*., 2015, Rahman *et al*., 2017 and Sahebi *et al*., 2020 used weighted and graded indicators to assess fire hazard vulnerability and risk. Based on the composite score and expert opinion, the buildings are grouped into high, medium, and low vulnerability levels.

Parameters for fire vulnerability assessment: Thirty-three (eighteen quantitative and fifteen qualitative) parameters were selected for the fire hazard vulnerability assessment (Table 1).

Development of weight: A weight value of 1-5 is assigned to each indicator (Table 2). Weighting is intended to identify the importance of the indicators in terms of the impact of fire hazards (Table 3). Thirty-three parameters (eighteen quantitative and fifteen qualitative) were selected for the fire hazard vulnerability assessment (Table 1). The weight of each indicator is detailed in Table 3.

Grading of parameters: Each indicator has been given a grade depending on the impact of those indicators on a particular building. The qualitative indicators are rated based on the description collected during the field survey with the help of expert opinion from excellent to very poor, with corresponding grading points detailed in Table 4. The quantitative indicators are rated based on the deviation from the required condition to comply with fire safety standards (Wadud *et al*., 2014).

Table 1. List of the quantitative and qualitative indicators.

Quantitative Parameters/Indicators	Qualitative Parameters/Indicators
1. Smoke detector	1. The practice of fire drill
2. Fire alarm	2. Ventilation of emergency exit
3. Unlocked emergency exit	3. Ventilation of the main staircase
4. Width of emergency exit	4. Lighting facilities of the main staircase
5. Refilled fire extinguisher	5. Lighting facilities of the emergency exit
6. Width of the main exit	6. Exit sign and refuge area
7. Distance from adjacent buildings	7. Accessibility of water
8. Sprinkler	8. Main electric switchboard
9. Skilled/trained people for firefighting	9. Emergency light
10. Fire door	10. Roof accessibility
11. Alternate power/ generator operator	11. Control room
12. The existence of a restaurant with kitchen	12. Electric connections checking
13. Distance from electric pole/transformer	13. Generator room
14. Main electric switchboard	14. Main exit
15. DoFSCD notice	15. Reserve water tank
16. Lift and lift operator	
17. Floor area	
18. Number of floors	

Table 2. Definition of weight for each indicator adopted from Wadud *et al.*, 2014.

Weight	Description of consequences
5	Most important—if absent, there could be serious damage to life and properties.
4	Important—if absent, life and properties could be considerably damaged.
3	Essential—in the absence, fatalities may be avoided. However, significant injuries and property damages still occur.
2	Essential—in the absence, loss of properties and injuries will be considerable.
1	Preferable —not essential, however desirable

Smoke detector: There should be one smoke detector in every 75 sq. meter area, according to Firefighting Rules 2014 (DoFSCD, 2014). The required smoke detector number has been calculated using the following formula for each building, and then the deviation has been calculated.

$$Number\ of\ smoke\ detector\ = \frac{total\ floor\ area\ (in\ sq\ m)}{75\ sq\ m}$$

Table 3. Indicators used in surveys with their average weight.

Indicators No.	Indicators/Parameters	Description of indicators/parameters	Weight (Xi)
1	Smoke detector	Availability and number of smoke detector	5
2	Fire alarm	Availability and number of fire alarms on each floor	5
3	Unlocked emergency exit	having unlocked emergency exits	5
4	Width of emergency exit	Deviation from ideal width	4.8
5	Main exit	Number of main exits for getting out of the building	4.6
6	The practice of fire drill	Provision and frequency of fire drill	4.6
7	Ventilation of emergency exit	The ventilation system in the emergency exit/ staircase	4.6
8	Lighting facilities of emergency exit	Availability and type of lighting facility in emergency exit/staircase	4.6
9	Refilled fire extinguisher	Number of refilled extinguishers	4.6
10	Exit sign and refuge area	Proper exit sign on each floor, provision of refuge area in the building	4.6
11	Accessibility of water	Availability of water for emergency use	4.6
12	Width of the main exit	Deviation from the ideal width	4.4
13	Main electric switchboard	Location of main electric switchboard (for easy access)	4.2
14	Roof accessibility	Unobstructed/easy access to the roof (with open space on the rooftop)	4.2
15	Emergency light	Availability and connection system of emergency light	4
16	Fire Door	Availability of a fire door on each floor separating the emergency exit	4
17	Sprinkler	Availability and number of sprinklers (deviation from required number)	4
18	Reserve water tank	Number of reserve water tanks (having an extra tank for firefighting)	4
19	Distance from adjacent buildings	Deviation from ideal distance	3.8
20	Lighting facilities of the main exit	Availability and type of lighting facility in main exit/staircase	3.8
21	Control room	Availability of a well-organized control room	3.8

22	Skilled/trained people for firefighting	Number of skilled people for firefighting and their level of skill	3.8
23	Electric connections checking	Yearly/monthly checking of all electric connections/equipment	3.8
24	Ventilation of the main exit/staircase	The availability of the ventilation system for the main exit/ staircase	3.6
25	Distance from the electric pole/transformer	Deviation from an ideal distance	3.5
26	Alternate power/ generator operator	Number of operators for generator	3.5
27	Main electric switchboard	Number of operators of the main electric switchboard	3.4
28	Generator room	Location and condition of the generator room	3.4
29	DoFSCD notice	DoFSCD notice (fire emergency advice) on each floor	3.25
30	The existence of a restaurant with kitchen	Number of floors having restaurant or kitchen	3.2
31	Lift and lift operator.	Type of lift (availability of fire lift) with operator number	2.8
32	Number of floors	Number of floors greater than six	2.6
33	Floor area	Total floor area	2

Table 4. Grade points of the indicators (Wadud *et al.*, 2014).

Grade point (Yi)	Qualitative indicator	Quantitative indicator based on deviation
1	Excellent	0- 25%
0.75	Good	26%-50%
0.5	Moderate	51%-75%
0.25	Poor	76%-100%
0	Extremely Poor (If it does not exist)	If it does not exist or deviation exceeds 100%

Fire alarm: According to experts, at least one fire alarm should be on each floor. So, the deviation was measured by calculating the number of floors with no fire alarm.

$$Deviation = \frac{number\ of\ floors\ having\ no\ fire\ alarm}{total\ floor\ number} * 100$$

Unlocked emergency exit: During the fire incident in the FR tower in 2019, emergency exits on many floors were locked, and the people in that building could not come out. Keeping emergency exits under lock and key is a common practice in Bangladesh. We calculated the percentage of floors with unlocked emergency exits in terms of the total number of floors and assigned grades according to Table 4.

Width of emergency exit: The FR tower had an emergency exit of approximately 0.61m iron staircase. Getting out of the building was risky, even in the normal time using that exit. The standard width of the emergency exit must be at least 1.5m, according to Fire Fighting Rules 2014 (DoFSCD, 2024b). We calculated the deviation of the emergency and main exit from 1.5m.

Refilled fire extinguisher: According to the opinion of experts, there should be one fire extinguisher in every 550 sq. ft. area. So, the required extinguisher has been calculated using the following equation.

$$Number\ of\ Required\ extinguisher = \frac{Floor\ area\ (in\ sq.ft.)}{550\ sq.ft}$$

Then the deviation has been calculated using the following equation:

$$Deviation = \frac{Required - Existing}{Required} * 100$$

Distance from adjacent buildings: Grading has been done based on the distance and description of buildings from survey and minimum requirements of side and rear space mentioned in BNBC for business and mercantile occupancy.

Sprinkler: Typically, one sprinkler is required within 120-200 sq. ft. However, the expert consulted for this study suggested that ideally there should be one sprinkler within 100 sq. ft. We employed the following formula to determine the spacing deviation:

$$Number\ of\ Required\ Sprinkler = \frac{Floor\ area\ (in\ sq.ft.)}{100\ sq.ft}$$

Then the deviation has been calculated as follows:

$$Deviation = \frac{Required - Existing}{Required} * 100$$

Skilled/trained people for firefighting: Trained people play a great role during fire hazards. All people using the building must have basic firefighting knowledge and be aware of the firefighting facilities of the building. There should be enough trained people for firefighting in each commercial building who can perform emergency responses

(dousing a fire with extinguishers, helping with evacuation) during any fire event. We have surveyed the building in detail (firefighting facilities, use of buildings) and collected information about the number of trained people, their training, and practice-related information. Then the building was graded based on the collected information.

Fire door: The spread of fire and smoke can be prevented by installing fire doors. Fire doors also ensure safe evacuation through the emergency exits. For assessment, the ratio between the floor with a fire door and the floor having no fire door was calculated. Additionally, we assessed whether the doors identified as fire doors complied with fire safety standards or were simply wooden or steel doors described as fire doors. Collected information was used to rate the performance of the building to fire susceptibility.

Alternate power/ generator operator: Each building should have three operators (according to experts). So, anyone can always be present. Buildings were graded based on the deviation of the number of operators and their duty hours.

Existence of a restaurant or kitchen: Fire can ignite in a restaurant. Building with no restaurant is rated as excellent. Buildings with restaurants are rated from extremely poor to good according to the number of restaurants and their safety compliance.

Distance from electric pole/transformer: The Bangladesh National Building Code stipulated that buildings must keep a minimum horizontal distance of 1.75 m from any high voltage electric lines (up to 33 kV) and 1.25 m for low to medium (<33 kV) voltage line during construction (MoHPW, 2024b). A building with no space with open electric wire is rated as extremely poor. Excellence is assigned to buildings having space more than 1.75 m. The building's space, however, is 1.75 m or less than 1.75 m is rated good to poor (Table 4) based on the calculated deviation during the field survey.

Main electric switchboard: There should be three operators (according to experts) in each building working in shifts to ensure twenty-four hours of coverage (safety of electricity and critical facilities). We collected information about operators along with their working procedures. Then, the buildings were rated based on the information.

DoFSCD notice: DoFSCD issues guidelines on actions to take during a fire with emergency contact information. It is recommended that the building authority display these notices evidently on every floor for quick communication during fire emergencies. The deviation has been calculated considering the number of floors without such notice.

Lift and lift operator: According to expert views, there should be at least one liftman for each lift; at least 1 of 2-3 lifts must be fire lifts. A fire lift is a lift specially designed and

operated safely during a fire in a building. The lift and lift operator information were collected and graded during the survey.

Floor area: A building with a large floor area typically requires more comprehensive firefighting facilities. In this study, buildings with a floor area under three thousand square feet are rated excellent, observing other factors such as fire alarms, smoke detectors, and additional safety measures to meet the requirements. In reverse, the floor area exceeding five thousand square feet was considered extremely poor if other safety measures were non-compliant with the standards. Moreover, during observation, it was noted that the allocation of fire safety equipment is sufficient regarding its accessibility and effectiveness across the building.

Number of floors: We considered buildings to have more than six floors as high-rise buildings (MoHPW, 2024a). The firefighting challenge increases with the number of floors or heights of buildings. We calculated % of deviation of the number of floors from the 6th floor.

Calculation of vulnerability score:

Finally, the fire hazard vulnerability score has been calculated using the following formula: $Fire\ Vulnerability = \sum_{i=1}^{n} Xi * Yi$

(Rahman *et al.*, 2015, Rahman *et al.*, 2017, Sahebi *et al.*, 2020)

Here, Xi = weight of the indicator and Yi = grade point of the indicators

Result and discussion

Assessment of fire safety condition: Based on 33 criteria, buildings are assessed and categorized from extremely poor to excellent, as outlined in Table 3 and Fig 4. Many buildings fall into extremely poor categories in different criteria due to non-compliance with safety standards regarding smoke detectors, fire drill practices, ventilation of emergency exits, emergency doors, lights, sprinklers, and control rooms (Fig 2). On the other hand, the highest number of buildings fall into good to excellent categories in the criteria of the main exit, lift and lift operator, electric connection checking, the width of the main exit, and the main switchboard (Fig 3).

The indicator-wise fire safety condition of the selected building is shown in Fig. 4. Most of the buildings (around 60%) perform extremely poorly to poor in DoFSCD notice, ventilation in main exit/staircase, trained firefighters, reserve water tank, sprinkler, smoke detector, fire door, exit sign and refuge area, lighting facilities and ventilation in

emergency exit, fire drill, condition of control room (see Fig. 4). The surveyed buildings perform (around 60%) well in indicators like lift operator, a restaurant in the building, electric switchboard safety, checking of electric connections, generator operator, the width of the main exit, emergency exit, accessibility of water and fire alarm (see Fig. 4).

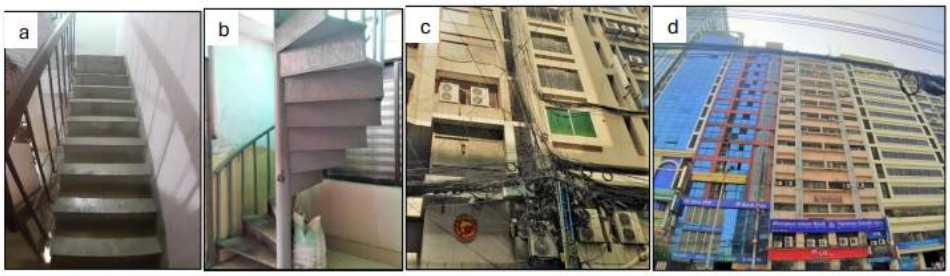

Fig. 2. Illustration of extremely poor to poor condition of exit (a.), narrow roof access (b.), dangerous electric wire (c.), and attached buildings (d.). (Source: Fieldwork, 2019-20).

Fig. 3. Illustration of excellent to good examples of well-equipped control room (a. inset), hydrant with pressurize valve (a.); Fire extinguisher (b.), fire alarm (b. inset upper right) and direction of extinguisher user procedure (b inset lower right); Well-ventilated exit (c.), emergency light (c. inset upper left), exit sign (inset upper middle) and exit doors (c. inset upper right). (Source: Fieldwork, 2019-20)

Assessment of Building Vulnerability: The aggregated vulnerability score for each building was derived from the combined score of the building. After multiplying the weight value and grade value of a particular indicator for a particular building, the products of all indicators have been summed up to have the final vulnerability score of a certain building. The buildings are categorized into low, medium, and highly vulnerable based on vulnerability scores and expert opinion (Table 5). The evaluation uses a scoring system where a higher score denotes less vulnerability to fire hazards—such buildings are safer in many criteria and categorized into good or excellent. On the contrary, a lower score pointed to a higher vulnerability, with many indicators rated as extremely poor or poor.

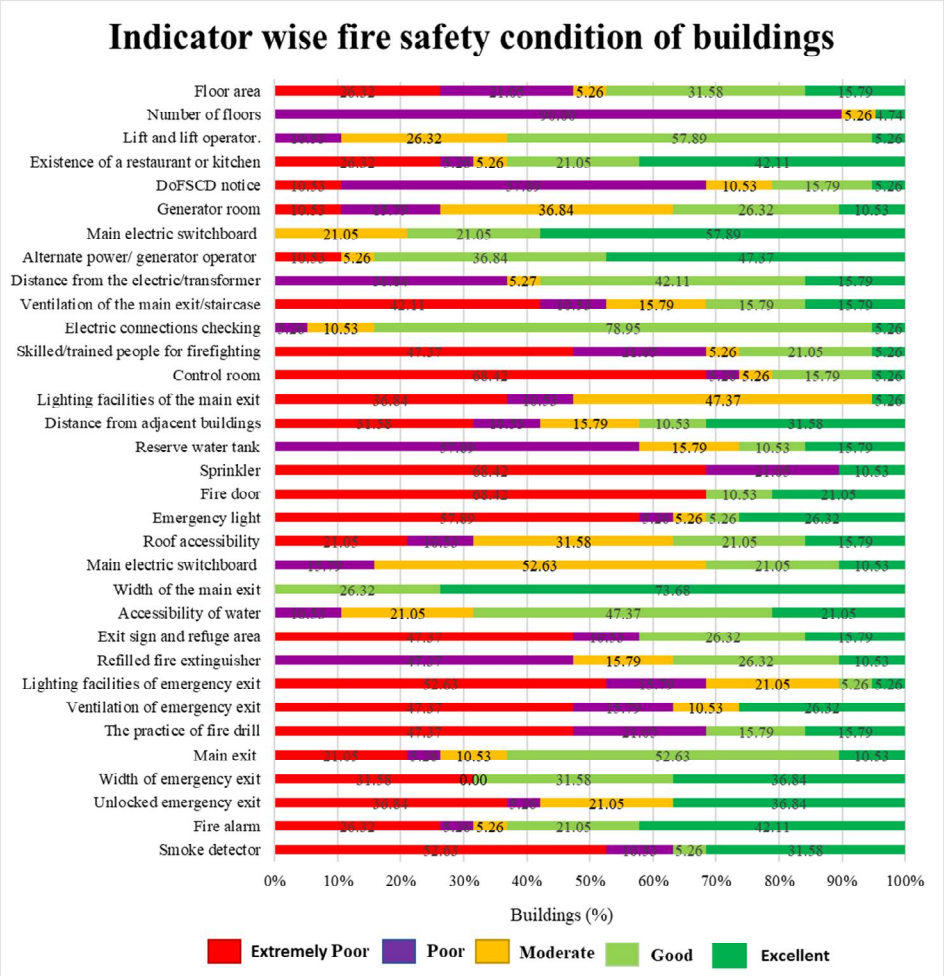

Fig. 4. Indicator-wise fire safety condition of surveyed buildings (Source: Fieldwork, 2019-20).

Table 5. Vulnerability score of buildings.

Vulnerability score range	Level of vulnerability	Number of buildings
29-55	High	9
56-82	Medium	7
83-109	Low	3

The Table 5 above shows that most buildings (9 out of 19) are highly vulnerable, with scores ranging from 29 to 55. Seven buildings are medium vulnerable, and only three are in low vulnerable conditions. So, the situation indicates that most buildings have been constructed flouting BNBC rules and are non-compliant with fire safety standards. Although some buildings have adopted some safety measures, they still need improvement (firefighting, fire emergency plan, fire safety drill) to prevent fire incidents and fire-related damages.

Building vulnerability, construction time, regulatory framework: The first act (the Building Construction Act 1952) on building construction in this region was promulgated in 1953 and has since undergone several amendments (Islam and Adri 2008). The first Bangladesh National Building Code was released in 1993. However, it was not officially gazetted until 2006 (Table 6). Out of nineteen surveyed buildings, three were constructed before 1993, eight between 1993-2006, and 7 after 2006 (Table 6). The evaluation reveals that nine are highly vulnerable, seven are medium vulnerable, and three are low vulnerable to fire hazards (Table 6).

Table 6. Building vulnerabilities in terms of construction time (Islam and Adri, 2008; Huda, 2022; Hossain *et al.*, 2022; Afrose, 2023; DoFSCD, 2024a).

Building Construction Time	Level of vulnerabilities		
	High	Medium	Low
Before 1993 (BNBC First Published)	3	0	0
1993-2006 (Fire Prevention and Extinguishing Act, 2003; however, BNBC was not Gazette.	5	3	0
After 2006 (BNBC gazette in 2006; Dhaka Metropolitan Building Construction Act of 2008 enforced, Fire Prevention and Extinction Rules, 2014 was formulated)	1	4	3

All the buildings built before 1993 are highly vulnerable to fire hazards (Table 6). Five buildings are highly vulnerable, and three are moderately vulnerable among the eight buildings, constructed between 1993 and 2006. Among the buildings built after 2006, only one is highly vulnerable, 4 are moderately vulnerable, and 3 are low vulnerable. Most of the buildings built before 2006 were identified as highly vulnerable. Though BNBC was already formulated then, it was not applied in the construction process, nor have any modifications been made to comply with safety standards. With the formulation of the legal framework, we have seen that the safety condition of the buildings has

improved (Table 6). However, it is not satisfactory. The reason may be a lack of monitoring from the planning and construction phase to the use phase.

Highly vulnerable buildings: There was no or less than the required space between these buildings. Moreover, this building lacks a proper emergency exit, or the exit is narrower than the 1.5 m standard. These buildings do not comply with necessary safety standards regarding a functional control room, the requisite number of smoke detectors, sprinkler systems, and professionally trained firefighting teams. There was no provision for firefighting drills. In some cases, exit signs are merely written on paper, which is unlikely to be effective during an emergency. Negligence is also observed in the maintenance of the emergency exit. The exit is often kept locked or blocked. The exits were not clean, lacked sufficient light, and were not well-ventilated.

Moderately vulnerable buildings: We found seven buildings in moderately vulnerable conditions (three constructed between 1993-2006 and four after 2006). These buildings are equipped with smoke detectors, fire alarms, and emergency exits that are not locked. These buildings have professionally trained firefighting personnel and well-ventilated main and emergency exits. These buildings achieve moderate to good ratings in most of the indicators. Even in some indicators, these have received excellent scores, for example, the width of the main exit. These building is rated as moderately vulnerable due to under-performance in several key areas, for example, space between adjacent buildings, frequency of practicing fire drills, functionality of control room, presence of sprinklers, provision of emergency exit door, smoke detector, emergency exit lighting facilities.

Low vulnerable buildings: Our research identified only three buildings in low vulnerable conditions constructed after 2006. The buildings are built in compliance with the BNBC. Most of the indicators of these buildings are rated as good or excellent. These buildings have sufficient space gaps with adjacent buildings and are located at a safe distance (1.75 m) from electric poles, transformers, and hanging electric wires. The main and emergency stairs are well-ventilated, with a width exceeding 1.5 m. Emergency exits are kept unlocked consistently. Fire extinguishers are routinely checked and refilled. Every building has the necessary smoke detectors and fire alarms. Furthermore, these buildings are well-equipped with a control room and a professionally trained firefighting team. These buildings have provisions for regular fire drills. None of the buildings have a restaurant on any floor. They have a well-equipped control room and a well-trained firefighting team. These buildings have a fire drill provided regularly (more than five times a year). The building authorities have installed necessary emergency signs and

safety notices of DoFSCD on different floors of the buildings. Smoking within these buildings is prohibited. The management team regularly checks electricity connections. They also have a reserve water tank for use in emergencies. However, the staircase to access the roof was narrow in two out of three buildings. One building does not have sprinklers but performs excellently in all other indicators.

Presently, there are many regulatory frameworks and safety standards for building safety (Table 6). However, most buildings surveyed in this research were non-compliant with safety standards. According to the Dhaka Metropolitan Building Construction Act of 2008 (Dhaka Mohanagar Imarat Nirman Bidhimala 2008), an occupancy certificate is compulsory. According to experts, most buildings do not have occupancy certificates or violate the certificate for space use. It is not practical to suggest the reconstruction of all these buildings. However, proper modification can improve the safety standards of these buildings. The expert interviewed in this study emphasizes the proper and corruption-free monitoring of the safety standards of the building (from planning and construction to the use phase) to improve fire safety in Dhaka.

Conclusion

Fire incidents are alarmingly increasing in Dhaka. The situation is worsening due to unplanned urbanization and the prolific growth of high-rises buildings. Building construction and use are sometimes done by flouting the BNBC, DoFSCD regulations, and the Dhaka Metropolitan Building Construction Act of 2008. Safety concerns were raised by the government and other stakeholders after the devastating FR tower incident in 2019. It is alarming that we found nine out of 19 buildings are highly vulnerable to fire incidents. These buildings lack proper fire safety measures (smoke detectors, adequate fire alarms, emergency lights, sprinklers, skilled workforce for fire safety, control rooms, and fire drills).

Moreover, in many cases, we found that emergency exits were blocked or locked and did not comply with safety regulations. However, regulation measures positively correlate with safety standards, as recently constructed buildings comply with fire safety standards. Those buildings built before 2006 (before the gazette of BNBC) are the most vulnerable, needing more fire safety measures. On the other hand, the newly constructed buildings (after the formulation and enactment of fire safety and building safety regulations) mostly comply with fire safety measures.

Reconstruction of these vulnerable buildings is not a practical solution. However, these buildings' fire safety standards and emergency management capabilities can be enhanced through modification and continuous monitoring.

References

Afrose, N. 2023. All you need to know about fire safety regulations in Bangladesh. Accessed on 26th February 2024 from https://www.thedailystar.net/law-our-rights/news/all-you-need-know-about-fire-safety-regulations-bangladesh-3285121.

Alam, M.J.B. and G. N. Baroi. 2004 Fire hazard categorization and risk assessment for Dhaka city in GIS framework. *J. Civ. Eng. (IEB)*, **32**(1): 35-45. Accessed on 10th March 2024 from: https://www.researchgate.net/publication/224767169_Fire_Hazard_ Categorization and_Risk Assessment for_Dhaka_City_using_GIS

Azad M.T.A., I. Hasan, M.K.Saha, R. Ahmmed, S.J. Moni and M.H. Kabir. 2018. Risk of fire disaster: Consequences on industry sectors in Bangladesh. Int. J. Sustain. Energy Dev. **3**(3): 52-63. Accessed on 26th February 2024 from https://www.researchgate.net/publication/330727323_Risk_of_Fire_Disaster_Consequences_on_Industry_Sectors_in_Bangladesh

Chisty, M.A. and M.M. Rahman. 2020. Coping capacity assessment of urban fire disaster: an exploratory study on ward no: 30 of Old Dhaka area. *Int. J. Disaster Risk Reduct.* **51**: 101878.

DoFSCD (Department of Fire Service and Civil Defence), 2024a. Fire Prevention and Extinguishing Act, 2003. Accessed on 26th February 2024 from: https://fireservice.gov.bd/site/page/6bb3bc22-8057-40b8-84f1-31b55bb805c9/-

DoFSCD (Department of Fire Service and Civil Defence), 2024b. Fire Prevention and Extinction Rules, 2014. Accessed on 26th February 2024 from: https://fireservice.gov.bd/site/page/6bb3bc22-8057-40b8-84f1-31b55bb805c9/-

Hossain, M.O., T. Rahman, S.K. Podder, M.H. Hasan and M.F. Momin. 2022. Evaluation of RC building under seismic load based on BNBC 2006 and BNBC 2020 using equivalent static force (ESF) method. J. Civ. Constr. Eng. **8**(3): 6-16

Huda, D.N. 2022. Vulnerability and user awareness level assessment of fire risks of high-rise buildings in Dhaka city: a study of Mohakhali commercial area. MS Thesis. BRAC University. Accessed on 20th February 2024 from: https://dspace.bracu.ac.bd/xmlui/handle/10361/17914

Islam, M.M. and N. Adri. 2008. Fire hazard management of Dhaka City: addressing issues relating to institutional capacity and public perception. *Jahangirnagar Plan. Rev.* **6**(6): 57-67. Accessed on 26th February 2024 from: https://www.researchgate.net/publication/293227526_Fire_hazard_management_of_Dhaka_City_addressing_issues_relating_to_institutional_capacity_and_public_perception

Jahan, N., S. Islam and M.I. Hossain. 2016. Fire hazard risk assessment of mixed-use chemical storage facilities: A case study of chemical warehouses in Old Dhaka. **9**: 113-124. Accessed on 26th February 2024 from: https://www.bip.org.bd/admin/uploads/bip-publication/publication-17/paper/20180607092512.pdf

MoHPW (Ministry of Housing and Public Works) 2024a. Bangladesh National Building Code (BNBC) 2006. Accessed on 26th February 2024 from: https://mohpw.gov.bd/

MoHPW (Ministry of Housing and Public Works) 2024b. Bangladesh National Building Code (BNBC) 2020. Accessed on 26th February 2024 from: https://mohpw.gov.bd/

Nazem, N.I. and S. Sultana. 2021. Slums, squatter settlements and affordable housing in the Dhaka metropolitan area. In: Huong L.T.T., Pomeroy G.M. (eds) AUC 2019. Advances in 21st century human settlements. Singapore: Springer.

Rahman, M.M., S. Akhter and M. Ashikuzzaman. 2017. Multi hazard vulnerability assessment of an urban area: a case study on ward 34 of Dhaka, *J. Asiat. Soc. Bangladesh, Sci.* **43**: 181-195.

Rahman, M.M., R. Avtar, A.P. Yunus, J. Dou, P. Misra, W. Takeuchi, N. Sahu, P. Kumar, B.A. Johnson and R. Dasgupta. 2020. Monitoring effect of spatial growth on land surface temperature in Dhaka. *Remote Sens.* **12**: 1191.

Rahman, M.M., S.J. Khan and K.N. Tanni. 2022. Holistic individual preparedness in an urban fire-prone area: the case of Dhaka City, Bangladesh. *Int. J. Disaster Risk Reduct.* **81**: 103274.

Rahman, N., M.A. Ansary and I. Islam. 2015. GIS based mapping of vulnerability to earthquake and fire hazard in Dhaka city, Bangladesh. *Int. J. Disaster Risk Reduct.* 1**3**: 291-300.

Rashid, K.J., T. Akter, A.S.M.I. Imrul Kayes and M.Y. Islam 2023. Exploring the spatio-temporal patterns and driving forces of urban growth in Dhaka megacity from 1990 to 2020. In: Chatterjee, U., Bandyopadhyay, N., Setiawati, M.D., Sarkar, S. (eds) Urban commons, future smart cities and sustainability. Springer Geography. Springer, Cham.

Sahebi, M.T., M.M. Rahman and M.M. Rahman. 2020. Fire risk situation analysis in the Nimtoli area of Old Dhaka. *J. Asiat. Soc. Bangladesh. Sci.* **46**: 91-102.

Tishi, T.R. and I. Islam. 2019. Urban fire occurrences in the Dhaka metropolitan area. *Geo Journal* **84**: 1417-1427.

Tongco, M.D.C. 2007. Purposive sampling as a tool for informant selection. Ethnobot. Res. Appl. **5**: 147-158.

UNDDR (United Nations Office for Disaster Risk Reduction) 2024. Vulnerability. Accessed on 26th February 2024 from https://www.undrr.org/terminology/vulnerability#:~:text=The%20conditions%20determined%20by%20physical,to%20the%20impacts%20of%20hazards

Wadud, Z., F.Y. Huda and N.U. Ahmed. 2014. Assessment of fire risk in the readymade garment industry in Dhaka, Bangladesh. Fire Technol. **50**: 1127-1145.

Woodruff, S., K.A. Vitro and T.K. BenDor. 2018. GIS and coastal vulnerability to climate change. Huang B. (ed) In Comprehensive geographic information systems; Elsevier: Amsterdam, The Netherlands. pp. 236-257.

(Revised copy received on 13/01/2025)

J. Asiat. Soc. Bangladesh, Sci. **51**(1): 19-38, June 2025
DOI: http://doi.org/10:3329/jasbs.v51i1.82788

SPATIOTEMPORAL CHANGES OF LAND USE, LAND SURFACE TEMPERATURE AND URBAN HEAT ISLAND IN BOGURA DISTRICT USING MULTISPECTRAL SATELLITE IMAGES

MD. RASHIDUL ISLAM, MD. BODRUDDOZA MIA*, MD. NASIF JAMIL, MASUMA CHOWDHURY AND ASM WOOBAIDULLAH
Geoinformatics Laboratory, Department of Geology, Faculty of Earth and Environmental Sciences, University of Dhaka, Dhaka-1000, Bangladesh

Abstract

This study presents an in-depth analysis of the spatiotemporal changes in land use/land cover (LULC) land surface temperature (LST) and urban heat islands (UHI) in Bogura District, with a focus on Bogura Municipality, utilizing multispectral satellite images from 1993 to 2023. The LULC of supervised classification identified significant shifts, including a sharp expansion of settlement areas, particularly by 2023, and a notable increase in vegetation cover, reflecting improved vegetation health. However, agricultural and fallow lands have shown a marked decline, especially post-2000, suggesting shifts in land use or a reduction in vegetation density. Water bodies have gradually decreased in areas, likely due to land conversion or the drying up of sources. The normalized difference vegetation index (NDVI) analysis corroborates these findings, highlighting fluctuations in vegetation health and coverage. Concurrently, LST analysis reveals an increase in higher temperature categories, closely linked to urbanization and the formation of urban heat islands (UHIs). The expansion of settlement areas has intensified the UHI effect, where urban zones exhibit significantly higher temperatures compared to surrounding rural areas. Additionally, areas of low temperature have expanded, indicating changes in land surface characteristics. The data underscores the dynamic nature of land use changes over the three-decade period, with urbanization and land cover alterations significantly impacting both vegetation and surface temperatures in the region. The study provides a framework for creating plans to counteract the negative effects of climate change, especially the UHI effect, and to direct sustainable urban planning.

Key words: Landuse, Land Surface Temperature, Urban Heat Island, Bogura District, Landsat image.

Introduction

Urbanization and environmental change are profoundly interconnected, affecting ecosystems, biodiversity, and local climates. Urban expansion's fast alteration of land use and land cover (LULC) has a profound effect on ecosystems, biodiversity, and the local and regional climate (Luck and Wu, 2002). The rapid urbanization in Bogura District has

*Corresponding author: bodruddoza@du.ac.bd

led to significant land use and land cover (LULC) changes over the past thirty years. Remote sensing techniques have a vital role in identifying and controlling different meteorological and environmental occurrences (Borges *et al.,* 2016). Utilizing satellite imagery from Landsat 5, 7, 8, and 9, this study investigates how these changes have influenced land surface temperature (LST) and contributed to the formation of urban heat islands (UHI). The Mono-window approach is a simplified method for calculating LST that only requires a small number of specific meteorological data (Jie *et al.*, 2008, Ding and Shi, 2013). Several recent studies have utilized satellite data to examine the impacts of Land Use and Land Cover Change (LULC) on Land Surface Temperature (LST) (Ahmed *et al.*, 2013; Zhang and He 2013). Previous studies highlight the impact of urban expansion on ecosystems and climate, noting that rising LST leads to reduced plant cover and increased heat island effects (Ramachandra *et al.,* 2012). Socio-economic advancement linked with urbanization often results in significant and lasting LULC changes. These changes exhaust agricultural lands, threaten biodiversity, and alter water resources, thereby affecting local and regional climates. The Bogura District, with its rapid population growth and extensive agricultural expansion, faces numerous environmental challenges exacerbated by climate change. This study aims to address these issues by monitoring biophysical data and analyzing their temporal and spatial relationships.

Despite the critical nature of LST and UHI phenomena, accurate assessments of land use patterns remain underexplored. According to (Weng *et al.*, 2004), there is a positive correlation between Land Surface Temperature (LST) and the percentage of impermeable surfaces, while there is a negative correlation between LST and the percentage of green vegetation. Land surface temperature is a crucial parameter in land surface modeling, influenced by various environmental factors and measurable through satellite thermal infrared sensors (Kustas and Norman, 1996). This technology employs satellite and airplane platforms, providing novel prospects for investigating the occurrence of HIs (Voogt and Oke, 2003). Understanding the formation and growth of UHIs, areas with significantly higher temperatures due to urbanization, is essential for developing mitigation strategies (Xie and Zhou, 2015). By selecting appropriate satellite images and utilizing remote sensing techniques, this study aims to enhance our understanding of LULC dynamics and UHI development in Bogura District. The findings will be crucial for mitigating socio-economic risks, such as drought, flooding, and biodiversity loss, which are aggravated by climate change. Studies in various regions, including Dhaka and Gazipur in Bangladesh, have shown significant LULC changes affecting LST. However, the Bogura District lacks comprehensive studies on LULC and LST changes. This study

aims to analyze LULC changes and their relation to UHI development in Bogura District using multi-spectral satellite imagery. Various Landsat TM/ETM+/TIRS sensor's images are used to study the urban heat island (UHI) effect.

Study area

The study area is Bogura District, and it is located in the northwestern part of Bangladesh under Rajshahi Division (Fig. 1). The latitude of Bogura District is 24°51`N -24°85`N and longitude is 89°22`E- 89°36`E.The area covers 2899 square kilometers (District Statistics 2011: Bogura). The climate of the Bogura District is intense tropical monsoon which consists of two main seasons which are dry season (November to March) and rainy season (June to October). The average precipitation rate of the area is 1760 mm per year (BMD, 2021). January is the coldest and April is the warmest month in the study area.The population of the area is 38,15,192 and the average density is 1,316/km^2 (BBS, 2022).

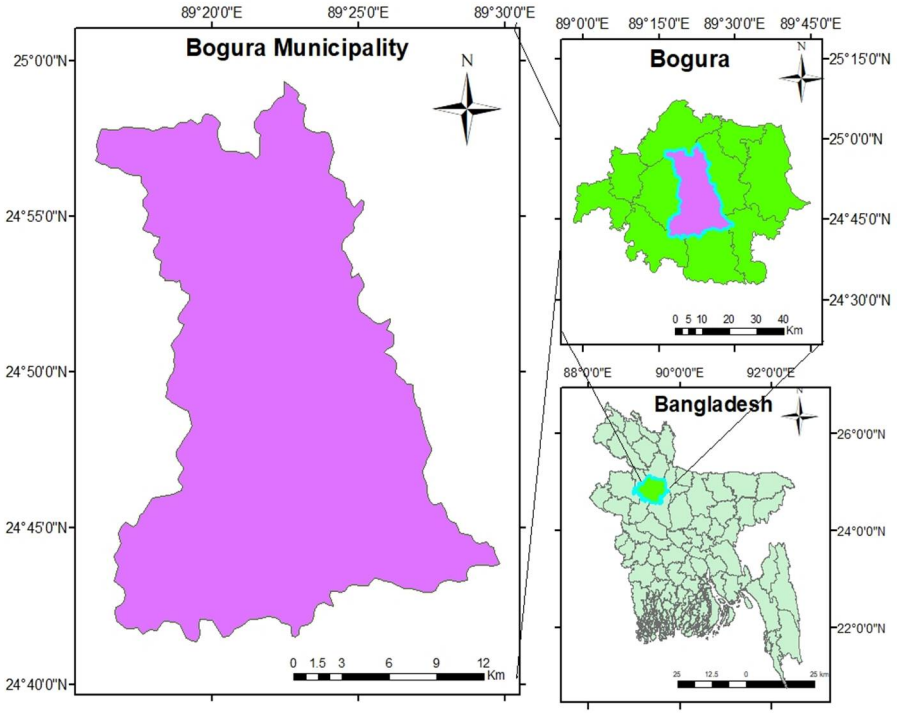

Fig. 1. Location map of the study area.

Materials and Methods

The study is conducted with Landsat satellite images using supervised classification and various indices approaches to quantify the spatiotemporal changes of landuse, and algorithm retrieved LST and UHI of the Bogura district in Bangladesh (Fig. 2).

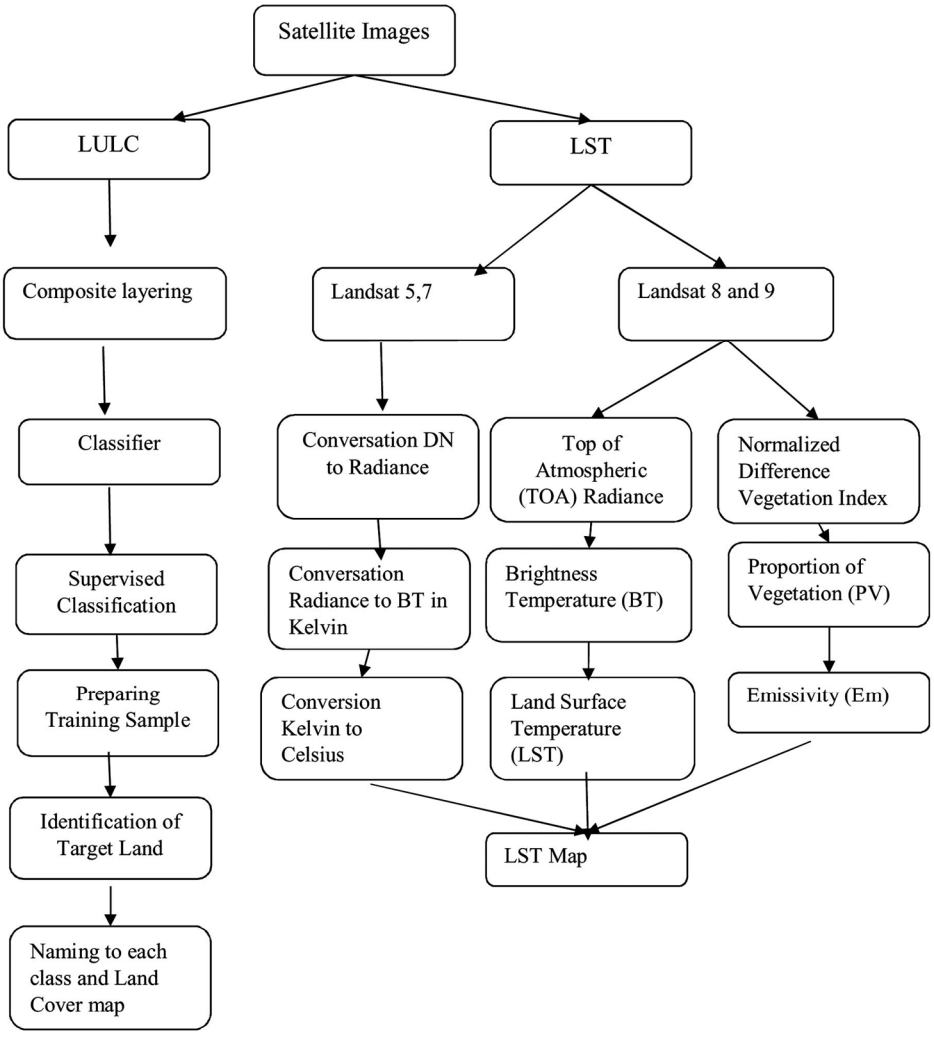

Fig. 2. Methodological flow chart of the study.

Satellite Images

Satellite imagery is often utilized to study the 'heat island effect' in metropolitan areas (Walawender *et al.*, 2014). To conduct this study, we obtained six sets of Landsat images in GeoTIFF format for free from the United States Geological Survey (USGS) collection, which is available at (https://earthexplorer.usgs.gov/). The images, which cover the Bogura District in the years 1993, 2000, 2005, 2010, 2017, and 2023, were chosen from three distinct path and row combinations to cover the full research region. These pictures were georeferenced using the Universal Transverse Mercator (UTM) zone 45N coordinate system, with reference to the World Geodetic System (WGS) 1984 datum, and taken during daylight hours. Due to the scarcity of images with less than 10% cloud cover along the required pathways and rows, there were random pauses between collections. (Table 1) summarizes the data gathered from the United States Geological Survey.

Table 1. Landsat Images Used in the Study.

Year	Sensor Platform	Acquisition Date	Resolution
1993	Landsat 5 TM	08-12-1993	30 m
2000	Landsat 7 ETM+	17-12-2000	
2005	Landsat 5 TM	07-11-2005	
2010	Landsat 5 TM	05-11-2010	
2017	Landsat 8 OLI	08-11-2017	
2023	Landsat 9 OLI	01-11-2023	

Methodology

Image Pre-Processing

This study utilized Landsat level-1 data from USGS Earth Explorer, specifically images from 1993, 2000, 2005, 2010, 2017, and 2023. These images underwent geometric correction to address distortions but often displayed radiometric anomalies due to atmospheric transparency issues, solar radiation variations, and scanning equipment flaws, necessitating radiometric correction for accurate representation.

Radiometric Correction

Radiometric correction is essential for comparing datasets over time, as it mitigates spectral property influences (Paolini *et al.*, 2006). This process involves calibrating pixel values, transforming the sensor's Digital Numbers (DN) into measurements like radiance, reflectance, or brightness temperature. Using sensor-specific metadata, the DN values are

converted into top of the atmosphere (TOA) reflectance and at-sensor radiance, with atmospheric correction achieved through the dark object subtraction method.

Layer Stack, Mosaic, and Subset

After image collection, the bands from the sensors were merged using layer stacking, requiring uniform spatial resolution. Bands that are neither panchromatic nor thermal were combined to enhance land feature distinction. The study area, defined by three images from distinct WRS path and row combinations, was processed using mosaic technique to create a cohesive image. The region of interest was selected and extracted using the subset method, and the research area was partitioned for further analysis.

Conversion of Digital Number (DN) to Radiance

The main procedure for standardizing picture data from various sensors and platforms involves converting DN values to Spectral Radiance, enabling consistent radiometric measurements. Familiarity with the initial scaling coefficients is necessary for this transformation. The spectral radiance (Lλ) has been computed using the equation specified by Zanter (2016).

$$L_\lambda = M_L * Q_{cal} + A_L \quad (1)$$

Where,

L_λ = Spectral radiance (W/ (m^2 * sr * μm))

M_L = Radiance multiplicative scaling factor for the band.

A_L = Radiance additive scaling factor for the band.

Q_{cal} = Pixel value in DN

To proceed with extra processing, it is necessary to convert the digital numbers (DN) to radiance for bands 2, 3, and 4 of the Landsat TM and ETM+ sensors in the years 1993, 2000, 2005, and 2010. To accomplish this, the radiance multiplicative and additive scaling factors for band 2, 3, and 4 of the corresponding images are acquired from the Landsat metadata files that accompany the downloaded images (Table 2).

Table 2. Parameters Used for DN to Radiance conversion.

Year	Sensor	Band No.	Rad. Mul. Scaling Factor (M_L)	Rad. Add. Scaling Factor (A_L)
1993	Landsat-5	2	1.3222	-4.16220
		3	1.0440	-2.21398
		4	0.87602	-2.38602
2000	Landsat 7	2	0.79882	-7.19882
		3	0.62165	-5.62165
		4	0.63976	-5.73976
2005	Landsat-5	2	1.32654	-4.16220
		3	0.72356	-2.62354
		4	0.63976	-5.65165
2010	Landsat-5	2	0.79882	-2.38602
		3	1.05644	-4.62165
		4	0.76543	-3.62165

Conversion of Radiance to TOA Reflectance

To create clear Landsat landscapes, spectral radiation can be converted into reflectance at the planetary or top of atmosphere (TOA) level. Converting photographs offers two advantages when comparing images captured by different sensors. The cosine effect can be utilized to minimize the influence of shifting solar zenith angles caused by variances in data gathering time. Moreover, the fluctuations in solar radiation outside the Earth's atmosphere caused by differences in spectral bands can also be modified. The radiance of the selected bands from the previous phase has been converted into images, which were then used to calculate reflectance. The calculation of the total reflectance from the Earth's surface and atmosphere for the years 1993, 2000, 2005, and 2010 has been conducted using Landsat TM and ETM+ data. The equation used for this calculation is the one supplied by Irish (2000).

$$Q_p = \frac{\pi d^2 L_\gamma}{ESUN_\gamma \cos\theta_s} \quad (2)$$

Where, ρ_p = Planetary Reflectance, L_γ = Spectral Radiance at the sensor's aperture

d = Earth-Sun distance in astronomical units, $ESUN_\gamma$ = Mean solar exoatmospheric irradiance, θ_s = Solar zenith angle in degrees

The solar zenith angle can be determined by subtracting the solar elevation angle, as indicated in the metadata file, from 90 degrees. Additionally, the mean solar exo-atmospheric irradiance (ESUNγ) and the Earth-Sun distance (d) are used in the radiometric correction process to account for variations in solar energy received at the Earth's surface derived using the Julian Calendar, are respectively provided in (Table 3 and Table 4).

Table 3. Solar irradiance for landsat 5(TM) and landsat 7(ETM+).

Band	Landsat 5 (TM) ($W/m^2*\mu m$)	Landsat 7 (ETM^+) ($W/m^2*\mu m$)
1	1957	1970
2	1826	1842
3	1554	1547
4	1036	1044
5	215.0	225.7
7	80.67	82.06
8	-	1369

Table 4. Parameters used for radiance to reflectance conversion.

Year (Landsat sensor)	WRS Path and Row	Earth-Sun distance in astronomical units (d)	Solar zenith angle in degrees (θ_s)	Mean solar exo-atmospheric irradiance ($ESUN_\gamma$)
1993 (TM)	138,42	0.99280	90 - 41.54147541	1826 (Band 2)
	138,43	0.99280	90 - 42.51407377	1554 (Band 3)
	139,42	0.99527	90 - 43.89935287	1036 (Band 4)
2000 (ETM+)	138,42	0.98724	90 - 38.81661247	1842 (Band 2)
	138,43	0.98724	90 - 39.97976610	1547(Band 3)
	139,42	0.98409	90 - 35.19818820	1044(Band 4)
2005 (TM)	139,88	0.98724	90 - 41.36576562	1825 (Band 2)
	138,43	0.99432	90 - 40.68539244	1554(Band 4)
	138,97	0.9967	90 - 43.23474323	1044(Band 4)
2010 (TM)	139,42	0.98724	90 - 39.78468454	1836 (Band 2)
	133,25	0.99543	90 - 41.64748456	1064(Band 4)
	136,89	0.98423	90 - 42.37835688	1044(Band 4)

Conversion of DN to TOA Reflectance

The process of transforming DN values to TOA for Landsat 8 and 9 images is a simple and efficient one-step procedure. This allows for the convenient conversion of data from 2017 and 2023 into reflectance images using the equation (Zanter, 2016).

$$\rho_\lambda = \frac{M_\rho * Q_{cal} + A_\rho}{\sin(\theta_{SE})} \quad (3)$$

Where, ρ_λ = TOA spectral reflectance.

M_ρ = Reflectance multiplicative scaling factor for the band.

A_ρ = Reflectance additive scaling factor for the band.

Q_{cal} = Pixel value in DN.

θ_{SE} = Local sun elevation angle (provided in degrees in the metadata).

To retrieve the Top of Atmosphere (TOA) reflectance values for bands 3, 4, and 5 of Landsat 8 images from the years 2017 and 2023, the reflectance multiplicative and scaling factor values, along with the local sun elevation angle, are extracted from the Landsat metadata files that accompany the downloaded images (Table 5).

Table 5. Parameters Used for DN to Reflectance Conversion.

Year (Landsat Sensor)	WRS path and row	Sun elevation angle in degrees (θ_{SE})	Reflectance multiplicative scaling factor (M_L)	Reflectance additive scaling factor (A_L)
2017 (OLI/TIRS)	138,42	38.24110398	0.00002	-0.100000
	138,43	39.45762644		
	139,42	40.00261158		
2023 (OLI/TIRS)	138,42	42.87747217		
	138,43	44.07959061		
	139,42	45.36241130		

Accuracy Assessment

To distinguish true land cover changes from potential classification errors, error matrices and per-class accuracy indices were calculated for the year 2023. In this process, 90 stratified random points were generated across the study area for the selected year using Google Earth imagery to determine the actual LULC classes. These verified classes, derived from the reference images, were then utilized to assess per-class accuracy (i.e.,

user's and producer's accuracy). Additionally, overall accuracy and the Kappa coefficient for the year were computed to provide a comprehensive evaluation of the classification performance.

Producer's Accuracy (PA): Measures how well a particular land cover class has been classified, from the perspective of the classifier (or producer). It indicates the probability that a reference pixel (ground truth) is correctly classified in the map.

User's Accuracy (UA): Measures the accuracy from the user's perspective, showing how often the class on the map represents the real-world category.

Both Producer's Accuracy and User's Accuracy are typically reported together, but Overall Accuracy is a combined metric that represents the proportion of correctly classified pixels across all classes.

Normalized Difference Vegetation Index (NDVI) Retrieval

The Normalized Difference Vegetation Index (NDVI) evaluates vegetation by quantifying the difference between near-infrared light, which is strongly reflected by plants, and red light, which is absorbed by plants. The vegetated sections are represented with a higher luminosity, whereas the non-vegetated portions are represented with a lower luminosity. The computation of NDVI can be executed utilizing the equation stated by (Rouse et. al in 1974).

$$\text{NDVI} = \frac{NIR - RED}{NIR + RED} \qquad (4)$$

Where, NIR =Reflectance of Near Infra-red band

RED = Reflectance of Red band

The Normalized Difference Vegetation Index (NDVI) is a quantitative measure that ranges from -1 to +1. Regions with abundant vegetation exhibit positive values close to +1, while places covered by snow, clouds, and bodies of water have lower values near -1. Band 4 of Landsat 5 (TM) and Landsat 7 (ETM+) corresponds to the Near Infrared (NIR) region, while band 3 represents the Red region.

$$\text{NDVI} = \frac{Band\ 4 - Band\ 3}{Band\ 4 + Band\ 3} \quad \text{(For Landsat 5 and 7)} \qquad (5)$$

On the other hand, band 5 and band 4 of Landsat 8 and 9 represent the reflectance of near-infrared (NIR) and red regions, respectively.

$$\text{NDVI} = \frac{Band\ 5 - Band\ 4}{Band\ 5 + Band\ 4} \quad \text{(For Landsat 8 \& 9)} \qquad (6)$$

Radiance to Brightness Temperature Conversion

By inputting the converted radiant thermal bands into the calculation provided by Zanter (2016), the brightness temperature is determined.

$$T_b = \frac{K_2}{\ln\left(\frac{K_1}{L_\lambda} + 1\right)} \qquad (7)$$

Where, T_b = Top of atmosphere brightness temperature (K)

K_2 = Second calibration constant (K)

K_1 = First calibration constant ($Wm^{-2}sr^{-1}\mu m^{-1}$)

L_γ = Spectral radiance ($Wm^{-2}sr^{-1}\mu m^{-1}$)

The values of the calibration constants are given in (Table 6).

Table 6. Thermal Band Calibration Constants.

Satellite	Constant K_1 ($Wm^{-2}sr^{-1}\mu m^{-1}$)	Constant K_2 (Kelvin)
Landsat 5 TM	607.76	1260.56
Landsat 7 ETM+	666.09	1282.71
Landsat 8 TIRS	774.89	1321.08
Landsat 9 TIRS	799.03	1329.24

Land Surface Emissivity Computation

Land Surface Emissivity (LSE) is the natural materials intrinsic property and is considered a prominent surface attribute. This method can be used to create maps of surface materials for geological studies on Earth as well as other worlds.

The equation used to compute LSE is as follows (Sobrino *et al.*, 2004):

$$\text{LSE} = 0.004 * P_v + 0.986 \qquad (8)$$

Where, P_v = Vegetation proportion

$$P_v = \left[\frac{(NDVI - NDVI_{min})}{(NDVI_{max} - NDVI_{min})}\right]^2 \quad (9)$$

Here, NDVI = Normalized Difference Vegetation Index obtained by previous equation.

$NDVI_{min}$ = Min. value of NDVI

$NDVI_{max}$ = Max. value of NDVI

Retrieval of Land Surface Temperature

The following equation has been employed to compute the Land Surface Temperature (Artis and Carnahan, 1982).

$$LST = \frac{T_b}{1+(\gamma T_b/\alpha)\ln \varepsilon} \quad (10)$$

Where, T_b = At-satellite brightness temperature (K)

γ = Wavelength of emitted radiance (μm)

α = h*c/K = 1.4388 * 10^{-2} m K = 14388 μm K

h = Planck's Constant (6.626 * 10^{-34} J-s)

c = Velocity of light (2.998 * 10^{8} m/s)

K = Boltzmann Constant (1.38 * 10^{-23} J/K)

ε = Land surface emissivity

The values of γ for different Landsat bands are given in (Table 7).

Table 7. Wavelength of emitted radiance used for LST retrieval.

Satellite	Band	Wavelength, γ (μm)
Landsat 4, 5 and 7	6	11.45
Landsat 8	10	10.8
Landsat 9	11	12

Results

Spatial-temporal Distribution of LULC in Bogura District

A systematic analysis was conducted utilizing supervised classification of thematic satellite images from 1993, 2000, 2005, 2010, 2017, and 2023 to examine the changes in land use and land cover (LULC) in the Bogura District (Fig. 3). LULC (Land Use/Land

Cover) Trends reflect a notable increase in settlement areas, which grew from 61.67 km² in 1993 to 625.71 km² in 2023 (Fig. 4). Agricultural land has decreased slightly from 1146.45 km² to 1089.70 km², while vegetation cover has diminished from 1497.06 km² to 831.99 km². The area of waterbodies has remained relatively stable, and bare soil/fallow land has increased from 96.67 km² to 232.30 km², indicating ongoing land degradation or reduced vegetation.

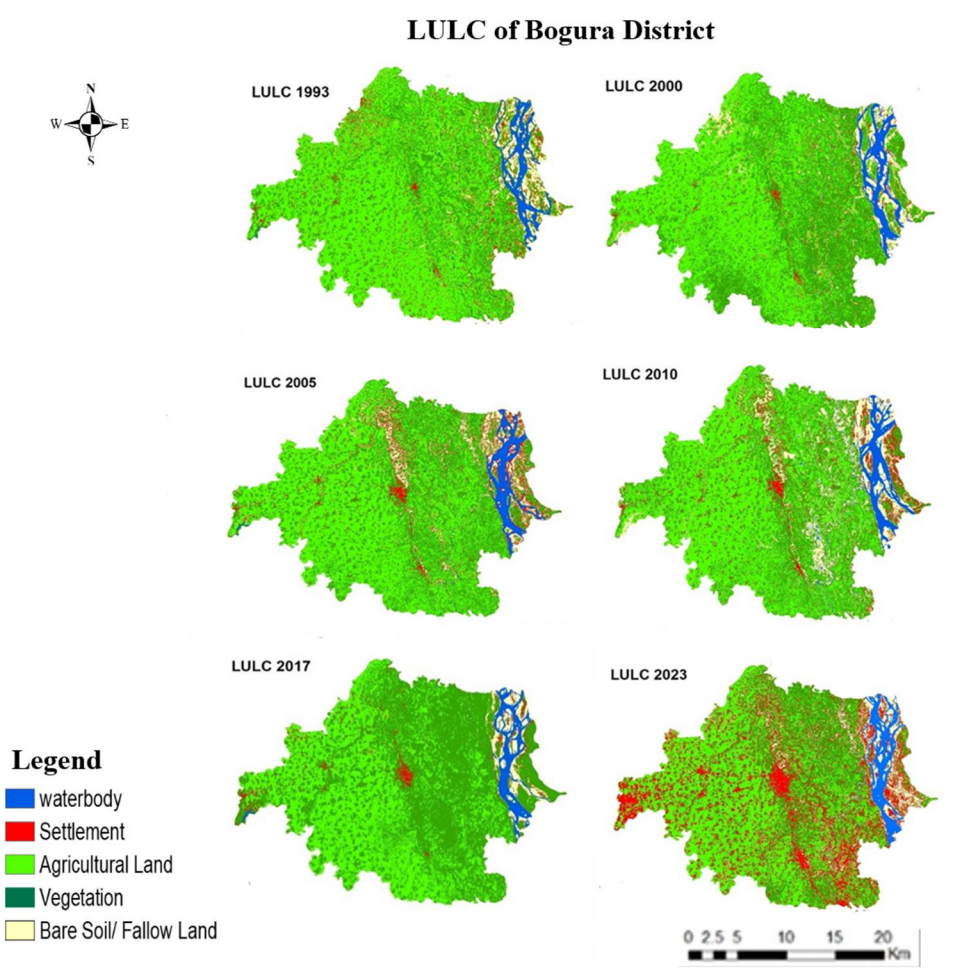

Fig. 3. Supervised classification based spatial distribution of LULC of Bogura District from 1993 to 2023.

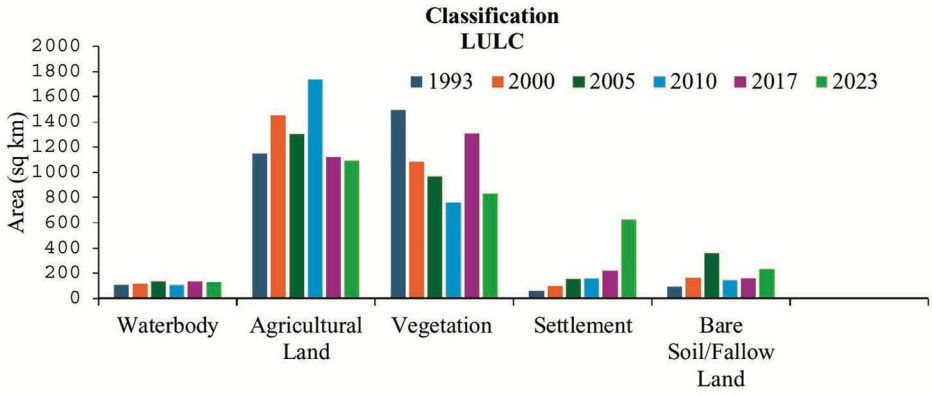

Fig. 4. Graphical representation of LULC calculation from 1993-2023.

Accuracy Assessment result

(Table 8 presents the results from the per-class accuracy assessment for the year 2023. User's accuracy (UA) and producer's accuracy (PA) for most land cover classes ranged between 60% and 88%. The Waterbody class exhibited high accuracy, with UA and PA values of 85% and 88%, respectively, reflecting reliable classification. Similarly, the Settlement class showed strong performance, with UA of 88% and PA of 82%. In contrast, the Agricultural Land and Bare Soil/Fallow Land classes demonstrated lower accuracies, with the lowest PA (62%) observed for Bare Soil/Fallow Land. This is likely due to the spectral similarity between these classes, which introduces misclassification errors. The Vegetation class achieved moderate accuracy, with UA and PA values of 72% and 75%, respectively, indicating some misclassification with other land cover types. Despite these variations, the overall accuracy was 89%, and the Kappa coefficient was 0.815, indicating strong agreement between the classified map and reference data.

Spatial-temporal Distribution of LULC in Bogura Municipality

Bogura Municipality (Bogura Sadar) is in the center of Bogura District and is heavily impacted by urbanization (Fig. 5). The municipality is undergoing massive urbanization development. The Bogura district municipality's settlement area is rapidly expanding. Vegetated and agricultural fields are declining, while habitation and barren lands are growing. Despite fast infrastructure development, the Bogura Sadar or Bogura municipality region faces threats of environmental deterioration and biodiversity loss.

Table 8. Per-class accuracy assessments of multi-temporal for the year 2023.

LULC Class	Samples (n)	User's Accuracy (UA)	Producer's Accuracy (PA)
Waterbody	15	0.85	0.88
Agricultural Land	20	0.65	0.68
Vegetation	20	0.72	0.75
Settlement	20	0.88	0.82
Bare Soil/ Fallow Land	15	0.60	0.62
overall accuracy		0.89	
Kappa coefficient		0.815	

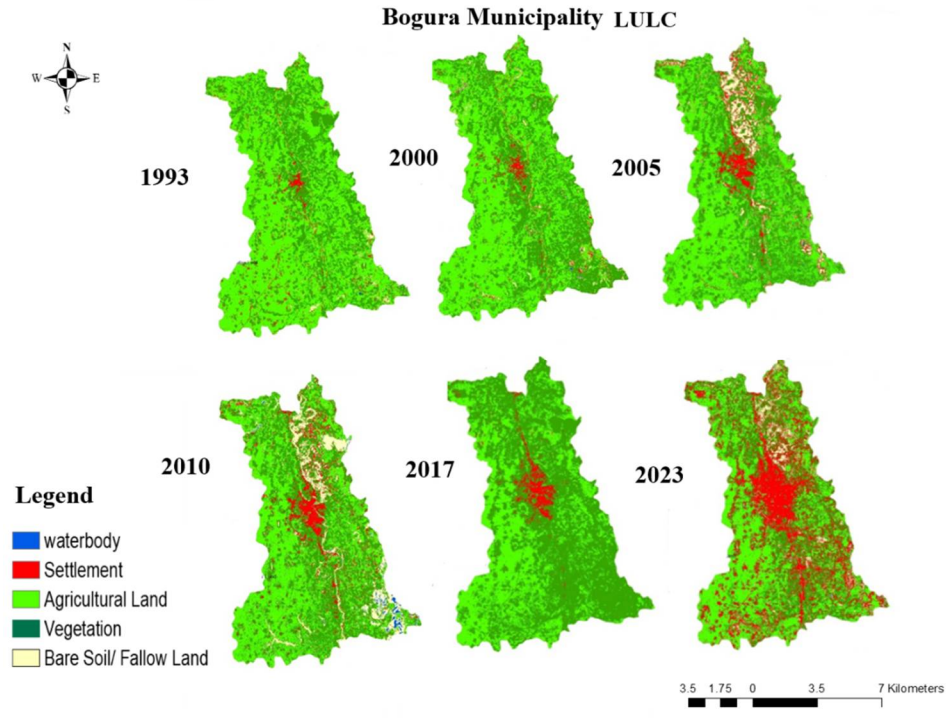

Fig. 5. Spatial Distribution of LULC of Bogura Municipality from 1993 to 2023.

Spatial-temporal Distribution of LST in Bogura District

The land surface temperature areas are classified into five classes which are very low temperature(<24°C), low temperature(24-26°C), moderate temperature(26-28°C), high temperature(28-30°C) and very high temperature (>30°C) covered areas (Fig. 6). The very low temperature category decreased sharply from 2817.96 km² in 1993 to just 61.78 km² in 2023 (Fig. 7). Conversely, areas experiencing low, moderate, high, and very high temperatures have all increased, with the most notable rise in the high temperature category, expanding from 0 km² in 1993 to 140.23 km² in 2023.

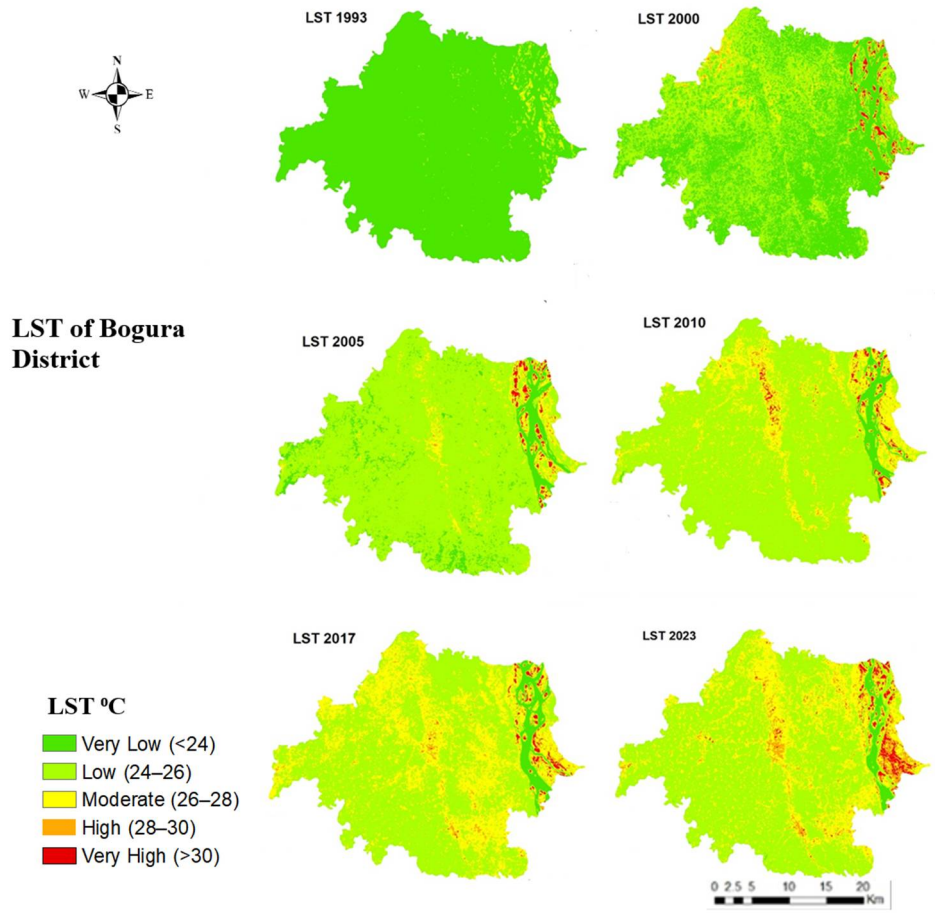

Fig. 6. Spatial Distribution of LST of Bogura District from 1993 to 2023.

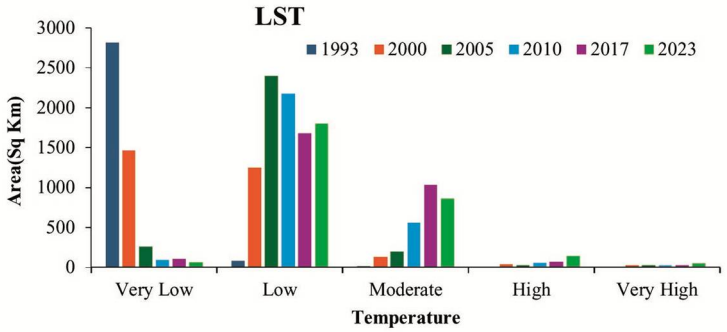

Fig. 7. Graphical representation of LST calculation from 1993-2023.

Spatial-temporal Distribution of NDVI in Bogura District

The NDVI data reveals changes in land cover and vegetation health from 1993 to 2023 (Fig. 8). Waterbody NDVI values declined from 298.86 km² in 1993 to 155.34 km² in 2023, indicating reduced waterbody areas or vegetation around them (Fig. 9). Fallow land

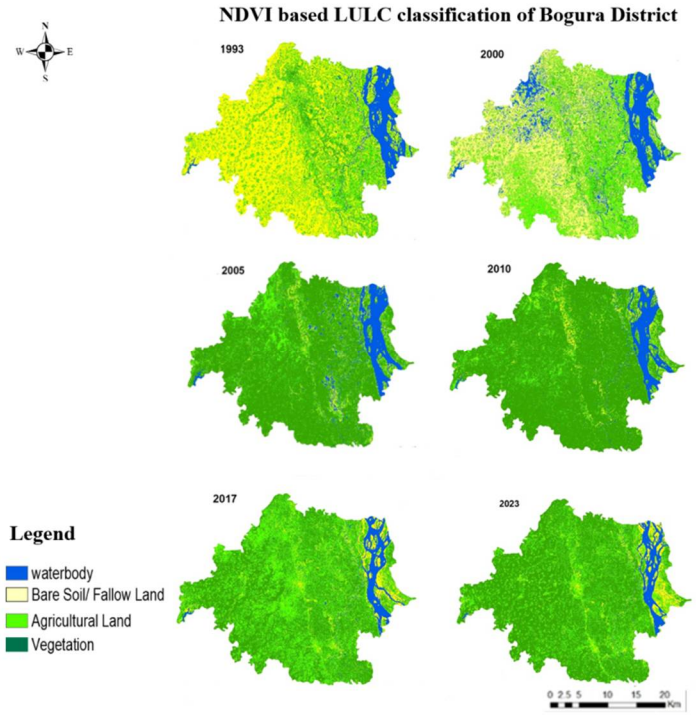

Fig. 8. Spatial Distribution of NDVI based LULC classification of Bogura District from 1993 to 2023.

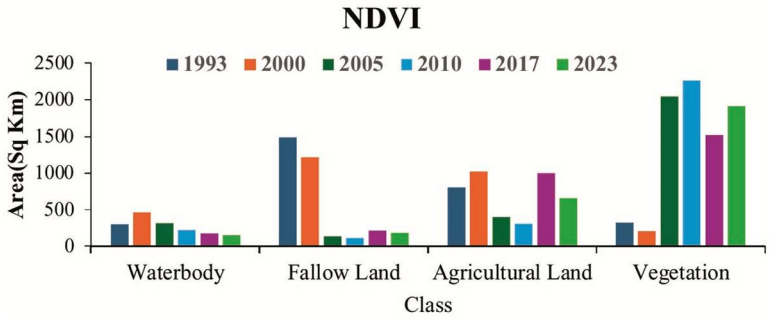

Fig. 9. Graphical representation of NDVI from 1993-2023.

NDVI values fluctuated significantly, dropping from 1489.71 km² in 1993 to 182.85 km² by 2023, reflecting a decrease in fallow land or vegetation changes. Agricultural land NDVI values increased from 802.85 km² in 1993 to 1003.45 km² in 2017 but then decreased to 657.90 km² in 2023, suggesting variations in agricultural practices. Vegetation NDVI values generally rose from 320.39 km² in 1993 to a peak of 2263.31 km² in 2010 before slightly decreasing to 1915.71 km² in 2023, indicating overall improved vegetation health with some fluctuations.

Discussion

The analysis of spatiotemporal changes in Bogura District from 1993 to 2023 reveals significant shifts in land use, land surface temperature (LST), and vegetation cover. The NDVI analysis highlights a substantial increase in vegetation cover, rising from 320.39 km² in 1993 to 1915.71 km² in 2023. This indicates overall improved vegetation health, although the increase in vegetation is somewhat counterbalanced by the notable decline in other land cover types. Waterbodies have decreased dramatically from 298.86 km² to 155.34 km², and fallow land has sharply reduced from 1489.71 km² to 182.85 km². Agricultural land has also seen a reduction, from 802.85 km² to 657.90 km², suggesting shifts in land use and potential impacts on local ecosystems.

The LST data reveals a significant shift towards higher temperature categories. The area classified under very low temperatures has decreased sharply from 2817.96 km² in 1993 to just 61.78 km² in 2023. Conversely, areas experiencing low, moderate, high, and very high temperatures have all increased, with the most notable rise observed in the high temperature category, expanding from 0 km² in 1993 to 140.23 km² in 2023. This shift reflects the intensifying urban heat island (UHI) effect driven by increased urbanization.

Land Use/Land Cover (LULC) trends further underscore the impact of urbanization. Settlement areas have expanded significantly from 61.67 km² in 1993 to 625.71 km² in 2023, highlighting rapid urban growth. Concurrently, agricultural land has decreased slightly from 1146.45 km² to 1089.70 km², while vegetation cover has diminished from 1497.06 km² to 831.99 km². The area of waterbodies has remained relatively stable, but bare soil and fallow land have increased from 96.67 km² to 232.30 km², indicating ongoing land degradation or reduced vegetation.

The strengths of this study lie in its comprehensive analysis using multispectral satellite images, which provides a detailed understanding of land use dynamics and their effects on surface temperatures. However, the study's reliance on satellite data alone may not capture all local variations, and integrating field surveys could enhance the accuracy of the findings.

This research is crucial for addressing the adverse impacts of urbanization and climate change. By identifying the key areas of change and their effects on temperature and vegetation, the study supports the development of strategies for sustainable urban planning and climate resilience. It provides a framework for mitigating the urban heat island effect and guiding efforts to balance urban growth with environmental conservation.

Conclusion

The strong link between land use-land cover (LULC) changes, Normalized Difference Vegetation Index (NDVI) variations, and land surface temperature (LST) help to understand the development of heat islands in Bogura District. Rapid urbanization has led to significant increases in settlement areas and surface temperatures, intensifying the urban heat island (UHI) effect. As urban areas expand, they replace vegetation and water bodies with impervious surfaces, contributing to higher LST and reduced NDVI values. The decline in fallow and agricultural lands, driven by growing food demands and urban sprawl, exacerbates habitat loss and environmental degradation. The findings underscore the urgent need for sustainable development strategies to mitigate the UHI effect, preserve biodiversity, and balance urban growth with ecological conservation.

Acknowledgement

Authors are gratefully acknowledged the USGS archive to provide satellite images with free of cost.

References

Ahmed, B., I. Kelman, M. Kamruzzaman, H. Mohiuddin, M.M. Rahman, A. Das and M. Shamsudduha. 2019. Indigenous people's responses to drought in northwest Bangladesh. *Environ. Develop.* **29**: 55-66.

Artis, D.A. and W.H. Carnahan. 1982. Survey of emissivity variability in thermography of urban areas. *Remote Sens. Environ.* **12**(4): 313-329.

Bangladesh Bureau of Statistics (BBS). 2022. *Population and housing census 2022*.

Bangladesh Meteorological Department (BMD). 2021. *Monthly maximum temperature*. Retrieved from http://live3.bmd.gov.bd/p/Monthly-Maximum-Temperature/ (Accessed September 6, 2021).

Borges, C.K., R.M. de Medeiros, R.E. Ribeiro, É. G. dos Santos, R. G. Carneiro and C.A. dos Santos. 2016. Study of biophysical parameters using remote sensing techniques to Quixeré-CE region. *J. Hyperspec. Remote Sens.* **6**(6): 283-294.

Ding, H. and W. Shi 2013. Land-use/land-cover change and its influence on surface temperature: A case study in Beijing City. *Inter. J. Remote Sens.* **34**(15): 5503-5517.

Jie, B., L. Shaomin and H. Guang. 2008. Inversion and verification of land surface temperature with remote sensing TM/ETM+ data. *Transactions of the Chinese Society of Agricultural Engineering*, **2008**(9).

Kustas, W.P. and J.M. Norman. 1996. Use of remote sensing for evapotranspiration monitoring over land surfaces. *Hydrol. Sci. J.* **41**(4): 495-516.

Luck, M. and J. Wu. 2002. A gradient analysis of urban landscape pattern: A case study from the Phoenix metropolitan region, Arizona, USA. *Landscape Ecol.* **17**(4): 327-339.

Pielke, R.A. 2005. Land use and climate change. *Science*, **310**(5754): 1625-1626.

Ramachandra, T.V., B.H. Aithal and D. Sanna. 2012. Land surface temperature analysis in an urbanizing landscape through multi-resolution data. *Research & Reviews: Journal of Space Science & Technology*, **1**(1): 1-10.

Rouse Jr, J., R.H. Haas, J. A. Schell and D.W. Deering. 1974. Monitoring vegetation systems in the Great Plains with ERTS.

Sobrino, J.A., L. Paolini, F.Grings, J.C. Jiménez-Muñoz and H. Karszenbaum. 2006. Radiometric correction effects in Landsat multi-date/multi-sensor change detection studies. *Inter. J. Remote Sens.* **27**(4): 685-704.

Voogt, J.A. and T.R. Oke, 2003. Thermal remote sensing of urban climates. *Remote Sens. Environ.* **86**(3): 370-384.

Walawender, J. P., M. Szymanowski, M.J. Hajto, and A. Bokwa. 2014. Land surface temperature patterns in the urban agglomeration of Krakow (Poland) derived from Landsat-7/ETM+ data. *Pure Appl. Geophy.***171**(6): 913-940.

Weng, Q. (2001). A remote sensing–GIS evaluation of urban expansion and its impact on surface temperature in the Zhujiang Delta, China. *Inter. J. Remote Sens.* **22**(10): 1999-2014.

Xie, Q., and Z. Zhou. 2015. Impact of urbanization on urban heat island effect based on TM imagery in Wuhan, China. *Environ. Eng. Manage. J.* **14**(3): 647-655.

Zanter, K. 2016. *Landsat 8 (L8) data users handbook. Landsat Science Official Website, 33*.

(Revised copy received on 18/03/2025)

J. Asiat. Soc. Bangladesh, Sci. **51**(1): 39-50, June 2025
DOI: http://doi.org/10:3329/jasbs.v51i1.82790

SUGARCANE WOOLLY APHID, *CERATOVACUNA LANIGERA* - AN INVASIVE PEST OF SUGARCANE AND ITS MANAGEMENT IN BANGLADESH

MD. MOHASIN HUSSAIN KHAN
Department of Entomology, Patuakhali Science and Technology University
Dumki, Patuakhali-8602, Bangladesh

Abstract

Study was conducted in homestead garden of Patuakhali Science and Technology University (PSTU) campus, Patuakhali during the period from November 2016 to October 2017. Results revealed that the length and width of the apterous adult female was 1.76 mm and 1.06 mm, respectively while the length and width of the alate adult was 2.09 mm and 6.4 mm, respectively. The nymphal stage varies from 15.8 (minimum) days to 32 (maximum) days of apterous, whereas of alate form the period is little longer, up to 40 days. The maximum population density of woolly aphid was observed in vegetative stage (47.12/2.5 sq.cm.) and the lowest population density was recorded in seedling stage (7.23/2.5 sq.cm.). The highest percent leaf area occupied by sugarcane woolly aphid was observed at vegetative stage (58.13%/leaf) and the lowest percent leaf area occupied by sugarcane woolly aphid was recorded in seedling stage (27.14%/leaf). No significant difference was found among leaves treated with 4 insecticidal treatments. But the lowest number (0.33 aphid/sq. cm) of woolly aphid per square cm area was found in leaf treated with Biotap plus extra 95EC @ 0.2 g/L of water followed by T4 (0.67 aphid/sq. cm) where Fija 70WG @ 0.074 g/L of water was sprayed. The highest number of woolly aphid was observed in untreated control treatment (41.33 woolly aphid/sq. cm). The highest percent reduction (99.20%) of woolly aphid over control was found in leaves treated with Biotap plus extra 95EC @ 0.2 g/L of water. Likewise, the percent reduction of leaf area occupied by woolly aphid was recorded maximum (99.41%) in leaves treated with Biotap plus extra 95EC @ 0.2 g/L of water while minimum percent (98.20%) was in leaves treated with Voliam flexi 300SC @ 0.5 ml/L of water. Application of Biotap plus extra 95EC @ 0.2 g/L of water could be the best treatment for the management of sugarcane woolly aphid.

Key words: sugarcane, woolly aphid, damage, incidence, insecticide.

Introduction

Sugarcane, *Saccharum officinarum* is an important cash crop of Bangladesh and it is the main source of processed sugar. It plays pivotal role in both agricultural and industrial economy of the country. Greater attention is given only in improving the sugar cane yield and not much in managing the cane trash. Sugarcane yield is markedly influenced by

*Corresponding author: mohasin1965@pstu.ac.bd

many factors like soil fertility, climate, variety, and cultural practices, prevalence of pests and diseases as well as environmental stress (Kumar and Pal, 2019). Among them, insect pests are known to cause considerable yield loss in sugarcane yield as well as sugar content. As sugarcane is a long duration crop of 10-18 months and therefore is liable to be attacked by a number of insect pests and diseases (Kumar and Pal, 2019). In sugarcane ecosystem the pests are classified into three categories *viz.*, internode bores, sucking pests and soil inhabiting pests. Internode borers like *Chilo infuscatellus* Snell (early shoot borer), *Scirpophaga excerptalis* Walker (top shoot borer), *Chilo sacchariphagus indicus* Kapur (internode stem borer), sucking pests are *Ceratovacuna lanigera* Zehnter (woollyaphid), *Pyrilla perpusilla* Walker (sugarcane leaf hopper), *Saccharicoccus sacchari* Cockerel (mealy bug), *Melanaspis glomeratus* Green (scale) and soil inhabiting pests like *Odontotermes obesus* Rhamb (termite) and *Holotrichia serrata* Fabricus (root grub) are the important pests of sugarcane in Indian situations (Vasantharaj and Ramamurthy, 2011). According to an estimate, sugarcane production declines by 20.0 and 19.0% by insect pests and diseases, respectively. Among the various factors, incidence of insect pests plays a vital role for low productivity and sugar recovery. About 103 insects were associated with sugarcane crop (Patil *et al*., 2007). Economical loss in sugarcane has been estimated to be 20 % in cane yield and 15 % in sugar recovery due to the ravages of the insect pests (Patil *et al*., 2011). Among different insect pests of sugarcane, sugarcane woolly aphid, *Ceratovacuna lanigera* Zehntner (Hemiptera: Aphididae), is one of the most destructive insect pests of sugarcane (Patil *et al*., 2007). It is a major leaf pest of sugarcane. The species is currently distributed in India, Nepal, Bangladesh, east and south-east Asia, Fiji and the Solomon Islands (Joshi and Viraktamath, 2004). It affects both the yield and quality of sugarcane in China. In India it has been reported from both tropical (Maharashtra, Karnataka, Gujrat, Andhra Pradesh and Tamilnadu) and subtropical belts (Assam, Nagaland, Tripura, Uttranchal, westen Uttar Pradesh and Haryana). Woolly aphid earlier was known to be minor pest in India has now assumed the status of economic pest after its severe outbreak in Maharashra during July 2002. The sugarcane woolly aphid bears huge content of white coloured woolly coating around it. Developed colonies looked like a white woolen mass and that is why this aphid is referred to as woolly aphid. It is often mistaken for a mealybug. Adult and nymphs of the sugarcane woolly aphid gather on the underside of leaves and suck the sap from the leaves (Girija 2012). The pests feed voraciously and convert excess sugar into honeydew. They produce honeydew that covers the entire upper surface of the leaf which causes the growth of sooty mold (Girija, 2012). This interrupts the plant's ability to photosynthesise and so results in a weaker plant with a reduced yield (Girija, 2015). The sugarcane plants wilt and gradually dry up from the tip downwards due to continuous

infestation and sap sucking from the leaves. This eventually leads to the reduction of the length, girth, and weight of the sugarcane, as well as the quality, yield, and sugar content (Patil *et al.*, 2011, Mukunthan *et al*., 2008). Management of agro-ecosystem which discourages the pest build-up like balanced use of fertilizers, avoiding excess irrigation, proper drainage, inter cropping and planting of least susceptible/resistant varieties (Joshi and Viraktmath, 2004). Use of less hazardous insecticides such as Metasystox 20 EC or endosulfan 35 EC @ 0.05% spray at 15-20 days interval where natural enemies are prevalent (Joshi and Viraktmath, 2004). No research report on incidence, damage severity and control of sugarcane woolly aphid is available in Bangladesh. Therefore, the present study has been undertaken to know the incidence pattern and damage of woolly aphid, and also to find out suitable chemical insecticide for controlling this pest.

Materials and Methods

Study was conducted in homestead garden of Patuakhali Science and Technology University (PSTU) campus, Patuakhali during the period from November 2016 to October 2017. The measurement of different stages of woolly aphid was performed by using stereo zoom trinocular microscope. The incidence and damage by woolly aphid on sugarcane leaves were observed from seedling to reproductive stages. Observations on the population of woolly aphid were recorded on 2.5 square cm area of sugarcane leaf in three randomly selected leaves per plant. The percentage of leaf area occupied by woolly aphid was measured on eye estimation. In case of control, there were five treatments viz., T_1 = Voliam flexi 300SC @ 0.5 ml/L of water, T_2 = Bioneem plus 1EC @ 1 ml/L of water, T_3 = Biotap plus extra 95EC @ 0.2 g/L of water, T_4 = Fija 70 WG @ 0.074 g/L of water and T_5= Untreated control. In this case, three leaves from each plant were used as three treatment replications for the application of each treatment. Data were also recorded on number of woolly aphid and leaf area occupied by woolly aphid. The percent reduction of woolly aphid and leaf area was calculated by following formula:

$$\% \text{ reduction over control} = \frac{\text{Control-treatment}}{\text{Control}} \times 100$$

Statistical analysis: Data were analyzed statistically following the analysis of variance (ANOVA) using WASP 1.0 software program. Means were separated by CD (critical difference) values.

Results and Discussion

Biology and characteristics of sugarcane woolly aphid

Different life stages of sugarcane woolly aphid is illustrated in Plate 1**.** Alate females produced first instar nymphs which were relatively active, had long and elliptical bodies. They were pale greenish white in colour. But apterous females produced first instar nymphs which were pale yellowish white in colour, had elongated ovoid bodies (0.75 mm length and 0.38 mm width). The dorsum was gradually covered by a white powdery secretion due to the development of nymph. Developed colonies looked like a white woollen mass, hence this aphid is referred to as woolly aphid (Table 1).

The length and width of the apterous adult female was 1.76 mm and 1.06 mm, respectively with broad, very soft, laterally depressed body which was densely covered by white, cotton like secretions. Its 5^{th} and 6^{th} segments of abdomen had circular cornicles through which it secretes waxy substance (Table 1).

Likewise, the length and width of the alate adult was 2.09 mm and 6.4 mm, respectively with expended wings. The head was black with enlarged brick red eyes (Table 1). The antennae had two thick basal segment and a flagellum composed of four segments. The legs had two tarsal segments with paired claws. The fore wing was very large and had 3 oblique veins emerging from subcostal vein. The hind wing was small with 2 oblique veins. Depending upon the temperature and relative humidity the nymphal stage varies from 15.8 - 16.5 (minimum) days to 23 - 32 (maximum) days of apterous, whereas of alate form the period is little longer, up to 40 days (Table 1).

Table 1. Characteristics of sugarcane woolly aphid.

Stages of woolly aphid	Size (mm)		Colour
	Length	Width	
Nymph	0.75 ± 0.2	0.38 ± 0.1	Pale greenish white
Apterous adult female	1.76 ± 0.6	1.06 ± 0.3	White
Alate adult	2.09 ± 0.5	6.4 ± 0.7	Head is black with brick red eyes
	Duration (Day)		
	Minimum	Maximum	
Apterous nymphal stage	15.8 - 16.5	23 - 32	
Alate nymphal stage		35-40	

Apterous females reproduced parthenogenetically giving birth directly to nymphs (Joshi and Viraktamath, 2004). In Woolly aphid thaleotoky type of parthenothenesis reproduction occurs where they reproduce viviparously. Immediately after ovulation, ova starts to develop within a viviparous reproducing female indicating that an embryo can exist inside another larger and mature embryo. These mode of reproduction provide an exceedingly rapid turnover of generations.

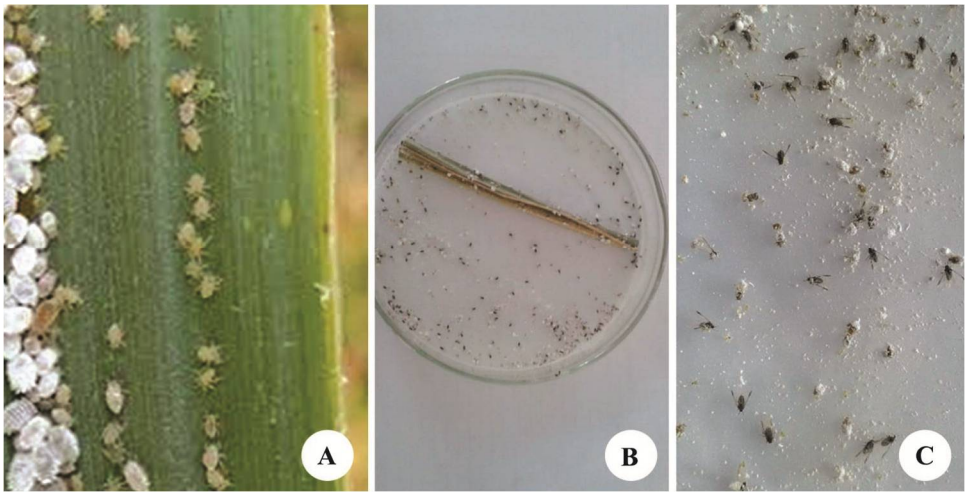

Plate 1. Different life stages (A- Nymphs, B-Adults, C-Adults in enlarged form) of sugarcane woolly aphid.

Incidence of sugarcane woolly aphid

Mean number of sugarcane woolly aphid per 2.5 square cm area in different growth stages of cane is presented in Fig. 1 and Plate 2. The maximum population density of woolly aphid was observed in vegetative stage (47.12/2.5 sq.cm.) which was followed by early vegetative stage (22.34/2.5 sq.cm.). The lowest population density was recorded in seedling stage (7.23/2.5 sq.cm.) and was followed by reproductive stage (12.68/2.5 sq. cm.), respectively.

Generally, the incidence of woolly aphid, scales and natural enemies was not appeared during seedling stage of crop since it requires cold climate and high relative humidity (80-95) and moderate temperature (19 to 30^0C). The colonies started developing in November and December and then gradually increased during winter, with phenomenal increase during summer. Measurements of the colony increased with decrease in

temperature from December to February. The pest population starts increasing in February and reaches its peak in April-June and decreases subsequently due to rains. The population peaked between the second half of April and the second half of June. Heavy precipitation coupled with high temperatures was the factors causing decline in the aphid population. The results are in conformity with Patil *et al*., (2003) who reported that the average population of sugarcane woolly aphid was 5.3 per 5 cm^2 leaf area during the month of July with corresponding leaf infestation being 42.11 per cent. Ghorpade *et al*., (2006) reported that the activity of sugarcane woolly aphid was started in the month of September and reached peak in the month of December. Thakur (2007) reported that apterous forms of *C. lanigera* showed maximum activity from mid October, 2003 to end of January, 2004 and their population vanished in May, 2004 and the late forms were appeared in first fortnight of July, 2003 and remained active till March, 2004 but the activity of predator, *D. aphidivora* was maximum (2.67/leaf/plant) in second fortnight of February, 2004. The incidence of Sugarcane Woolly Aphids was found sever in the months of September, October and November, 2011, but later on with increase in maximum temperature and decrease in relative humidity in the month of December, the population of woolly aphids declined (Mane *et al*., 2016).

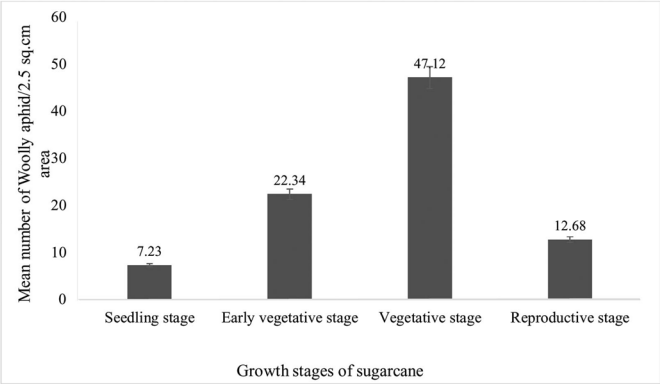

Fig. 1. Mean number of sugarcane woolly aphid at different growth stages of cane

The aphid emerged before sunset and continued to emerge until early morning (Arakaki, 1989). This probably helped aphids to escape desiccation due to high day temperatures. The incidence of this pest starts immediately after rainy season and becomes severe during summer and when there are prolonged dry spells coupled with high relative humidity. Therefore, more population density of woolly aphid, scales and natural enemies

was gradually increased during vegetative stage (Shruthi *et al*., 2018). While, incidence of sucking pests: pyrilla, derbid plant hopper, woolly aphid and mite were recorded as 0.92 per leaf, 4.2 per plant, 7.17 per leaf and 11.25%, respectively. Similar trend was also observed during 2018-19.

The incidence of stem borer, wooly aphid, pyrilla, grasshopper and mite occurs in July to February. The average incidence ranged from 1.86 to3.51 woolly aphids per leaf during 2017-18. During 2018-19, its average incidence ranged from 1.77 to 4.96 per leaf and the maximum incidence of 12.27 wooly aphids per leaf at village Salmara. The incidence started from August and continued up to February and reached the maximum during October till December. Rabindra *et al.* (2002) reported that serious infestation by the sugarcane woolly aphid, *C. lanigera*, on the leaves of 4 to 9 month old sugarcane plants was observed in Kolhapur and Pune districts of Maharashtra in September-October 2002.

The pest is transmitted by wind as well as by the transportation of sett and cane from an affected field to other areas. The pest survives on the ratoon crop as well as on hosts like grasses and banana during the off season. Rao *et al*., (2009) made roving survey in sugarcane fields both in planted and ratoon crops revealed that, among various and insect and non-insect pests, early shoot borer, internode borer, scale insect and mealybugs were considered as key pests, while whitefly, pyrilla, woolly aphid, red mite, yellow mite, white grub, termites and grasshoppers as localized pests and they also opined that, the suitable surveillance periods for different sugarcane pests i.e. March to May for early shoot borer, mealybugs and red mite, june to august for grasshopper, internode borer and yellow mite and June to October for grasshoppers, root grub, scale insect, termites, whitefly and woolly aphid.

Plate 2. Incidence pattern of sugarcane woolly aphid (cottony growth of woolly aphid on sugarcane leaf)

Damage severity by sugarcane woolly aphid

The average percentage of leaf area occupied by sugarcane woolly aphid at different growth stages of cane is presented in Fig. 2 and Plate 3. The highest percent leaf area occupied by sugarcane woolly aphid was observed at vegetative stage (58.13%/leaf) which was followed by early vegetative stage (43.41%/leaf). The lowest percent leaf area occupied by sugarcane woolly aphid was recorded in seedling stage (27.14%/leaf) and was followed by reproductive stage (36.32%/leaf) respectively.

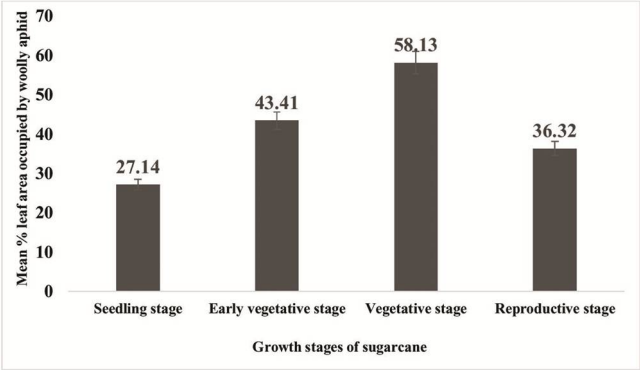

Fig. 2. Percentage of leaf area occupied by woolly aphid at different growth stages of sugarcane.

Plate 3. Damage severity of sugarcane woolly aphid.

The findings of the present study are supported by several authors who stated that both nymphs and adults of woolly aphid suck the cell sap from lower surface of leaves. They suck the sap from phloem by inserting their stylets through the stomata of the plants

leaves. Cell-sap concentration was a major factor in inducing susceptibility in different cane varieties (Yamazaki and Arikado, 1939). Mature leaves were more prone to aphid attack compared to young leaves (Uichanko, 1928). Takano (1937) observed that narrow and erect leaves were affected to a great extent while Patil (2002) found that soft, broad and drooping leaves were more suitable for aphid build-up. They excrete huge amount of honey dew on the leaves which provide a sticky coating on leaves that favours black sooty mould (*Capnodium* sp.) develops making the leaves look all black. The white powder on the ground and leaves confirms the presence of the aphids. If uncontrolled, it spreads very quickly and can cause yield losses of up to 20% (Girija, 2012). Due to the thick coating of sooty mould process of photosynthesis is significantly hampered in severely infested plants, thereby, considerable reduction in cane yield (25%) and sucrose content (26.71%), whereas, during the early growth period plants may die (Patil *et al*., 2011; Mukunthan *et al*., 2008). From above results it can be concluded that, occurrence of woolly aphid decreased during reproductive stage. Because cane become hard and sap is not available for survival of sucking pests so reduced during reproductive stage.

Management of sugarcane woolly aphid

The effect of selected insecticides on sugarcane woolly aphid at vegetative stage is presented in Table 2 and Plate 4. The lowest number (0.33 aphid/sq. cm) of woolly aphid per square cm area was found in leaf treated with Biotap plus extra 95EC @ 0.2 g/L of water followed by T_4 (0.67 aphid/sq. cm) where Fija 70 WG @ 0.074 g/L of water was sprayed. However, no significant difference was found among the treated leaves. The highest number of woolly aphid was observed in untreated control treatment (41.33 woolly aphid/sq. cm). The highest percent reduction (99.20%) of woolly aphid over control was found in leaves treated with Biotap plus extra 95EC @ 0.2 g/L of water followed by T_4 (98.38%) while the lowest percent reduction (96.78%) of woolly aphid over control was found in leaves treated with Voliam flexi 300SC @ 0.5 ml/L of water followed by T_2 (97.58%) where Bioneem plus 1EC @ 1 ml/L of water was sprayed. In case of percent leaf area occupied by woolly aphid, similar trend was also observed

where the lowest percent leaf area occupied (0.33 %) by woolly aphid was recorded in leaves sprayed with Biotap plus extra 95EC @ 0.2 g/L of water and the highest percent leaf area occupied (55.67%) by woolly aphid was recorded in leaves without spraying (T_5).

Table 2. Effect of selected synthetic insecticides on sugarcane woolly aphid at vegetative stage

Treatment	No woolly aphid/2.5 sq cm area	% reduction over control	Leaf area occupied by woolly aphid (%)	% reduction of leaf area occupied by woolly aphid over control
T_1 = Voliam flexi 300SC @ 0.5 ml/L of water	1.33b	96.78	1.00b	98.20
T_2 = Bioneem plus 1EC @ 1 ml/L of water	1.00b	97.58	0.67b	98.80
T_3 = Biotap plus extra 95EC @ 0.2 g/L of water	0.33b	99.20	0.33b	99.41
T_4= Fija 70 WG @ 0.074 g/L of water	0.67b	98.38	0.67b	98.80
T_5= Untreated control	41.33a	-	55.67a	-
CD (1%)	2.20		3.24	
CV (%)	13.08		14.76	

Values are average of three replications.

Plate 4. Leaves of sugarcane treated with selected insecticides (4 treatments).

The percent reduction of leaf area occupied by woolly aphid was recorded maximum (99.41%) in leaves treated with Biotap plus extra 95EC @ 0.2 g/L of water while minimum percent (98.20%) was in leaves treated with Voliam flexi 300SC @ 0.5 ml/L of water. The percent reduction of woolly aphid population ranged from 96.58 to 99.20% and leaf area reduction ranged from 98.20 to 99.41%, respectively. These results are in conformity with Patil *et al.* (2004) and Shankar and Shitole (2004) who found that soil application of phorate 10G @ 2.5 and 3.0 kg a.i./ha reduced the aphid population to the tune of 90 per cent.

Conclusions

The length and width of alate adult was higher compared to apterous adult female. The maximum population density and the highest percent leaf area occupied of woolly aphid was observed at vegetative stage than those of seedling and reproductive stages. The highest percent reduction of woolly aphid and its damage was recorded in leaves treated with Bitap extra plus 95EC @ 0.2 g/L of water at vegetative stage.

References

Arakaki, N. 1989. Flight periodicity and the effect of weather conditions on the take-off of *Ceratovacuna lanigera* Zehntner (Homoptera: Aphididae). *Appl. Entomol. Zool*. **24**: 264-272.

Ghorpade, S. A., D. S. Pokharkar, P. Sinha and R. J. Rabindra. 2006. Biological suppression of sugarcane woolly aphid, *Ceratovacuna lanigera* Zehntner in Maharashtra. Proceedings of National Symposium on Biological control of sucking pests in India, PDBC, Bangalore, May 26-27, pp. 39.

Girija, G. 2012. Factsheets for Farmers. CAB International. Plantwise. www.plantwise.org

Girija, G. 2015. Factsheets for Farmers. PlantwisePlus Knowledge Bank.

Joshi, S. and C.A. Viraktamath. 2004. The sugarcane woolly aphid, *Ceratovacuna lanigera* Zehntner (Hemiptera: Aphididae): its biology, pest status and control. *Curr. Sci*. **87** (3): 307-316.

Kumar, A. and S. Pal. 2019. Survey and surveillance of sugarcane insect pests under Terai zone of Northern West Bengal. *J. Entomol. Zool. Stud.* **7**(3): 47-50.

Mane, M.A., P.B. Mohite and S.A. Patil. 2016. Population dynamics and management of sugarcane woolly aphids, *Ceratovacuna lanigera* (Zehntner) (Hemiptera : Aphididae) with new molecules of insecticides. *Int. J. Adv. Res*. **4**(10): 2047-2050.

Mukunthan, N., J. Srikanth, B. Singaravelu, S. Asokan, N.K. Kurup and Y.S. Goud. 2008. Assessment of woolly aphid impact on growth, yield and quality parameters of sugarcane. *Sugar Tech.* **10**: 143-149.

Patil, A.S. 2002. Pandhrya lokari mavyapasun us wachavinyasathi. Rathnagiri Sthani, Sheti Puravani, 26 September 2002.

Patil, R.K., G.K. Ramegowda, V. Rachappa, S. Lingappa and P. S. Tippannavar, 2003. Records of woolly aphid, *Ceratovacuna lanigera* Zehntner (Homoptera: Pemphigidae) on sugarcane in North Karnataka, *Ins Envt*, **9**: 57-59.

Patil, A.S., V.D. Shinde, S.B. Mager, R.G. Yadav and Y.S. Nerkar, 2004. Sugarcane woolly aphid (*Ceratovacuna lanigera*) its history and control measures. Proceedings of Sugarcane Technologists Association in India, pp.133-155.

Patil, A.S., S.B. Magar, and V.D. Shinde. 2007. Biological control of the sugarcane Woolly Aphid (*Ceratovacuna lanigera*) in Indian sugarcane through the release of predators. In Proceedings of the XXVI Congress, International Society of Sugar Cane Technologists (ISSCT), Durban, South Africa, 29 July–2 August 2007; pp. 797-804.

Patil, N.B., C.P. Mallapur and Y.H. Sujay. 2011. Efficacy of Acremonium zeylanicum against sugarcane wooly aphid under laboratory conditions. *J. Biol. Control*, **25**: 124-126.

Rabindra R.J., P. Mohanraj, J. Poorani, S.K. Jalali, S. Joshi and Ramani, S. 2002. *Ceratovacuna lanigera* Zehntner (Homoptera: Aphididae) a serious pest of sugarcane in Maharashtra and attempts at its management by biological means. *J. Biol. Control*. **16**:171-172.

Rao, C.V.N., N.V. Rao, B. Bhavani and N.V. Naidu. 2009. Survey and surveillance of sugarcane insect pests in Andhra Pradesh. *Indian. J.Pl. Prot*. **37**(1/2): 24-28.

Shankar, G. and D. M. Shitole. 2004. Management of Sugarcane woolly aphid, *Ceratovacuna lanigera* Zehntner (Homoptera : Aphididae), *Pestology*, **28**: 25-26.

Shruthi, N. A.P., Biradar and S. Muzammil. 2018. Occurrence of insect pests and activity of selected natural enemieson sugarcane crop in Northern dry zone of Karnataka. *Internat. J. Plant Protec*. **11**(1) : 80-86, DOI : 10.15740/HAS/IJPP/11.1/ 80-86.

Takano, S. 1937. Relation of sugarcane varieties to insect pests. *J. Sugarcane Plant. Assoc*. **15**: 195-198.

Thakur, S.G., 2007. Studies on Biology and Management of sugarcane woolly aphid, *Ceratovacuna lanigera* Zehntner (Homoptera: Aphididae), Ph.D. Thesis, Mahatma Phule Krishi Viyapeeth, Rahuri, India.

Uichanko, L. B. 1928. Rep. Comm. Cane Varieties and Fertilizers. 6th Ann. Conv. Philipp. Sugar Assoc., p 16.

Vasantharaj, D.B. and V.V. Ramamurthy. 2011. Elements of ecomomic entomology. Namrutha Publications, Chennai, Tamil Nadu, pp. 385.

Yamazaki, M. and H. Arikado. 1939. Relation between the resistance of sugarcane varieties to *Ceratovacuna lanigera* Zehnt. and the concentration of the cell sap (in Japanese). *Rep. Jpn. Assoc. Adv. Sci.*, **14**: 153-155.

(Revised copy received on 22/10/2024)

J. Asiat. Soc. Bangladesh, Sci. **51**(1): 51-72, June 2025
DOI: http://doi.org/10:3329/jasbs.v51i1.82791

REMOTE SENSING TELLS KINSHIP: AGRICULTURAL LAND USE BASED STUDY IN RURAL BANGLADESH

TANJINUL HOQUE MOLLAH[1*], MUNIA TAHSIN[2], MD. MASUK MOWLA AUNKUR[1], MONALISHA FERDOUS[1], MD. HABIBUR RAHMAN[3] AND MOHAMMAD ARIFUR RAHMAN[4]

[1]*Department of Geography and Environment, Jahangirnagar University, Savar, Dhaka-1342, Bangladesh*
[2]*ICCCAD-IUB, Bangladesh*
[3]*Center for Environmental and Geographic Information Services CEGIS), Bangladesh*
[4]*Department of Statistics, Jahangirnagar University, Savar, Dhaka-1342, Bangladesh*

Abstract

Remote sensing senses the land cover, which is indirectly linked to social structure, economic condition, and environmental issues. For instance, collateral information from remote sensing can be used in certain economic conditions and social aspects such as kinship detection, family structure, economic condition, habitat fragmentation, biodiversity, and structure of the villages. The Manikdi *Mouza*, Netrokona, Bangladesh was chosen as a case study because of its homogeneous landscape. This study conducted a household questionnaire survey, involving 370 respondents with a 95% confidence level whereas the margin of error is 5%. CS, RS, and Worldview-3 images were used to map the agricultural boundary and interpret the associated family structure changes over the study period. Besides that, three primary methods such as cluster analysis, multiple regression modeling, and Fuzzy Cognitive Mapping (FCM) were employed to examine plot parcelization, identify the driving forces influencing land parcelization, and determine their respective weights. The results indicate that, over the study period from 1950 to 2023, the total number of plots increased from 359 to 1,048 due to land fragmentation, while 404 plots remained unchanged. Unaltered plots are associated with combined families, while fragmented plots correspond to nuclear families. From the Cadastral Survey (CS) to the Revisional Survey (RS), approximately 26.98% of plots remained unchanged, and from the RS to the present, 38.55% of plots have stayed unaltered. The study's investigation into agricultural land fragmentation and its effects on kinship dynamics in rural Bangladesh highlights crucial implications for local governance and national policy frameworks, advocating for informed, community-centric strategies in land management.

Key words: Remote sensing, Kinship, Plot fragmentation, Family structure and Agricultural plot size.

*Corresponding author: e-mail: thmollah@juniv.edu

Introduction

Kinship, a social bond formed through blood ties, is primarily concerned with future generations. Consequently, kin-based groups are also linked to their land possession (Dister, *et al.,* 1993). Therefore, this land possession is handed down from generation to generation. According to the Muslim Family Laws Ordinance, 1961 (Ordinance NO. VIII OF 1961)-"In the event of the death of any son or daughter of the propositus before the opening of the succession, the children of such son or daughter, if any, living at the time the succession opens, shall per stirpes receive a share equivalent to the share which such son or daughter, as the case may be, would have received if alive." On the contrary, the Muslim Family Laws Ordinance of 1961 also contains information on property ownership, which states that individuals can gain land ownership rights through purchase, inheritance, gift, or settlement by the government (Van schendel and Rahman, 1997). Therefore, in Bangladesh, the spatial orientation of landscape boundaries changes over time as family structures change (Mollah *et al.,* 2023). For example, when a combined family is divided into a single family, the land ownership is delineated as well. As a result, instead of farmland, an individual cropland notion is created (Abdullah, 1976).

Bangladesh is a developing nation with an emphasis on agriculture where more than 85% of the rural poor are directly or indirectly involved in agricultural activities (BBS, 2011). There are two distinct kinds of agricultural land such as farmland and scattered/fragmented agricultural land (Mollah *et al.,* 2023). These two types of land differ in terms of size, location, management techniques, and land use regulations (Mollah *et al.,* 2023). In Bangladesh, agricultural land that is scattered throughout an area is made up of smaller pieces of land because of its large population size (Hassan, 2017). Therefore, scattered agricultural land is operated by small-scale farmers in the rural areas of Bangladesh who grow crops for personal, local consumption and sometimes for large-scale agricultural operations (Rahman *et al.,* 2020).

The relationship between kinship and land fragmentation in Bangladesh is not a straightforward one (Wood, 1981). While kinship often plays a role in land ownership and distribution, land fragmentation can occur due to various socio-economic reasons, including population growth, economic pressure, or changes in livelihood options (Mollah *et al.,* 2023 and Siddik *et al.,* 2022). Hence, using kinship as a sole explanation for land fragmentation can be limiting and should be critically examined in relation to other potential driving forces. In general, remote sensing allows for direct dimensions of the earth's surface as well as the spatial distribution of its physical entities whereas social science is more interested in why things happen rather than where they happen (Turner,

1998). But both disciplines are connected through perceptions, concepts, and related spatial contextual information like area boundary, settlement distribution pattern, shape, size, and height of the buildings as well as vegetation and forest cover (Taubenbock *et al.,* 2009). This confluence of events paves the way to utilize remotely sensed data for distinctive socio-economic rural morphology that is strongly correlated with the characteristics of physical and human dimensions (National Research Council, 1998).

Through the reflection of the objects, remote sensing gives socio-economic information indirectly (Walker, 1994). For instance, the rural morphology in a satellite image is the physical reflection of a society which is influenced by the historical, social, cultural, economic, political, demographic, and natural variables, as well as their changes (Taubenbock *et al.,* 2009). However, these implicit variables have not yet been sufficiently studied. While remote sensing has been widely used to study land use and environmental changes, its application in assessing kinship is unprecedented (Rahman, 2022). Researchers have not previously discussed implicit aspects such as kinship. This interpretation of satellite data will aid in understanding socioeconomic conditions, land fragmentation, and land loss, among others. Thus, this study focuses on remote sensing to detect kinship in rural Bangladesh based on agricultural land use. To achieve this, a more nuanced approach is required, identifying specific kinship-related factors that drive land fragmentation. Therefore, this research has major three key goals. These are (1) know the family structure of the study site; (2) map the agricultural land boundary according to *Mouza* Maps and finally; (3) identify driving forces those are responsible for agricultural plot size fragmentation.

Materials and Methods

Selection of the study area: Manikdi *Mouza* is situated in the *Gohalakanda* Union, Purbadhala Upazila, Netrokona District, Bangladesh. Geographically it is situated between 24º43´2´´N to 24º43´36´´N Latitude and 90º 35´33´´E to 90º36´14´´E Longitude. The *Kulla Mouza* no. 165 and *Telihati Mouza* no. 169 are located in the southern and eastern parts of the Manikdi *Mouza* respectively (Fig. 1).

The total population of Manikdi *Mouza* is 7,507. Manikdi *Mouza* of Netrokona district is known for its homogeneous floodplains and scattered waterbodies. Agricultural practices of the area are extensive with rice, jute, wheat, and vegetables among the most common.

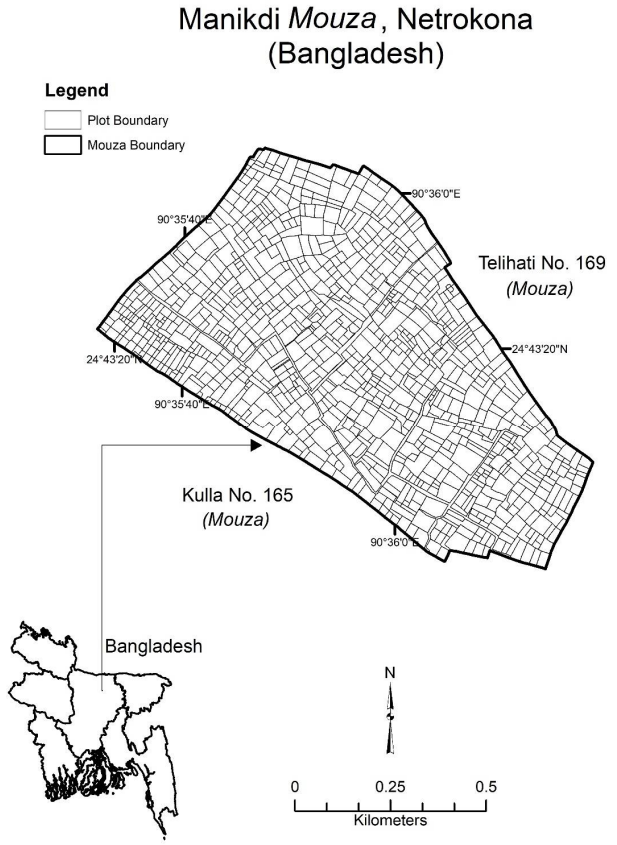

Fig. 1. The study area of Manikdi *Mouza*, Netrokona, Bangladesh.
Source: Compiled by authors, 2024 from CS, RS, and WorldView 3 satellite images.

Data sources: Primary data: To conduct this study, primary data were gathered from a variety of respondents through questionnaires and FGDs survey. Following is an explanation of the primary data gathering and requirements:

(a) Selection of local respondents: There are 370 questionnaires and 10 FGDs (each group consists of 7 to 8 respondents whereas male was 4 to 5 and female was 2 to 3) were conducted randomly with a 95% confidence level and 5% error margin for collecting data such as age, sex, education, earning sources or occupation, the total size of the family members, amount the of agricultural land acquired from the ancestor, the relationship among the family members, family status like combined or nuclear, driving forces that responsible for plot size fragmentation.

(b) KII: Key Informant Interviews (KIIs) were also conducted for data collection from the local experts and the Bangladesh Institute of Development Studies (BIDS) for identifying driving forces which are responsible for plot size fragmentation.

(c) Ground Control Points (GCPs): For accuracy assessment, Ground Control Points (GCPs) were used to geo-reference images and related *Mouza* maps like RS and CS. There are 9 GCPs were used for the datasets using the GPS survey.

(d) Error matrix was measured through GPS survey: There are 282 agricultural plots were surveyed for detecting error matrix.

Secondary data: In this study, secondary data were carefully collected from government as well as non-government organizations and used in figure 2. Listed below is a description of the secondary data collection:

(e) CS-1950 (Fig. 2a) and RS-1998 (Fig. 2b) *Mouza* maps were collected from DLRS (Department of Land Records and Surveys).

(f) The multispectral satellite image was collected through Maxar technologies, WorldView 3-November, 2023 (Fig-2c). The resolution of the image is 0.3m.

(g) Administrative/political maps were collected from the Center for Environmental and Geographic Information Services (CEGIS).

(h) Literature was reviewed from different national and international journals and books.

(i) Population data were collected from the Bangladesh Bureau of Statistics (BBS) in 2011.

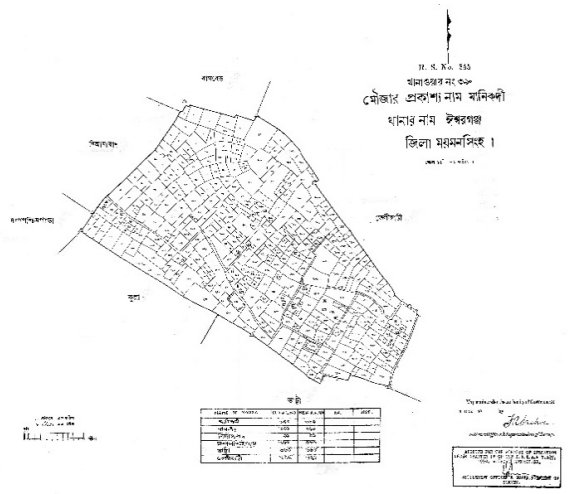

Fig. 2(a) Map made under the authority of government in 1909-1910 by settlement officer and superintendent of the survey which was adopted in 1950

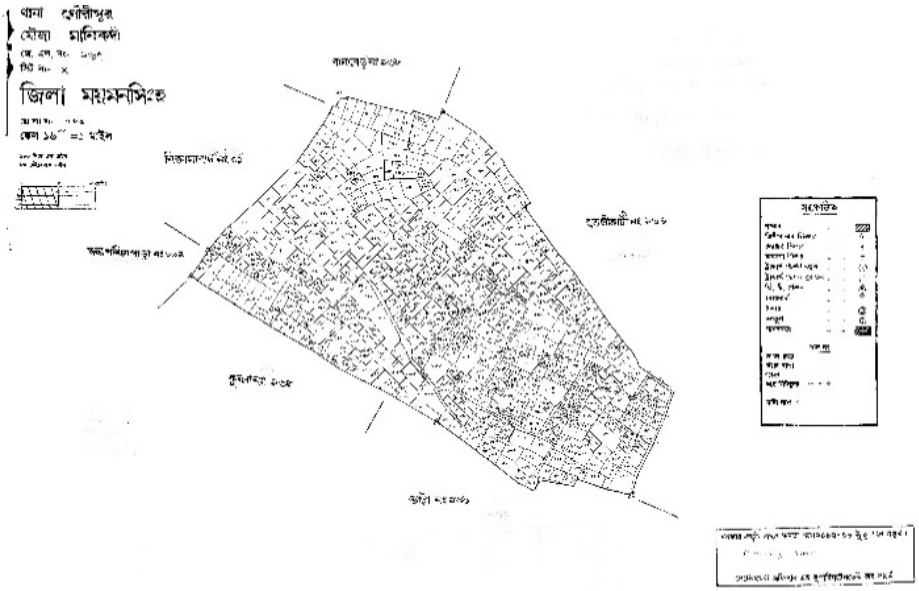

Fig. 2(b) Map made under the authority of government in 1984-1998 by settlement officer and superintendent of the survey which was adopted in 1998

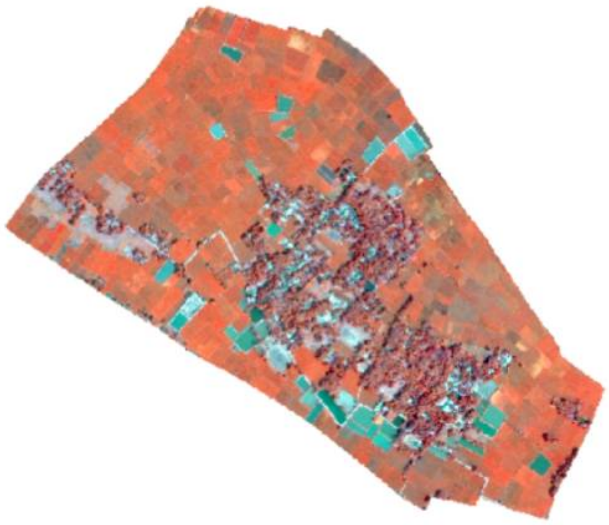

Fig. 2(c) Multispectral satellite imagery collected from Maxar technologies, WorldView 3; Nov, 2023, 0.3-meter resolution: Projection parameter: UTM N46

Fig. 2 (a-c). CS, RS, and Current WorldView-3 multispectral satellite imagery of the study area of Manikdi *Mouza*, Netrokona, Bangladesh.

Source: Compiled by authors, 2024 from CS, RS (collected from DLRS Bangladesh) and WorldView 3 satellite images.

Several methods were employed in this study to identify the relationship between plot size and family bonding. These methods include on-screen digitizing, multiple regression analysis, FCM (Fuzzy Cognitive Maps) and cluster analysis. Additionally, kappa statistics were utilized to measure the error matrix for nuclear and combined family data collected from agricultural plot boundaries in April 2024.

a. Georeferencing

Ground Control Points (GCPs) were collected through a field survey to georeference the CS and RS *Mouza* maps. The GCP data were processed and integrated into ArcGIS software for georeferencing purposes. Subsequently, the georeferenced maps were further adjusted using georeferencing tools to align with a WorldView satellite image, allowing for accurate plotting of boundaries.

b. On-screen digitizing

On-screen digitizing is an interactive technique used to generate vector data from previously scanned documents or raster information. In this study, the on-screen digitizing method was employed to digitize the CS map from 1950, the RS map from 1998, and satellite images from 2023, enabling the measurement of agricultural plot boundaries. Each digitized plot boundary is accompanied by metadata related to the landowners, including a unique plot number assigned to each plot on the map.

c. Cluster analysis

Cluster analysis is a statistical data processing technique that categorizes objects into clusters based on their degree of similarity. In this study, the hierarchical clustering algorithm was employed to analyze the fragmentation of agricultural plot sizes. Cluster analysis was utilized to identify similar groups within the dataset related to the parcelization of agricultural land.

d. Multiple regression model

According to Kutner, Nachtsheim, Neter, and Li (2005), the multiple regression model is expressed as: $Y = \beta0 + \beta1X1 + \beta2X2 + ... + \beta p*Xp + \varepsilon$ Where, Y = Dependent variable, X1, X2, ..., Xp = Independent variables, β0, β1, β2, ..., βp = Regression coefficients (parameters), and ε = Error term (representing the Y variance that could not be explained by the set of independent variables).

The coefficients β1, β2, ..., βp show how much the dependent variable changes when the corresponding independent variable changes by one unit, while all other independent variables stay the same. The intercept term, β0, is the value of the dependent variable when all the independent variables are zero. Multiple regression aims to estimate the regression coefficient values that best suit the observed data by minimizing the sum of the squared differences between the actual and anticipated values of Y based on the independent variables. Ordinary least squares (OLS) regression is commonly used for

this. Based on the values of the independent variables, the resulting model can be used to generate predictions about the value of the dependent variable.

e. *Kappa* statistics

In this study, the cross-validation method was used to validate data accuracy (Hussain *et al.,* 2022). Cross-validation was conducted through GPS Survey (Mishra *et al.,* 2020). From the evaluation samples, an error matrix was calculated. From the error matrix table, the producer's accuracy, user accuracy, overall accuracy, and the *Kappa* coefficient were calculated (Yesuph and Dagnew, 2019). The formula of Cohen's kappa coefficient (Hua, 2017): $K = \frac{PO - Pe}{1 \quad Pe}$, Where, *K*= Kappa Coefficient; *PO*= relative observed agreement among raters; and *Pe*= the hypothetical probability of chance agreement.

f. Fuzzy Cognitive Maps (FCMs)

In this study, the FCM was constructed to model the interactions between key factors influencing agricultural plot fragmentation. Each factor's influence was quantified through an adjacency matrix, where the weights w_{ij} indicate the strength and direction of influence from factor C_j to factor C_i. The activation values for each factor were updated iteratively using the equation$A_i^{(t+1)} - f\left(A_i^{(t)} + \sum_j^n w_{ij} . A_j^{(t)}\right)$, where f is a threshold function ensuring the activations remain within a standard range (Kosko, 1986). This iterative process continued until the system reached a stable state, where activation values indicated the relative influence of each factor on land fragmentation.

g. GIS, Remote sensing, and statistical tools

This study employed several software applications, including ArcGIS 10.8, IDRISI Silva, JMP Pro 16, and Microsoft Excel. ArcGIS 10.8 was utilized for primary data preparation and map composition. The transition probability matrix, which analyzes land use gains and losses from the CS *Mouza* map (1950) to the WorldView satellite image (2023), was examined using IDRISI Silva. JMP Pro 16 was used for cluster modeling and multiple regression analysis. Microsoft Excel facilitated attribute generation, data table creation, and tabular data management.

Results and Discussion

Agricultural plot boundaries can be accurately mapped with the use of remote sensing. Agricultural field identification and delineation is made possible through the use of remote sensing and imaging techniques (Wang *et al.,* 2022). The distribution of land in Bangladesh is determined by kinship relationships and cultural norms. Land may be

transferred and inherited in a variety of ways, including through ancestral systems (Wang *et al.*, 2022 and Tambiah, 1958). Therefore, land fragmentation techniques, such as the percelization and inheritance of agricultural plots within a family members, can be influenced by kinship as a significant social component (Tambiah, 1958; Yalcin and Gunay, 2016). Detailed findings and analysis are presented and discussed below:

*LULC changes from CS (1950) to the current year (*November, 2023*) with different dynamics:* This research investigates the use of geographic information system (GIS) and remote sensing techniques for mapping the percelization of agricultural land in order to ascertain the familial relationships among the family members. However, it also examines the use of GIS frameworks to precisely identify and map the physical boundaries of agricultural plots through the incorporation of high-resolution satellite images and field survey data. Figure 3 depicts the existing LULC divisions by area for the years 1950, 1998, and 2023. Comparative analysis of the shifting pattern of LULC revealed that the internal LULC categories diverged significantly. As a consequence, a massive transformation has been conceivable over the years as a result of one category LULC to others. The study was able to detect gain, loss, and net change for the three temporal periods 1950-1998, 1998-2023, and overall 1950-2023 by LULC category for a better understanding (Figure 3).

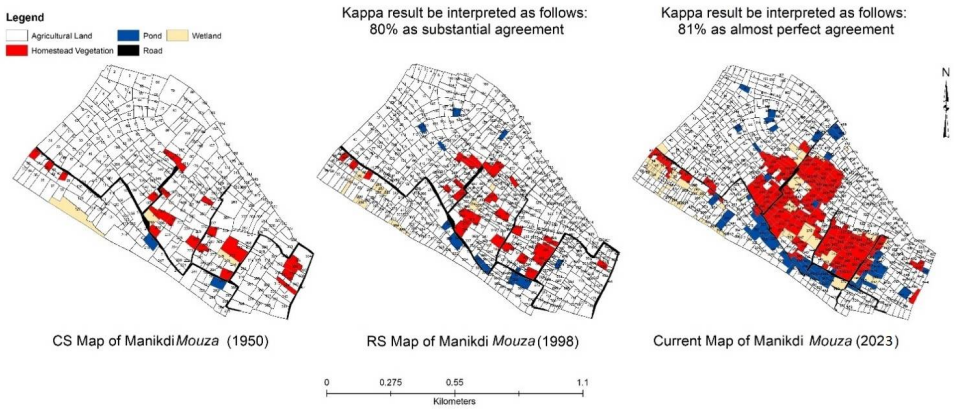

Fig. 3. Land use and land cover changes from CS (1950) to RS (1998) and RS to the Current Year (November, 2023) of Manikdi *Mouza*, Netrokona, Bangladesh.
Source: Compiled by authors, 2024 from CS, RS, and WorldView 3 satellite images.

A change area matrix was created for the aforementioned periods to examine the outcomes of land use/cover conversion. It displays the areas of change concerning other LULC categories during the specified periods. Figure 3 shows that agricultural land

dominates the entire research region, with homestead vegetation taking up the majority of the area throughout each of the three study periods.

Table 1. Transition probability matrix derived from the land use maps such as CS, RS, and Landsat TM multispectral satellite imageries in HSCZ during 1950–1998

Changing from	Probability of changing by RS (1998) to:					Subtotals	
CS (1950)	Agricultural land	Homestead vegetation	Pond	Road	Wetland	Total	Loss
Agricultural land	0.7366	0.1473	0.0597	0.0079	0.0486	1	0.2635
Homestead vegetation	0.0162	0.9224	0	0.0037	0.0577	1	0.0776
Pond	0.0553	0.004	0.7426	0.0283	0.1698	1	0.2574
Road	0.2983	0.0941	0.0839	0.5153	0.0085	1	0.4848
Wetland	0.2222	0	0	0	0.7778	1	0.2222
Total	1.3286	1.1678	0.8862	0.5552	1.0624		
Gain	0.592	0.2454	0.1436	0.0399	0.2846		

*** Halgurd-Sakran Core Zone (HSCZ) of the Manikdi *Mouza* in the Netrokona district, Bangladesh;
*** CS (Cadastral Survey), 1950 land survey system used to establish and maintain land records in Bangladesh;
*** RS, 1998- A land surveying method known as RS (Record of Rights Survey) is used to establish and keep records of land ownership and use; and
*** *Mouza* Boundary- Smallest administrative units of Bangladesh.
Source: Compiled by authors, 2024 using CS and RS *Mouza* boundary.

The probability matrix for significant LULC conversions for all classes in HSCZ that occurred between 1950 and 1998 is summarised in Table 1. While agricultural land has a chance of 73.66% in 1998 to continue to be agricultural land, the likelihood of conversion from agricultural land to homestead vegetation is 14.73%. Other fields like agricultural land to the pond, agricultural land to the road, and agricultural land to wetland transformation probability are 5.97%, 0.79%, and 4.86%.

Homestead vegetation has a 92.24% probability of remaining as homestead vegetation, a 1.62% chance of becoming agricultural land, a 0% chance of being a pond, a 0.37% chance of turning roads, and a 4.86% chance of becoming wetlands. In comparison to other categories, homestead vegetation is less likely to alter under the impact of population increase and homestead expansion from 1950 to 1998. Pond-to-pond conversion is 74.26% likely, compared to 5.53% for the pond to agricultural land, 0.4% for pond-to-homestead vegetation, 2.83% for pond-to-road, and 16.98% for pond-to-wetland. Road has undergone the most alteration between 1950 and 1998. Road has a 51.53% chance of still being a road, compared to 29.83% for a road to an agricultural field, 9.41% for a road to homestead vegetation, 8.39% for a road to a pond, and 0.85% for a road to a wetland. Less change was made to wetland at that time. Wetland remained

wetland 77.78% of the time, with transitions to agricultural land occurring just 22.22% of the time.

Table 2 shows the second scenario of transition probability from RS to WorldView 3 multispectral satellite imageries during 1998-2023. The classification categories remain the same as the scenario 1st from 1950-1998. For agricultural land, there is a 96.09% chance that it will continue to be unchanged. However, there is a 1.86% chance that it will be transformed into homestead vegetation, a 0.633% chance that it will become pond, a 0.51% chance that it will be road, and a 0.91% chance that it will become wetland.

The second least amount of change occurred on agricultural land among the various categorization groups. The likelihood that homestead vegetation will stay homestead vegetation is 71.37%, compared to the probabilities for homestead vegetation to be converted to agricultural land, ponds, roads, and wetland, which are all 0%. Pond categorization category had the least amount of change. Pond stayed a pond 96.48% of the time, changed into agricultural land 3.52%, changed into homestead vegetation 0%, changed into a road 0%, and changed into a wetland 0%.

Table 2. Transition probability matrix derived from the land use maps such as RS and WorldView 3 multispectral satellite imageries in HSCZ during 1998–2023.

Changing from	Probability of changing by the current year (2023) to:					Subtotals	
RS (1998)	Agricultural land	Homestead vegetation	Pond	Road	Wetland	Total	Loss
Agricultural land	0.9609	0.0186	0.0063	0.0051	0.0091	1	0.0391
Homestead vegetation	0.2634	0.7137	0	0.0228	0	1	0.2862
Pond	0.0352	0	0.9648	0	0	1	0.0352
Road	0.1744	0.0402	0.011	0.7743	0	1	0.2256
Wetland	0.5148	0.076	0	0.019	0.3902	1	0.6098
Total	1.9487	0.8485	0.9821	0.8212	0.3993		
Gain	0.9878	0.1348	0.0173	0.0469	0.0091		

*** Halgurd-Sakran Core Zone (HSCZ) of the Manikdi *Mouza* in the Netrokona district, Bangladesh; Source: Compiled by authors, 2024 using RS *Mouza* boundary and WorldView 3 multispectral satellite imageries.

Road retained road 77.43% while experiencing the second-highest shifting. Road conversions to agricultural land, homestead vegetation, ponds, and wetlands total 17.44%, 4.02%, 1.1%, 0.1%, and 1.1%, respectively. Wetland underwent the greatest

alteration of all for the final classification category. From 1950 to 1998, wetlands remained wetlands 39.02% of the time, but wetlands changed into agricultural land 51.48% of the time, the greatest likelihood of changing from wetlands to other classified categories. 7.6% of wetlands were converted to homestead vegetation, 0% to ponds, and 1.9% to roads. During the period, agricultural land had the biggest gains and wetlands saw the highest losses, which shows the intense pressure on land used for agriculture.

The spatial orientation of plot size boundaries changes over time: There are 1048 plots in total in November, 2023, and 684 of them are set aside for agriculture. Agricultural plot numbers grew from 1998 to 2023 from 646 to 684, with 299 plots fragmenting into 337 plots over this research period representing the nuclear family while 347 plots representing the united family stayed the same. The number of homestead vegetation plots was 20 in 1950; in 1998, it was broken into 31 plots, with 12 plots remaining the same as previously and 8 plots representing the nuclear family, adding 19 plots. The number of homestead vegetation plots rose from 187 in the previous research year (1998) to 215 between 1998 and 2023, with 28 plots remaining the same.

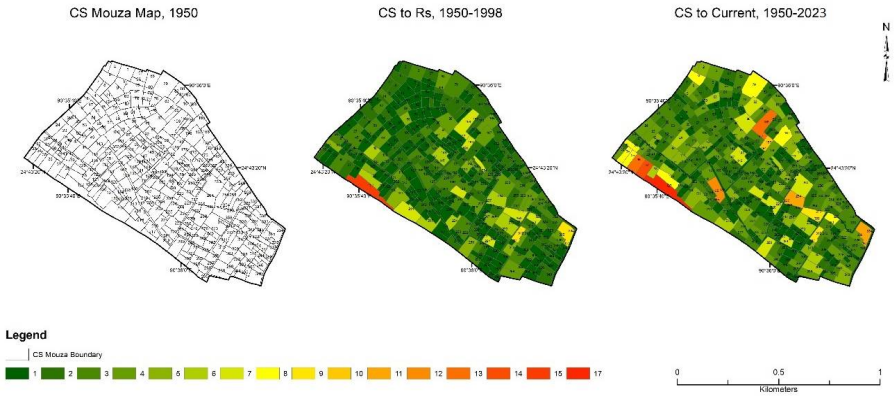

Fig. 4. The spatial orientation of plot size boundaries changes over time as family structures change from CS (1950) to RS (1998) and RS to Current Year (November, 2023) of Manikdi *Mouza*, Netrokona, Bangladesh.

Source: Compiled by authors, 2024 from CS, RS, and WorldView 3 satellite images.

Table 3. Identify the nuclear and combined family using CS, RS, and WorldView 3 multispectral satellite imageries during 1950–2023.

LULC/ Year	Total plot no- CS (1950)	Total plot no- RS (1998)	Nuclear family/LULC changes of plot numbers	No changes plot boundaries (RS-1998)	Total plot no. current (2023)	Nuclear family/LULC changes of plot numbers	No changes plot boundaries (Current-2023)
Agricultural land	327	646	471*	175**	684	337*	347**
Homestead vegetation	20	31	19*	12**	215	187*	28**
Pond	2	14	12	2	54	41	13
Road	7	7	3	4	8	6	2
Wetland	3	21	20	1	87	73	14
Total Plot No	359	719		194	1048		404

* Nuclear family in the Manikdi *Mouza*, Netrokona, Bangladesh from CS to the Current year of November, 2023; and

** Combined family in the Manikdi *Mouza*, Netrokona, Bangladesh from CS to the Current year of November, 2023.

Source: Compiled by authors, 2024 from CS, RS, and WorldView 3 satellite images.

Table 3 shows the total number of plots and how they were divided into nuclear and combined family groups over this study period. According to the CS map, there were 359 total plots in 1950. By combining the various categorization types of agricultural land, homestead vegetation, pond, road, and wetland, it fragmented into a total 719 number of plots. The two categorization groups with the greatest representation are agricultural land and homestead vegetation. The fragmentation of the entire plot number is shown by the fact that the overall plot number rose to 719 in 1998 from 359. According to this research, the number of agricultural plots expanded from 327 to 646 throughout the study period, while 175 plots stayed the same as they were in 1950, representing the combined family, and 152 agricultural plots are divided into 471 plots, which indicates the nuclear family.

Cluster analysis for plot size fragmentation: Cluster analysis is a statistical method for determining subsets of a dataset which have characteristics such as a high degree of similarity or close physical proximity. The use of cluster analysis allows for an investigation of temporal and spatial trends in the distribution of plot boundaries with the changes of family ties. Figure 5 displays the cluster analysis for plot size fragmentation over the research period. This diagram shows three clusters of plot fragmentation. Cluster 1 represents a plot that has been divided into 1-6 plots. Cluster 2 depicts the division of a plot into 7–12 plots, whereas Cluster 3 shows the division of a plot into 13–18 plots.

From CS until the present, there were a total of 359 plots, which were divided into 1,048 plots. Of them, 219 plots are part of Cluster 1, 37 plots are part of Cluster 2, and 103 plots are part of Cluster 3.

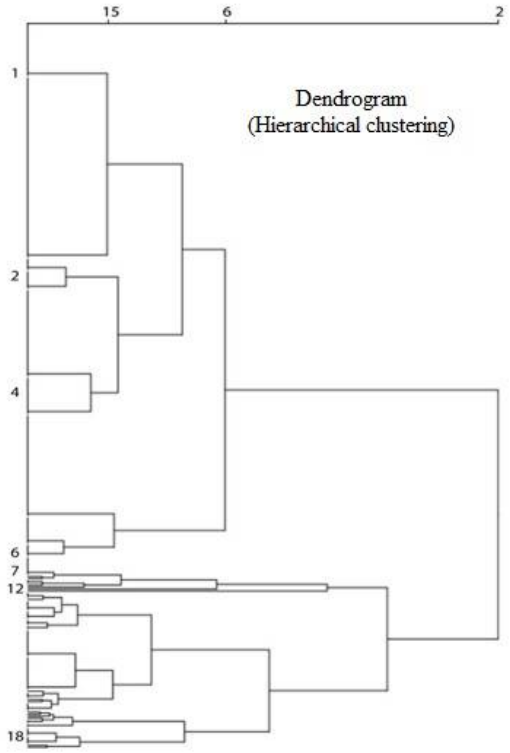

Fig. 5. Cluster analysis (Hierarchical clustering) for plot size fragmentation from 1950-2023. Source: Made by authors, 2024 from CS, RS, and WorldView 3 satellite images.

Driving forces that are responsible for agricultural plot size fragmentation using multiple regression model

Scenario-1: CS to RS (1950-1998)

There are a number of forces that directly influence parcelization of land. From 1950 to 1998, the primary propelling forces were economic development, demographic factors, social structure, resource scarcity, and land tenure systems. In this case, economic development plays the leading role, while demographic factors also play a significant role in land valuation. As the population development rate was high during that time period, particularly after independence, the rate of land fragmentation was also high. Social

structure also influenced the fragmentation of the narrative. The tendency toward nuclear families determines the size of plots. With 12% and 8%, resource scarcity and land price systems play a less significant role.

Table 4. Driving factors for changing of land ownership between combined family to nuclear family from 1950-1998.

Contributing/influencing factors for changing of land ownership between combined family to nuclear family	Percentage according to multiple regression models
Economic development	35%
Demographic factors	25%
Social structure	20%
Resource scarcity	12%
Land tenure systems	8%

Source: Made by authors, 2024 using multiple regression models

Combined to Nuclear= 0.35Ed+0.25Df+0.20Ss+0.12Rs+0.8Lt

Here, Ed=Economic development, Df= Demographic factors, Ss=Social Structure, Rs=Resource scarcity and Lt=Land tenure systems

Scenario- 2: RS to Current (1998-2023)

For 2nd scenario, economic development, demographic factors, technological innovation, urbanization, land tenure systems, and resource scarcity are the main controlling factors of percelization of land. From 1998 to 2023, over 23 years, economic development and demographic factors influence the land fragmentation most having 40% and 30% contribution respectively.

Table 5. Driving factors for changing of land ownership between combined family to nuclear family from 1998 to 2023.

Contributing/influencing factors for changing of land ownership between combined family to nuclear family	Percentage according to multiple regression models
Economic development	40%
Demographic factors	30%
Technological innovation	15%
Urbanization	10%
Land tenure systems	3%
Resource scarcity	2%

Source: Made by authors, 2024 using multiple regression models

Combined to Nuclear= 0.40Ed+0.30Df+0.15Ti+0.10U+0.03Lt+0.02Rs

Here, Ed= Economic development, Df= Demographic Factors, Ti= Technological innovation, U= Urbanization, Lt= Land tenure systems and Rs=Resource scarcity

From CS to RS (1950-1998), the percentage of factors influencing the shift from combined to nuclear family land ownership found that economic development, demographic factors, and social structure were the most influential, while resource scarcity and land tenure systems had a relatively smaller impact.

The percentage change from RS to Current (1998-2023) shows that technological innovation and urbanization are the most important factors influencing the shift from combined to nuclear family land ownership. Resource scarcity and land ownership structures play a smaller role in this model.

FCM analysis

The FCM analysis highlights that economic development, with an activation value of 0.40, is the most influential driver of agricultural plot fragmentation, reflecting the strong role economic progress plays in driving land division. As economic growth increased land value, families divided their landholdings to capitalize on these rising values, marking economic development as the central force in plot fragmentation. Demographic factors, at 0.30, significantly contribute by intensifying land subdivision due to rapid population growth, particularly after Bangladesh's independence, which led to larger plots being split among more people. Social structure, with a value of 0.20, also plays an essential role, as the shift toward nuclear families increased the demand for individual landholdings, accelerating fragmentation. Technological innovation (0.15) and urbanization (0.10) add to this trend, with advancements in technology making smaller plots manageable and urban expansion pressuring rural areas. While resource scarcity (0.02) and land tenure systems (0.03) have lesser weights, they impose constraints that indirectly reinforce land division trends. Together, these factors underscore the cumulative impact of economic, demographic, social, and technological forces in reshaping agricultural land ownership in Bangladesh.

The discussion focuses on interpreting the results of this study, which analyzed land use and land cover (LULC) changes in Manikdi *Mouza*, Netrokona, Bangladesh, over the period from 1950 to 2023. Using remote sensing and GIS techniques, the analysis sheds light on the influence of family structures such as nuclear and combined families on

agricultural land parcelization. The significant LULC transformations observed suggest that cultural shifts and evolving family dynamics have played a critical role in shaping

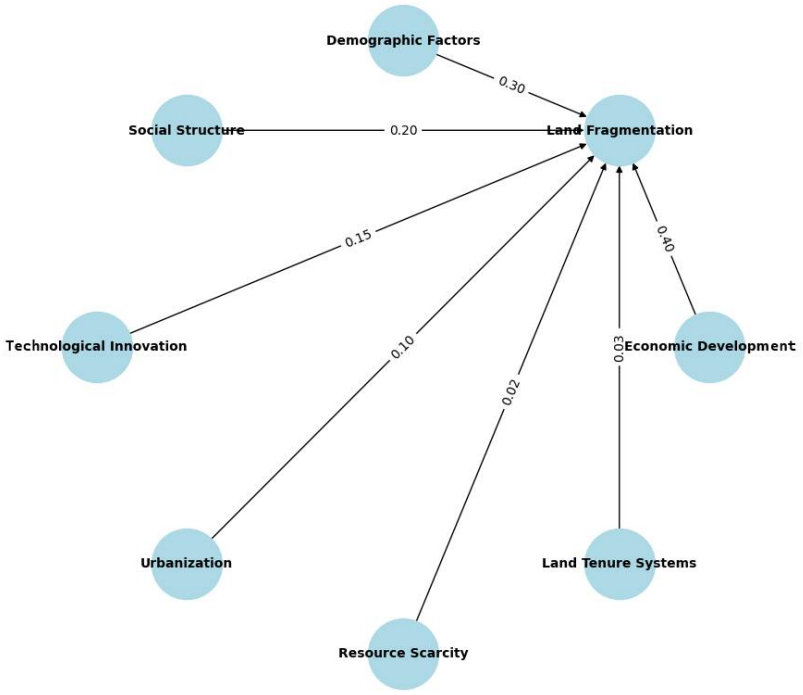

Fig. 6. The Fuzzy Cognitive Map (FCM) analysis using different driving forces that influences plot size fragmentation from 1950-2023.
Source: Made by authors, 2024 from surveyed data.

land fragmentation trends. These findings are examined in the broader context of rural development, economic impacts, and potential policy interventions to address the consequences of increasing land parcelization. The most significant changes were agricultural land and homestead vegetation. Agricultural land increased from 327 plots in 1950 to 646 plots in 1998 and further to 684 plots in 2023. Among these, 471 plots were fragmented into smaller plots representing nuclear families, while 175 plots remained unchanged and were associated with combined family units. By 2023, 337 of the total agricultural plots were associated with nuclear families, while 347 plots remained unchanged. Homestead vegetation, which initially consisted of only 20 plots in 1950, saw an increase to 31 plots in 1998, with 19 of these being associated with nuclear family units and 12 remaining unchanged. By 2023, homestead vegetation expanded

dramatically to 215 plots, of which 187 represented nuclear family plots, leaving only 28 unchanged. The trend of land fragmentation in ponds, roads, and wetlands was also notable. Ponds expanded from just 2 plots in 1950 to 14 in 1998, and then to 54 plots by 2023, with the majority of this change attributed to nuclear family land use. Wetlands saw an even greater shift, increasing from 3 plots in 1950 to 21 in 1998, and then to 87 plots by 2023. Much of the wetland fragmentation occurred in nuclear family structures, with a significant portion of wetlands being repurposed for agricultural use. In total, the number of plots increased from 359 in 1950 to 1048 in 2023. This reflects the broader trend of land parcelization in Manikdi *Mouza*, as nuclear families sought to divide ancestral land among family members, leading to a significant increase in the number of plots, particularly in agricultural and homestead categories. The increase in nuclear family plots indicates the growing trend of land fragmentation in response to evolving family structures, with a shift from large, combined family landholdings to smaller, more fragmented parcels.

The multiple regression model reveals that from 1950 to 1998, economic development (35%), demographic factors (25%), and social structure (20%) were primary drivers of agricultural plot fragmentation, with resource scarcity (12%) and land tenure (8%) playing smaller roles. From 1998 to 2023, economic and demographic factors remained influential, while technological innovation (15%) and urbanization (10%) gained prominence. The FCM analysis corroborates these findings, highlighting economic (0.40) and demographic (0.30) factors as central, with social structure (0.20) and technology (0.15) reinforcing land fragmentation trends.

The spatial analysis demonstrates how kinship and cultural practices directly influence land use patterns, as seen in the breakdown of agricultural plots and homestead vegetation over time. This research highlights the significant socio-cultural factors driving land fragmentation and the implications this has for agricultural productivity, land management, and rural development in the region. The continued parcelization of land poses challenges for sustainable land use, particularly in maintaining agricultural productivity and addressing the increasing pressure on natural resources.

Accuracy Assessment/Validation: To evaluate the classification's accuracy, each LULC map was compared to reference data. Using ERDAS Imagine 9.1 software, a GPS field survey was used as ground truth data to confirm the categorization accuracy. The accuracy assessment process is a particularly effective approach to portray accuracy since it identifies the accuracies of each category as well as any inclusion- and exclusion-related mistakes (commission errors and omission errors) that may have occurred during

the classification (Congalton, 1991). The image from 1950 and 1998 was found to have an overall accuracy of 85.98% and 82.13%, respectively, with matching kappa coefficients of 0.84 and 0.86. Both the accuracy of the producer and the user were over 82%.

Table 6. User's accuracy, producer accuracy, overall accuracy, and kappa statistics for Nuclear and Combined family from agricultural plot boundary, 2023.

Features	CS in 1950		RS in 1998		Current year-2023	
	User's accuracy	Producer's accuracy	User's accuracy	Producer's accuracy	User's accuracy	Producer's accuracy
Nuclear family	85.00%	81.73%	80.00%	83.33%	91.11%	95.35%
Combined family	82.00%	85.42%	85.00%	86.73%	92.22%	90.22%
Overall accuracy	85.98%		82.13%		89.52%	
Kappa statistics	84.90%		86.37%		82.50%	

Source: Compiled by authors, 2024 using Kappa statistics

Implications

This research introduces a novel cultural perspective on remote sensing by examining kinship detection and its impact on rural land use in Bangladesh, offering significant insights for local governance and national policies. By identifying familial connections, kinship detection can enhance various policy areas, including social welfare programs by validating family ties for benefit distribution, inheritance rights by clarifying family claims to prevent disputes, and public health by understanding genetic disease patterns. Additionally, it can support disaster response by reconnecting separated family members, inform socio-economic policies on wealth distribution and social mobility linked to familial land fragmentation, and improve census accuracy by identifying kin-based land use and hidden households in rural areas. The study suggests that integrating kinship detection with remote sensing can drive advancements in socio-economic policy, public health, and disaster management, expanding the applications of remote sensing in cultural studies.

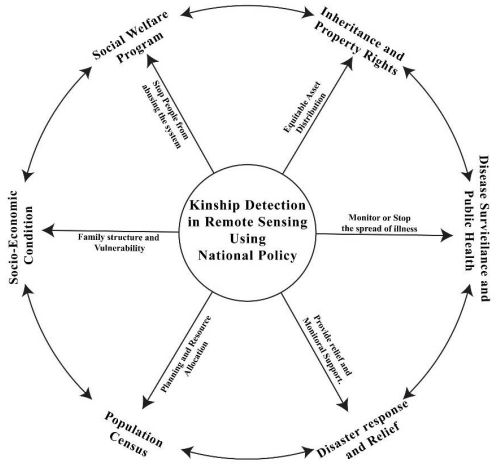

Fig. 7. Implications of kinship detection using remote sensing can indeed play a vital role in national policy in a number of ways.
Source: Made by authors, 2024 from KII, questionnaire survey and FGDs.

Conclusion

Land cover can be interpreted both implicitly and explicitly using remote sensing data. Through the use of remote sensing data, this study identifies the implicit aspect of kinship. From CS to RS, the rate of land parcelization was 73.02%, but from RS to the present day, it has decreased to 61.45%. High percelization of land from CS to RS indicates that the number of nuclear families increased between 1950 and 1998, despite the influence of population growth and economic development during this time period. Due to an increase in population, the agricultural land boundary changed significantly from CS to RS and then from RS to the present. Technical innovation and urbanisation were added to these factors, which essentially represent the kinship of Manikdi Mauza.

Acknowledgment

I'd like to thank the local community of Manikdi *Mouza* for contributing their time for interviews on agricultural land fragmentation, the Bangladesh Bureau of Statistics (BBS) for providing census data, and the Centre for Environmental and Geographic Information Systems (CEGIS) for various datasets. Additionally, I am grateful to Jahangirnagar University for providing the funds necessary to conduct this study. I would like to express my gratitude to Dr. Mohd. Shamsul Alam, Professor, Department of Geography

and Environment, Jahangirnagar University, Bangladesh, for his helpful advice in conducting the research successfully.

References

Abdullah, A. 1976. Land reform and agrarian change in Bangladesh. The Bangladesh Development Studies, 4(1): 67-114.

Bangladesh Bureau of Statistics. 2011. Population and housing census 2011. http:// 203.112. 218.66/WebTestApplication/userfiles/Image/BBS/Socio_Economic.pdf

Congalton, R.G. 1991. A review of assessing the accuracy of classifications of remotely sensed data. *Remote Sens. Environ.* 37(1): 35-46. https://doi:10.1016/0034-4257(91)90048-b.

Dister, S., L. Beck, B. Wood, R. Falco and D. Fish. 1993. The use of GIS and remote sensing technologies in a landscape approach to the study of Lyme disease transmission risk. *Proceedings of GIS*, **93**: 15-18.

Hassan, M.M. 2017. Monitoring land use/land cover change, urban growth dynamics and landscape pattern analysis in five fastest urbanized cities in Bangladesh. *Remote Sensing Applications: Soc. Environ.* **7**: 69-83.

Hua, A.K. 2017. Application of CA-Markov model and land use/land cover changes in Malacca river watershed, Malaysia. *Appl. Ecol. Environ. Res.*, **15**(4), 605-622. https://doi.org/10.15666/aeer/1504_605622

Hussain, S., L. Lu, M. Mubeen, W. Nasim, S. Karuppannan, S. Fahad, A. Tariq, B.G. Mousa, F. Mumtaz and M. Aslam. 2022. Spatiotemporal Variation in Land Use Land Cover in the Response to Local Climate Change Using Multispectral Remote Sensing Data. *Land*, **11**(5): https://doi.org/10.3390/land11050595

Kosko, B. 1986. Fuzzy cognitive maps. *International Journal of Man-Machine Studies*, **24**(1): 65-75. https://doi.org/10.1016/s0020-7373(86)80040-2

Kutner, M. H., C.J. Nachtsheim, J. Neter and W. Li. 2005. *Applied Linear Statistical Models* (5th ed.). McGraw-Hill.

Mishra, P.K., A. Rai and S.C. Rai 2020. Land use and land cover change detection using geospatial techniques in the Sikkim Himalaya, India. *Egyptian Journal of Remote Sensing and Space Science*, **23**(2): 133-143. https://doi.org/10.1016/j.ejrs.2019.02.001

Mollah, T.H., M.A. Habib, M. Tahsin, N. Mollah, M.M.M. Aunkur, M. Ferdous and S.R. Shefa. 2023. Changes in agricultural crop suits and landscape: A time-series study using multispectral imageries from rural Bangladesh. *J. Asiat. Soc. Bangladesh, Sci.* **49**(1): 85-100. https://doi.org/10.3329/jasbs.v49i1.67598

National Research Council. 1998. *People and pixels: Linking remote sensing and social science.* National Academies Press.

Rahman, A., R. Ali, S.N. Kabir, M. Rahman, R. Al Mamun and A. Hossen. 2020. Agricultural mechanization in Bangladesh: Status and challenges towards achieving the sustainable development goals (SDGs). *AMA, Agricultural Mechanization in Asia, Africa and Latin America*, **51**(4): 106-120.

Rahman, M.H. 2022. A study on determining land use/land cover changes in Dhaka over the last 20 years and observing the impact of population growth on land use/land cover using remote sensing. *Malaysian J. Civil Engineering* **34**(2)*:* 1-9. https://doi.org/10.11113/ mjce.v34.17812

Siddik, M.A., M.A. Rahman and M.A. Rahman. 2022. Causes and impacts of rural land fragmentation in the coastal belt of Bangladesh. *Indonesian J. Geography*, **54**(2): 206-212. https://doi.org/10.22146/ijg.67314

Tambiah, S.J. 1958. The Structure of Kinship and its Relationship to Land Possession and Residence in Pata Dumbara, Central Ceylon. *The Journal of the Royal Anthropological Institute of Great Britain and Ireland* **88**(1): 21. https://doi.org/10.2307/2844073

Taubenbock, H., M. Wurm, N. Setiadi, N. Gebert, A. Roth, G. Strunz, J. Birkmann, and S. Dech. 2009. Integrating remote sensing and social science. *2009 Joint Urban Remote Sensing Event*. https://doi.org/10.1109/urs.2009.5137506

The Muslim Family Laws Ordinance, 1961 (Ordinance NO. VIII OF 1961). http://bdlaws.minlaw.gov.bd/act-305.html

Turner, B.L.I.I. 1998. Frontiers of Exploration: Remote Sensing and Social Science Research. In *Pecora 13 Symposium, Human interaction with theEnvironment: Perspectives from Space (August 20-22, 1996, Souix Falls, SD)* pp. 15-19.

Van schendel, W. and M. Rahman. 1997. Gender and the inheritance of land: Living law in Bangladesh. In *The village in Asia revisited* pp. 237-276.

Walker, B.H. 1994. Landscape to regional-scale responses of terrestrial ecosystems to global change. *Ambio (Journal of the Human Environment, Research and Management); (Sweden)*, **23**(1).

Wang, M., J. Wang, Y. Cui, J. Liu and L. Chen. 2022. Agricultural Field Boundary Delineation with Satellite Image Segmentation for High-Resolution Crop Mapping: A Case Study of Rice Paddy. *Agronomy*, **12**(10): 2342. https://doi.org/10.3390/agronomy12102342

Wood, G.D. 1981. Rural class formation in Bangladesh, 1940–1980. *Bulletin of Concerned Asian Scholars*, **13**(4): 2-17.

Yalcin, H. and B. Gunay. 2016. Delineation of parcels in agricultural lands in remote sensing. *2016 Fifth International Conference on Agro-Geoinformatics (Agro-Geoinformatics)*. https:// doi.org/ 10.1109/agro-geoinformatics.2016.7577601

Yesuph, A.Y. and A.B. Dagnew. 2019. Land use / cover spatiotemporal dynamics , driving forces and implications at the Beshillo catchment of the Blue Nile Basin , North Eastern Highlands of Ethiopia. *Environmental Systems Research*. https://doi.org/10.1186/s40068-019-0148-y.

(Revised copy received on 07/12/2024)

J. Asiat. Soc. Bangladesh, Sci. **51**(1): 73-86, June 2025
DOI: http://doi.org/10:3329/jasbs.v51i1.82792

COMPARATIVE EFFECTS OF SOME ORGANIC AMENDMENTS ON ACIDIC SANDY LOAM SOIL: *IN VITRO* STUDY

RAZIA SULTANA SHAKY[1,2] AND SABRINA SHARMEEN ALAM[1*]
[1]*Department of Soil Science, University of Chittagong, Chattogram-4331, Bangladesh.*
[2]*Ondokuz Mayıs University, Faculty of Agriculture, Department of Soil Science and Plant Nutrition, Samsun, Turkey.*

Abstract

An incubation study was conducted to investigate the effects of four organic amendments (e.g., banana peel, BP; eggshell, ES; tea waste, TW; and vermicompost, VC) on chemical properties of an acidic sandy loam soil. Three incubation periods *viz.* 38, 120, and 240 days (d) and two rates, e.g., 4% and 8% (w/w) of amendments with three replicates were considered. Amendments and incubation time had significant impacts on soil chemical properties. It was revealed that soil pH, EC, OC, TN, extractable P, K, Ca, Mg, Fe, Cu, Mn, and Zn were increased in most of the amended soils. However, ES had no impact on TN and K. Moreover, it decreased micro-nutrients concentrations. BP and TW had no impact on Ca and Cu, respectively. Soil pH raised (> 8.0) in ES and BP amended soils. Highest OC was recorded in VC and TW amended soils. Highest EC, P, Mg, and micronutrients, except Fe, was recorded in VC amended soils. Both K and Fe was highest in BP; and Ca was highest in ES amended soils. Overall, soil pH, OC, TN, extractable K, Mg, Cu, and Mn significantly reduced with incubation time. In contrast, soil EC, extractable P, Fe, and Zn increased.

Key words: Sandy loam soil, Incubation, Organic amendments, Cost-effective, Extractable nutrients, Bangladesh.

Introduction

Sandy loam soils are poorly fertile soils because of low moisture, low organic matter and poor nutrients content. These soils occupy mostly the southeastern parts of Bangladesh (Huq and Shoaib, 2013). Not only in Bangladesh, in many regions of the world, the marginal and nutrient-deteriorated soils are often used for crop production only after large quantities of chemical fertilizers are applied (Manyanga *et al.*, 2024). Suitability of sandy loam soils for crop cultivation become even worse when they are acidic. In Bangladesh, satisfying food demand for a large population is challenging while land resources are very limited. Soil fertility is declining day by day due to extreme utilization

*Corresponding author: ssalam@cu.ac.bd

of artificial fertilizers without paying much attention to soil health. Therefore, it is urgent to nourish the poorly fertile soils in a way that will protect them from any sorts of degradation. Use of eco-friendly organic amendments (OAs) could be the solution in this regard. Application of OAs to infertile soils could bring suitable physical, chemical, and biological conditions for crop production if are provided in a rational way. In this *in vitro* study, four cost-effective, easily available, and environment-friendly organic amendments e.g., banana peel (BP), eggshell (ES), tea waste (TW), and vermicompost (VC), were selected for organically modification of an acidic sandy loam soil, collected from Chittagong University campus.

Previously, many studies showed that OAs, often with chemical fertilizers, were efficient in improving soil reaction (Candemir and Gülser 2011); and other chemical properties (Ch'Ng *et al.*, 2014; Chen *et al.*, 2018; Anwar *et al.*, 2018). The BP, ES, and TW are relatively new soil modifiers that have been used recently, while VC has been widely used over few decades. Literatures on the effects of BP, ES, and TW on soil properties seemed to be very limited. However, research showed that BP wastes and its biochar was effective in improving soil bio-chemical properties (Sial *et al.*, 2019a). Banana wastes could also reduce heavy metals like Cd, Pb, and Cu in contaminated soil (Wedayani *et al.*, 2024). The ES powder was effective in treating acid mine drainage effluents and increased soil pH and basic cations (Luo *et al.*, 2018; Muliwa *et al.*, 2018; Mahajabin *et al.*, 2019). It also effectively reduced heavy metals in soils (Ok *et al.*, 2011a; Almaroai *et al.*, 2014). Toxic metals uptake was reduced by TW-biochar application (Peiris *et al.*, 2022). The VC amended soils showed increases in OM, TN, pH, EC, available P, K, Ca and Mg but decreases in DTPA-extractable metals (Angelova *et al.*, 2013). Again, soil pH, OC, N, available P, and micronutrients increased with VC application rate in drylands of Ethiopia (Teka *et al.*, 2024; Terefe *et al.*, 2024). Overall, crops grown under organic farming system contained more nutritional values than crops grown in artificially fertilized soils (Mi *et al.*, 2018; Hernandez *et al.*, 2021).

Amendment's effects on soil depends on amendment type, its application dose, characteristics of soil treated, and incubation time. Due to chemical compositional variability in OAs, it is unrealistic that amendments used in the present study would have similar impact on soil chemical properties. Hence, to obtain desired soil characteristics for crop production, proper selection of OAs is important. In this study, we used different organic materials for soil amendment to compare their impacts on a locally present sandy loam soil. We hypothesized that application of OAs to such soil could have positive impacts on chemical soil properties. Therefore, the objectives of this study were: i) to assess the characteristics of OAs, ii) to compare the effects of OAs on soil pH, EC, OC,

TN, and extractable macro- and micro-nutrients, and iii) to observe the effects of incubation time on selected soil properties.

Materials and Methods

Materials description: Dried pieces of ripen banana peel (BP), poultry eggshell (ES), and tea waste (TW) was ground by a grinder machine to get powder form; however, cow-dung derived vermicompost (VC) was used in its original but air-dried condition. OAs were passed via a 2 mm sieve before storage. Sandy loam soil was collected from mineral horizon (0-15 cm) of a field at Chittagong University campus (22°46′N; 91°78′E), Bangladesh. Soil was developed under tropical climatic conditions with 1551 mm mean annual precipitation and 26°C mean annual temperature. This soil belongs to 'Brown Hill soils' (FAO/UNDP, 1988). World Reference Base (WRB) classified these type of soils as Dystric Cambisols, Haplic and Ferric Alisols. Soil was disintegrated, air-dried, and passed via a 2 mm sieve. The OAs and initial sandy loam soil were investigated for several parameters (Table 1).

Experimental design: A 240 d incubation study was conducted on sandy loam soil under controlled condition at ~25°C. Experimental design was randomized complete block (RCB) with 9 treatments, 3 replications, and 3 incubation time. Treatments were control (unamended soil), BP4% (banana peel 4%), BP8% (banana peel 8%), ES4% (eggshell 4%), ES8% (eggshell 8%), TW4% (tea waste 4%), TW8% (tea waste 8%), VC4% (vermicompost 4%), and VC8% (vermicompost 8%). Exactly, 315 g soil (dry weight) was mixed with each treatment on a clean tray before transferring to 500 mL plastic jars with perforated lids. Field capacity of soil was maintained with distilled water throughout the study. At 38, 120, and 240 d soil samples were taken out from jars (27 ×3 = 81 jars) for air-drying. Soils that were not analyzed immediately, were kept in refrigerator.

Laboratory analyses: OAs were scanned via wavelength dispersive X-ray fluorescence (XRF) spectrometer (Rigaku ZSX Primus IV) for rapid investigation of elements (Musa *et al.,* 2021). XRF showed high efficiency in nutrients analyses in many OAs and composts (López-Núñez 2022). Particle size distribution was analyzed following hydrometer method. Soils were investigated for pH, EC, OC, TN, extractable P, Ca, Mg, K, Fe, Cu, Mn, and Zn. pH of soil:water suspension (1:2.5, w/v) and of amendment:water suspension (1:10, w/v) was measured by digital pH meter (Adwa, AD1020). EC (using suspension of 1:5 soil:water (w/v), and 1:10 amendment:water (w/v)) was measured by portable EC meter (Adwa, AD330). The OC was determined followed by wet-oxidation method (Walkley and Black 1934). The TN was determined followed by micro-Kjeldahl

digestion and distillation. Extractable P determination followed Bray & Kurtz extraction (Bray and Kurtz 1945), and ascorbic acid blue color method (Murphy and Riley, 1962). Samples were extracted with 1 N NH_4OAC at pH 7.0 for Ca, Mg, and K; and with DTPA for Fe, Cu, Mn and Zn measurement. Concentrations of elements in extracts were determined by Shimadzu AA-7000® atomic absorption spectrophotometer (AAS).

Table 1. Characteristics of the OAs and initial soil used in the present study.

Characteristics	BP	ES	TW	VC	Initial soil
Minerals identified by XRD	-	-	-	-	Quartz, albite, muscovite
Sand (%), Silt (%), Clay (%)	-	-	-	-	69, 15, 16
Moisture (%)	7.4	0.5	4.6	8.25	2.0
$pH_{(in\ water)}$	8.8	8.5	5.3	6.5	4.85
EC (dS m^{-1})	7.38	0.30	1.08	3.79	0.103
OC (%)	24.2	1.28	20.43	9.08	0.39
Total N (%)	1.34	0.12	1.4	0.95	0.02
Total P (g kg^{-1})	11.6	1.86	17.5	17.6	-
Total K (g kg^{-1})	580	1.0	129	83.2	-
Total Ca (g kg^{-1})	88.1	691	265	68.7	-
Total Mg (g kg^{-1})	14.6	4.16	26.8	19.0	-
Total Fe (g kg^{-1})	10.9	0.29	30.7	139	-
Total Cu (g kg^{-1})	ND	ND	3.19	0.44	-
Total Mn (g kg^{-1})	9.14	ND	60.8	12.5	-
Total Zn (g kg^{-1})	2.68	ND	5.74	2.22	-
Extractable P (mg kg^{-1})	-	-	-	-	6
Extractable K (mg kg^{-1})	-	-	-	-	35
Extractable Ca (mg kg^{-1})	-	-	-	-	122
Extractable Mg (mg kg^{-1})	-	-	-	-	65
Extractable Fe (mg kg^{-1})	-	-	-	-	38
Extractable Cu (mg kg^{-1})	-	-	-	-	0.32
Extractable Mn (mg kg^{-1})	-	-	-	-	9.3
Extractable Zn (mg kg^{-1})	-	-	-	-	1.3

Note. Elements that were beyond detection limit by XRF were indicated as ND i.e., Not detected.

Statistical analysis: Data were analyzed using SAS software version 9.4 and Microsoft Excel 2010. A two-way Analysis of Variance (ANOVA) was performed to test effects of treatments and incubation times on soil properties. Treatment and incubation time means was considered statistically significant at $P < 0.05$, according to Tukey's test.

Results and Discussion

Soil pH, EC, OC and TN: Amendments, incubation time, and their interaction had significant influence on soil pH, EC, OC and TN (Table 2). Overall, OAs increased soil pH, EC, OC and TN compared to control, except ES, which had no impact on TN (Table 2). The extent of increment depended on amendment type and application rate. Highest value was obtained with highest rate. Soil parameters increased because OAs were higher in pH, EC, OC, and TN than that of initial soil (Table 1). The BP and ES increased soil pH up to 8.5 similar to previous study (Ashrafi *et al.,* 2015). High pH could be due to high to medium K, Ca, and Mg in BP; and extremely high Ca in ES (Table 1). BP and ES was thus efficient in ameliorating soil acidity (Zhang *et al.,* 2023; Gurmessa 2021; Luo *et al.,* 2018). Despite having a pH 6.5, and considerable quantities of Ca and Mg in VC, it did not increase soil pH to that extent. The presence of high-soluble salts in VC could depress soil pH (Naramabuye and Haynes 2006) but remarkably increased soil EC (Demir 2019). EC in amended soils (except BP8%) didn't surpass critical limit of 4 dS m^{-1}, which is in agreement with others (Angelova *et al.,* 2013; González *et al.,* 2010; Demir 2019). High EC in BP amended soils could be due to presence of high total K in BP. Overall, OC content was almost similar among the amended soils, except ES treated soil (Table 2). However, at least 2% OC (a major threshold for soil OC) was maintained in TW and VC amended soils at higher application rate (Ouda and Mahadeen 2008; Teka *et al.,* 2024). As expected, highest TN in TW amended soils was due to highest TN in TW (Candemir and Gülser 2011). Increased OC resulted in increased TN content (Angelova *et al.,* 2013; Demir 2019).

Overall, soil pH, OC, and TN was significantly decreased but EC increased during incubation period (Table 2). More specifically, soil pH, EC, OC and TN showed variable trends during incubation depending on amendments type (Fig. 1). Soil pH slightly decreased over incubation period in control and in VC but remarkably decreased in TW amended soils at 120 d (Fig. 1a). A decline of pH might be attributed to NH^{4+}, CO_2, H^+ production and release of various organic acids from organic matter mineralization (Thite *et al.,* 2022). Soil pH seemed stable in BP and ES amended soils (Fig. 1a). This could be due to excellent buffering capacity of BP and ES. Gradual EC increment in all soils (Fig. 1b) could be attributed to release of bases and soluble salts from decomposing amendments (Thite *et al.,* 2022). Overall, soil OC and TN showed a decreasing trend over incubation period for all treatments (Fig. 1c and Fig. 1d). Decrease of OC and TN reflected the mineralization of the amendments with time. Soil OC in organically amended Inceptisols started to decrease at 30 d of incubation (Thite *et al.,* 2022).

Table 2. Effects of amendments and incubation time on soil pH, EC, OC, and TN.

	pH	EC	OC	TN
		dS m^{-1}	%	
Amendment				
Control	4.05 ± 0.52 g	0.17 ± 0.03 g	0.33 ± 0.06 g	0.05 ± 0.02 e
BP4%	7.37 ± 0.15 b	1.44 ± 0.28 e	1.27 ± 0.33 e	0.11 ± 0.04 d
BP8%	8.50 ± 0.36 a	3.11 ± 0.90 b	1.77 ± 0.42 c	0.16 ± 0.05 b
ES4%	7.93 ± 0.15 b	0.37 ± 0.13 f	0.54 ± 0.11 f	0.04 ± 0.02 e
ES8%	8.17 ± 0.35 b	0.47 ± 0.29 f	0.61 ± 0.12 f	0.05 ± 0.02 e
TW4%	4.57 ± 1.86 f	1.36 ± 0.39 e	1.54 ± 0.36 d	0.14 ± 0.03 c
TW8%	5.37 ± 1.10 d	1.71 ± 0.68 d	2.25 ± 0.66 a	0.20 ± 0.07 a
VC4%	5.03 ± 0.51 e	2.29 ± 0.24 c	1.79 ± 0.52 d	0.16 ± 0.03 c
VC8%	5.27 ± 0.42 e	3.68 ± 0.37 a	2.05 ± 0.06 b	0.18 ± 0.01 a
Incubation time (T, days)				
38	6.80 ± 1.33 a	1.33 ± 1.07 c	1.65 ± 0.86 a	0.15 ± 0.05 a
120	6.19 ± 1.89 b	1.51 ± 1.11 b	1.23 ± 0.63 b	0.11 ± 0.06 b
240	5.87 ± 2.04 c	2.04 ± 1.37 a	1.18 ± 0.65 b	0.11 ± 0.05 b
Source of variation				
Amendment (A)	***	***	***	***
Incubation time (T)	***	***	***	***
A × T	***	***	***	***

Note: Values are mean ± standard deviation of three replications. Means followed by different lowercase letters are significantly different (within amendment or incubation time) at $P < 0.05$ (Tukey's test). ***, significant at the 0.001 probability level.

*Extractable P, K, Ca, and Mg***:** Amendments, incubation time, and their interaction had significant impact on soil extractable P, K, Ca, and Mg, excepting that incubation time had no impact on Ca variation (Table 3). Compared to control, most of the treatments enhanced soil macro-nutrients to the extent of their respective element content, and their application rate (Table 1 and Table 3). Accordingly, highest P, K, and Ca was observed with VC, BP, and ES applications, respectively. ES had no significant impact on K, and BP had no significant impact on Ca. Enrichment in amended soils suggested the release

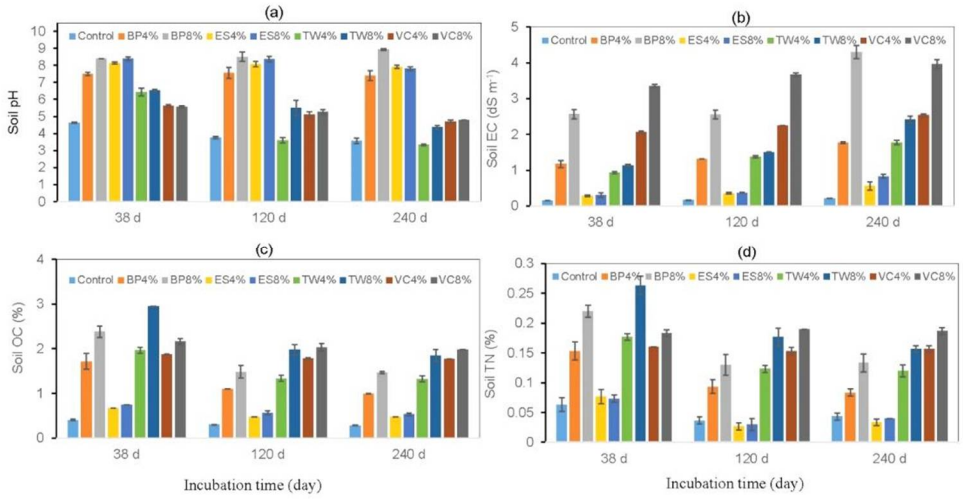

Fig. 1. Variation in Soil pH (a), EC (b), OC (c) and TN (d) during 240 days incubation. Bars represent standard errors of the mean (*n*=3).

of available plant nutrients from the amendments during incubation. ES and TW showed least impact on P, whereas VC8% contributed to ~94% increase in extractable P over control. Large fraction of P in VC could remain in labile form (López *et al.*, 2021). Soil P increment with increased VC rate proved its efficiency as P supplement in Ethopian sandy soil (Teka *et al.*, 2024). In acid soil, P might increase due to OAs application as they raised soil pH, which allowed Al or Fe fixation instead of P (Ch'Ng *et al.*, 2014). BP8% contributed to ~96% increment in K. Research showed BP and its biochar remarkably accelerated soil available K (Panwar 2015; Islam *et al.*, 2019). ES8% contributed to ~90% increase in Ca over control because of its extraordinary Ca level. Surprisingly, though VC contained relatively lower amount of total Ca among amendments, it supplied greater extractable Ca than BP or TW did. This suggested VC contained nutrients mostly in plant available forms (Angelova *et al.*, 2013). Highest extractable Mg in VC amended soils also reflected similar attribute.

Overall, P showed increasing trend until end of incubation. K and Mg decreased slightly. Ca seemed stable as was not impacted by incubation time (Table 3). More specifically, maximum P was observed at 240 d upon VC application followed by BP. P increment stopped at 120 d in TW amended soils, whereas P did not change in ES amended soils with incubation time (Fig. 2a). However, TW was unable to supply much extractable P as VC supplied. The dynamic of P release from VC suggested its high efficiency in

correcting soil P deficiency. K was noticeably decreased only in VC amended soils, whereas it seemed stable in others (Fig. 2b). Often, available K can be fixed by soil minerals. Ca slightly increased in VC amended soils until 240 d (Fig. 2c). Gradual increase in Ca suggested slow release of Ca from VC (Dey et al. 2019). Mg seemed stable throughout the incubation study (Fig. 2d).

Table 3. Effects of amendments and incubation time on soil extractable P, K, Ca, and Mg.

	P	K	Ca	Mg
		mg kg^{-1}		
Amendment				
Control	12.23 ± 5.94 h	51 ± 7.80 g	101 ± 18.15 g	82 ± 13.84 g
BP4%	37.55 ± 2.42 d	961 ± 9.01 b	111 ± 6.11 g	188 ± 8.40 d
BP8%	75.97 ± 10.35 c	1344 ± 19.24 a	114 ± 15.10 g	212 ± 5.92 bc
ES4%	15.82 ± 2.46 g	61 ± 2.25 g	900 ± 27.50 b	86 ± 6.62 g
ES8%	16.43 ± 2.10 fg	61 ± 4.50 g	1028 ± 55.43 a	100 ± 5.23 f
TW4%	17.26 ± 3.21 f	173 ± 9.81 f	288 ± 10.58 f	182 ± 8.68 e
TW8%	27.67 ± 7.98 e	242 ± 14.06 e	397 ± 24.03 e	206 ± 9.70 c
VC4%	182.51 ± 9.23 b	345 ± 120.86 d	479 ± 111.18 d	214 ± 7.81 ab
VC8%	230.42 ± 21.00 a	480 ± 169.59 c	681 ± 111.88 c	218 ± 3.17 a
Incubation time (T, days)				
38	60.93 ± 75.11 c	459 ± 445 a	450 ± 340.86 a	167 ± 58.58 a
120	68.37 ± 75.57 b	397 ± 449 b	462 ± 331.74 a	166 ± 55.81 a
240	75.64 ± 84.28 a	393 ± 437 b	460 ± 339.46 a	163 ± 55.00 b
Source of variation				
Amendment (A)	***	***	***	***
Incubation time (T)	***	***	**NS**	***
A × T	***	***	***	***

Note: Values are mean ± standard deviation of three replications. Means followed by different lowercase letters are significantly different (within amendment or incubation time) at $P < 0.05$ (Tukey's test). ***, significant at the 0.001 probability level.

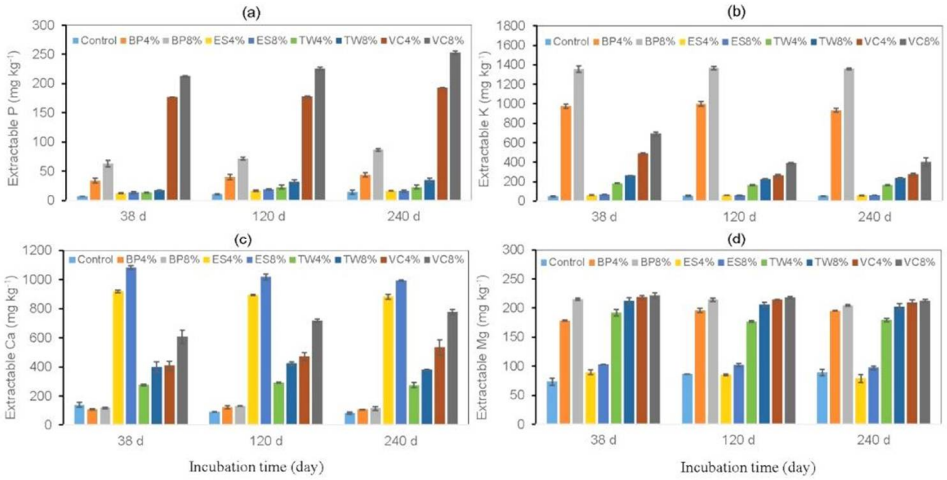

Fig. 2. Variation in soil extractable P (a), K (b), Ca (c) and Mg (d) during 240 days incubation. Bars represent standard errors of the mean (*n*=3).

Extractable Fe, Cu, Mn, and Zn: Amendments, incubation time, and their interaction had significant impact on DTPA extractable Fe, Cu, Mn, and Zn (Table 4). Overall, amendments, except ES, increased Fe, Cu, Mn, and Zn content to the extent of their application rate. Study revealed that ES was highly effective in minimizing micro-nutrients (metals) in soil. This was probably due to alkaline condition in ES amended soil, favorable for metal immobilization (Ashrafi *et al.*, 2015; Luo *et al.*, 2018). However, despite high pH in BP amended soil, Fe, Cu, Mn, and Zn was still higher than ES amended soil because BP naturally contained more of these elements than ES (Table 1). Banana stem amendment did not decreased Pb and Zn in sandy soil (pH 7.83) but ES decreased (Ashrafi *et al.*, 2015). Several other factors also control metal immobilization (Ruttens *et al.*, 2010; Zhou *et al.*, 2012; Houben *et al.*, 2012). TW addition increased Fe, Mn, and Zn but had no impact on Cu. At least 60% Fe increment in BP8% and TW8% amended soils suggested that both amendments were potential in releasing bio-available Fe. TW supplied higher extractable Mn as contained highest total Mn among amendments. VC showed highest efficiency in increasing Cu, Mn, and Zn (Table 4). Surprisingly, despite high Fe content in VC (Table 1), extractable Fe did not increased with its application. Moreover, Fe declined with increased addition of VC. This could be due to complex formation of Fe as insoluble $FePO_4$ in VC amended soil.

Table 4. Effects of amendments and incubation time on DTPA soil extractable Fe, Cu, Mn, and Zn.

	Fe	Cu	Mn	Zn
		mg kg^{-1}		
Amendment				
Control	40.98 ± 0.08 d	0.31 ± 0.03 d	12.56 ± 1.99 g	1.61 ± 0.10 f
BP4%	75.74 ± 29.51 b	0.38 ± 0.07 c	13.18 ± 5.12 f	1.70 ± 0.17 e
BP8%	113.33 ± 53.57 a	0.52 ± 0.15 b	23.71 ± 1.62 e	2.63 ± 0.18 c
ES4%	6.81 ± 2.54 f	0.20 ± 0.03 e	0.31 ± 0.12 h	0.47 ± 0.14 g
ES8%	5.71 ± 2.19 f	0.16 ± 0.01 e	0.30 ± 0.17 h	0.47 ± 0.12 g
TW4%	45.15 ± 23.61 c	0.32 ± 0.02 d	42.11 ± 13.89 d	2.27 ± 0.71 d
TW8%	109.18 ± 53.66 a	0.31 ± 0.02 d	57.05 ± 5.59 c	2.24 ± 0.55 d
VC4%	42.11 ± 12.97 d	0.52 ± 0.08 b	67.52 ± 27.05 b	5.69 ± 0.21 b
VC8%	26.05 ± 7.49 e	0.76 ± 0.28 a	123.00 ± 46.94 a	6.11 ± 0.52 a
Incubation time (T, days)				
38	32.82 ± 19.43 c	0.41 ± 0.25 a	45.79 ± 55.98 a	2.55 ± 2.12 b
120	52.61 ± 42.77 b	0.36 ± 0.13 c	35.00 ± 32.69 b	2.55 ± 1.88 b
240	70.16 ± 56.04 a	0.38 ± 0.17 b	33.22 ± 30.97 c	2.66 ± 1.87 a
Source of variation				
Amendment (A)	***	***	***	***
Incubation time (T)	***	***	***	***
A × T	***	***	***	***

Note: Values are mean ± standard deviation of three replications. Means followed by different lowercase letters are significantly different (within amendment or incubation time) at $P < 0.05$ (Tukey's test). ***, significant at the 0.001 probability level.

Overall, Fe and Zn significantly increased but Cu and Mn decreased at 240 d of incubation (Table 4). However, these nutrients showed variable patterns with incubation time depending on types of amendments (Fig. 3). Fe was remarkably increased in BP and TW amended soils but slightly increased in VC amended soils. However, it was stable in ES amended soil (Fig. 3a). Though total Fe level was superior in VC among all (Table 1), extractable Fe content could be low in VC. Cu was ultimately decreased in VC and increased very slowly in BP amended soils at higher application rates at 240 d. It remained unchanged in ES and TW amended soils (Fig. 3b). Presence of high content of extractable Cu in VC could led faster Cu release during early stage of incubation (Fig. 3b). Slow increase of Cu in amended soils with time indicated low content as well as

minimum release. Mn dramatically decreased with incubation time in VC amended soil but negligibly increased in TW amended soil. It remained stable in ES and BP amended soils (Fig. 3c). Highest extractable Mn in VC amended soils at 38 d indicated maximum content of readily available Mn in VC (Dey *et al.*, 2019). Variations in time-dependent Cu and Mn release could be attributed to formation of stable complexes of Cu and Mn with C fractions present in OAs in amended soils (Stevenson 1991). Mn stability in ES and BP amended soils was due to its poor content (below detection limit) in amendments (Table 1). With incubation period, extractable Zn was remarkably increased in TW treated soil, which was directly related with total Zn as well as higher extractable Zn content in TW (Table 1, Fig. 3d). Zn remained stable in other soils. This might be due to lower Zn content in the amendments.

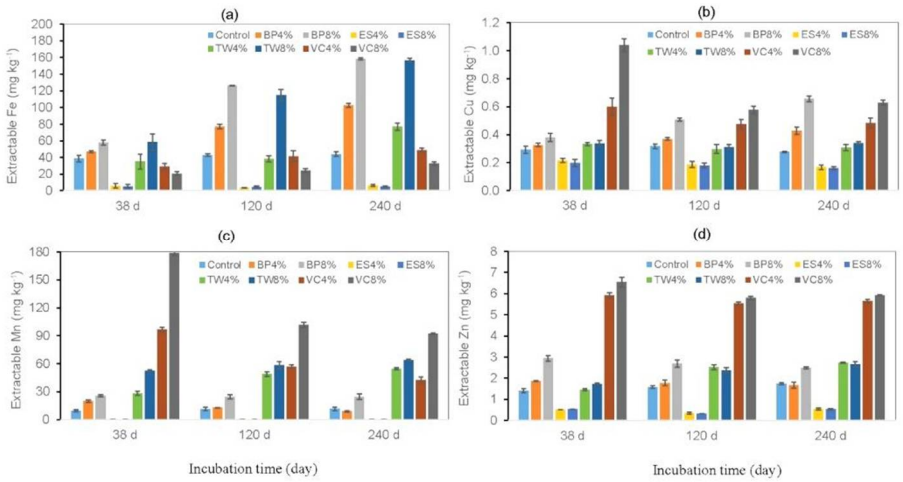

Fig. 3. Variation in soil extractable Fe (a), Cu (b), Mn (c) and Zn (d) during 240 days incubation. Bars represent standard errors of the mean (n=3).

Conclusion

In this study, organic amendments proved their significant efficiencies in improving chemical fertility of sandy loam soils. The amendments were cost-effective, eco-friendly, and easily accessible. The extent of impacts of amendments was dependent on amendment characteristics, their application rate, and incubation time. Overall, the amendments improved soil pH, EC, OC and nutrient properties. According to this study, TW and VC are suggested as the best choice for OC increment whereas, ES and BP are recommended for improving soil pH in acid soil. In heavy metals contaminated soils, ES can be highly effective in metal immobilization. Overall, VC is highly recommended for

improving EC, soil P, and micronutrients. In future, field application of BP, ES, TW and VC is suggested to assess their potentiality for crop production. In conclusion, organic amendment selectivity is important considering the characteristics of soil to be treated.

Acknowledgement

This research was conducted in the laboratory of the Department of Soil Science, University of Chittagong, Bangladesh. A part of analyses was carried out in Soil Resources Development Institute (SRDI), Sylhet division. The first author acknowledges Professor Dr. Coskun Gülser, Ondokuz Mayıs University, Turkey for his valuable suggestions during manuscript writing.

Funding

This research received no specific funding from any institution or agency.

References

Almaroai, Y.A., A.R.A. Usman, M. Ahmad, D.H. Moon, J.S. Cho, Y.K. Joo, C. Jeon, S.S. Lee and Y.S. Ok. 2014. Effects of biochar, cow bone, and eggshell on Pb availability to maize in contaminated soil irrigated with saline water. *Environ. Earth Sci*. **71**(3): 1289-1296.

Angelova, V.R., V.I. Akova, N.S. Artinova and K.I. Ivanov. 2013. The effect of organic amendments on soil chemical characteristics. *Bulg. J. Agric. Sci*. **19(**5): 958-971.

Anwar, Z., M. Irshad, A. Ping, F. Hafeez, and S. Yang 2018. Water extractable plant nutrients in soils amended with cow manure co-composted with maple tree residues. *Int. J. Agric. Biol. Eng*. **11**(5): 167-173.

Ashrafi, M., S. Mohamad, I. Yusoff, and F.S. Hamid. 2015. Immobilization of Pb, Cd, and Zn in a contaminated soil using eggshell and banana stem amendments: Metal leachability and a sequential extraction study. *Environ. Sci. Pollut. Res*. **22**(1): 223-230.

Bray R.H and L.T. Kurtz. 1945. In Soil Science. 39-45 pp.

Candemir, F., and C. Gülser. 2011. Effects of different agricultural wastes on some soil quality indexes in clay and loamy sand fields. *Commun. Soil Sci. Plant Anal*. **42**: 13-28.

Ch'Ng, H.Y., O.H. Ahmed and N.M.A. Majid. 2014. Improving phosphorus availability in an acid soil using organic amendments produced from agroindustrial wastes. *The Sci. World J*. **2014**: 1-6.

Chen, Y., M. Camps Arbestain, Q. Shen, B. Singh and M.L. Cayuela. 2018. The long-term role of organic amendments in building soil nutrient fertility: a meta-analysis and review. *Nutr. Cycl. Agroecosystems*. **111**.

Demir, Z. 2019. Effects of Vermicompost on Soil Physicochemical Properties and Lettuce (Lactuca sativa Var. Crispa) Yield in Greenhouse under Different Soil Water Regimes. *Commun. Soil Sci. Plant Anal*. **50**(17): 2151-2168.

Dey, A., P.C. Srivastava, S.P. Pachauri and A.K. Shukla. 2019. Time-dependent release of some plant nutrients from different organic amendments in a laboratory study. *Int. J. Recycl. Org. Waste Agric*. **8**(0123456789): 173-188.

González, M., E. Gomez, R. Comese, M. Quesada, and M. Conti. 2010. Influence of organic amendments on soil quality potential indicators in an urban horticultural system. *Bioresour. Technol*. **101**(22): 8897-8901.

Gurmessa, B. 2021. Soil acidity challenges and the significance of liming and organic amendments in tropical agricultural lands with reference to Ethiopia. *Environ. Dev. Sustain*. **23**(1): 77-99.

Hernandez, T., J.G. Berlanga, I. Tormos and C. Garcia. 2021. Organic versus inorganic fertilizers: Response of soil properties and crop yield. *AIMS Geosci*. **7**(3): 415-439.

Houben, D., J. Pircar and P. Sonnet. 2012. Heavy metal immobilization by cost-effective amendments in a contaminated soil: Effects on metal leaching and phytoavailability. *J. Geochemical Explor*. **123**: 87-94.

Huq, S.M.I. and J.U.M. Shoaib. 2013. *The Soils of Bangladesh. Netherlands:* Springer Netherlands.

Islam, M., M. Halder, M.A.B. Siddique, S.A.A. Razir, S. Sikder and J.C. Joardar. 2019. Banana peel biochar as alternative source of potassium for plant productivity and sustainable agriculture. *Int. J. Recycl. Org. Waste Agric*. **8**(1): 407-413.

López-Núñez, R. 2022. Portable X-ray Fluorescence Analysis of Organic Amendments: A Review. *Appl. Sci*. **12**(14).

López, R., J. Antelo, A.C. Silva, F. Bento and S. Fiol. 2021. Factors that affect physicochemical and acid-base properties of compost and vermicompost and its potential use as a soil amendment. *J. Environ. Manage*. **300**(113702).

Luo, W., Y. Ji, L. Qu, Z. Dang, Y. Xie, C. Yang, X. Tao, J. Zhou and G. Lu. 2018. Effects of eggshell addition on calcium-deficient acid soils contaminated with heavy metals. *Front. Environ. Sci. Eng*. **12**(3): 1-10.

Mahajabin, S., S. Rahman, A. Chamon, M. Mondol and M. Rahman. 2019. Effect of eggshell and lime on growth and mineral nutrition of kalmi (Ipomoea aquatica: Convolvulaceae) grown on lead contaminated soil. *J. Biodivers. Conserv. Bioresour. Manag*. **5**(1): 85-92.

Manyanga, M.A., J. Marumure, N. Chigede, M. Mubvuma, C.P. Mudzengi, I. Nyambiya and M. Muteveri. 2024. *Vermicomposting for Improved Soil Health: Prospects for Degraded Soils BT -The Marginal Soils of Africa: Rethinking Uses, Management and Reclamation*. Springer Nature Switzerland. 325-337 pp.

Mi, W., Y. Sun, S. Xia, H. Zhao, P. Brookes, Y. Liu and L. Wu. 2018. Effect of inorganic fertilizers with organic amendments on soil chemical properties and rice yield in a low-productivity paddy soil. *Geoderma*. **320**: 23-29.

Muliwa, A.M., T.Y. Leswifi and M.S. Onyango. 2018. Performance evaluation of eggshell waste material for remediation of acid mine drainage from coal dump leachate. *Miner. Eng*. **122**(March): 241-250.

Murphy, J. and J.P. Riley. 1962. A modified single solution method for the determination of phosphate in natural waters. *Anal. Chim. Acta*. **27**: 31-36.

Musa, A.M.M., S.F.U. Farhad, M.A. Gafur and A.T.M.K. Jamil. 2021. Effects of withdrawal speed on the structural, morphological, electrical, and optical properties of CuO thin films synthesized by dip-coating for CO2 gas sensing. *AIP Adv*. **11**(11).

Naramabuye, F.X. and R.J. Haynes. 2006. Effect of organic amendments on soil pH and Al solubility and use of laboratory indices to predict their liming effect. *Soil Sci*. **171**(10): 754-763.

Ok, Y.S., S.S. Lee, W.T. Jeon, S.E. Oh, A.R.A. Usman and D.H. Moon. 2011. Application of eggshell waste for the immobilization of cadmium and lead in a contaminated soil. *Environ. Geochem. Health*. **33:** 31-39.

Ouda, B. and A.Y. Mahadeen. 2008. Effect of fertilizers on growth, yield, yield components, quality and certain nutrient contents in broccoli (Brassica oleracea). *Int. J. Agri. Biol*. **10**: 627-632.

Panwar, N. 2015. Studies on physicochemical characteristics and fertility of soil by addition of banana peels-waste management. *International J. Sci. Res. Dev*. **3**(01): 2321-0613.

Peiris, C., P.D. Wathudura, S.R. Gunatilake, B. Gajanayake, J.J. Wewalwela, S. Abeysundara and M. Vithanage. 2022. Effect of acid modified tea-waste biochar on crop productivity of red onion (Allium cepa L.). *Chemosphere*. **288**(132551).

Ruttens, A., K. Adriaensen, E. Meers, A. De Vocht, W. Geebelen, R. Carleer, M. Mench and J. Vangronsveld. 2010. Long-term sustainability of metal immobilization by soil amendments: cyclonic ashes versus lime addition. *Environ. Pollut*. **158**(5): 1428-1434.

Sial, T.A., M.N. Khan, Z. Lan, F. Kumbhar, Z. Ying, J. Zhang, D. Sun and X. Li. 2019. Contrasting effects of banana peels waste and its biochar on greenhouse gas emissions and soil biochemical properties. *Process Saf. Environ. Prot*. **122:** 366-377.

Stevenson, F.J. 1991. *Organic matter-micronutrient reactions in soil*. In J. J. Mortvedt (Ed.), Soil Science Society of America Inc, Wisconsin (Issue 4).

Teka, K., B. Abraha, S. Mebrahtom, A. Tsegay, Y. Welday, T.A. Gessesse, M. Ostwald and L. Hansson. 2024. Effect of Vermicompost on Soil Fertility and Crop Productivity in the Drylands of Ethiopia. *Compost Sci. Util*. **31**(3-4): 75-85.

Terefe, Z., T. Feyisa, E. Molla and W. Ejigu. 2024. Effects of vermicompost and mineral fertilizers on soil properties, malt barley (*Hordeum distichum* L.) yield, and economic benefits. *Agrosystems, Geosci. Environ.* **7**(3): e20550.

Thite, M.D., S.R. Ingle and A.S. Gaikwad. 2022. Effect of incubation duration of incorporated organic manures on chemical properties of Inceptisol. *The Pharma Innov. J*. **11**(1): 162-166.

Walkley, A. and I.A. Black. 1934. An Examination of the Degtjareff method for determining soil organic matter, and a proposed modification of the chromic acid titration method. *Soil Sci*. **37**(1): 29-38.

Wedayani, N.M., I.N. Rai, I.G. Mahardika and I.M.S. Wijana. 2024. Utilization of banana waste biochar to reduce heavy metal contamination in soil and maize plants. *J. Degrad. Min. Lands Manag*. **11**(2): 5475-5483.

Zhang, S., Q. Zhu, W. de Vries, G.H. Ros, X. Chen, M.A. Muneer, F. Zhang and L. Wu. 2023. Effects of soil amendments on soil acidity and crop yields in acidic soils: A world-wide meta-analysis. *J. Environ. Manage*. **345**, 118531.

Zhou, Y.F., R.J. Haynes and R. Naidu. 2012. Use of inorganic and organic wastes for in situ immobilisation of Pb and Zn in a contaminated alkaline soil. *Environ. Sci. Pollut. Res. Int*. **19(**4): 1260-1270.

(Revised copy received on 18/05/2025)

J. Asiat. Soc. Bangladesh, Sci. **51**(1): 87-102, June 2025
DOI: http://doi.org/10:3329/jasbs.v51i1.82793

OCCUPATIONAL HEALTH HAZARDS AND TREATMENT SEEKING BEHAVIOR OF SALT PAN WORKERS IN KUTUBDIA AND MAHESHKHALI ISLANDS OF COX'S BAZAR, BANGLADESH

MD. HUMAYUN KABIR*[1], MD. AMZED HOSSEN[1] AND MUHAMMAD FERDAUS[2]

Department of Geography & Environment, University of Dhaka, Dhaka-1000, Bangladesh
[2] Postgraduate Programs in Disaster Management, BRAC University, Bangladesh

Abstract

This study aimed to illuminate the prevailing occupational health issues faced by salt pan workers in Kutubdia and Maheshkhali Islands of Cox's Bazar, Bangladesh. Utilizing qualitative methodologies, the research conducted individual interviews, focus group discussions, and key informant interviews with salt farmers, and community leaders, and experts. Data were analyzed using thematic analysis method to explore demographic attributes, health status, challenges, and concerns of the workers. Findings revealed that salt farmers frequently encounter heat stresses, dehydration, respiratory health problems, musculoskeletal issues, dermatological problems, and vision-related complications. The study also highlighted the lack of access to protective equipment, inadequate medical facilities, and substantial treatment expenses faced by the workers. The study emphasizes the urgent need for multifaceted interventions, emphasizing access to protective gear, community awareness enhancement, collaborative efforts, and sustainable practices. Addressing the occupational health challenges faced by salt pan workers in Kutubdia and Maheshkhali Islands requires concerted efforts from stakeholders, policymakers, and community leaders.

Key words: Occupational health, Salt farming, salt pan workers, Health hazard.

Introduction

Occupational health plays a pivotal role in safeguarding the well-being of workers and ensuring a productive, sustainable work environment. The joint estimates of WHO/ILO shows that about 1.9 million people died from occupational health hazards in 2016 with 81% from diseases and 19% from injuries (WHO and ILO, 2021). The geographic variations of these occupational health risks and associated impacts are related to the economic development of the regions with workers in the developing nations suffering more. The Decent Work Agenda of International Labour Organization (ILO, 1999) and

*Corresponding author: E-mail: mh_kabir@yahoo.com

later incorporation of Decent work in the United Nations' 2030 Agenda for Sustainable Development (UN, 2015.), all emphasized the creation of safe and secure working environments and promoting occupational health and safety standards and reducing work-related injuries and illnesses.

Occupational hazards pose health and well-being risks inherent to specific professions with industrial and agricultural sectors face the greatest risks (WHO, 1983). Distinct work-related risks entailed in differential professions are associated with specific tasks, environments, and exposures associated with that profession. Construction workers face hazards like falls and machinery (Dong *et al*., 2017; Eom and Lee, 2020; Alateeq *et al*., 2023), while healthcare workers confront biological risks such as infections (Ali *et al*., 2020; Ayenew *et al*., 2022). Agricultural workers encounter dangers like pesticide exposure (Gilson *et al*., 2011; Shaik and Padma, 2017; Manwani and Pandey, 2016; Nguyen *et al*., 2018; Joshi *et al*., 2020; Tchir and Szafron, 2020) and miners face dust and underground risks (Azad, 2017; Agwa-Ejon and Pradhan, 2018; Son et. al., 2020; McCulloch and Miller, 2023). In such, salt pan workers confront unique challenges due to their specialized tasks and the distinctive environmental conditions they operate in.

Salt workers face challenges such as- direct contact with salt crystals, physical strain, and intense sunlight glare (Cherian *et al*., 2015). Breathing in salt particles can elevate blood pressure (Haldiya *et al*., 2005, Glad Mohesh and Sundaramurthy, 2016), and many exhibit increased oral health issues, indicating limited access to dental care (Sanadhya, 2013). Prolonged heat exposure in these agricultural settings can lead to kidney function decline and conditions like chronic kidney disease of unknown etiology (CKDu) (Luangwilai *et al*., 2021). Recent research from Thailand reveals this kidney function decline in workers during peak harvest periods (Luangwilai *et al*., 2022). A study in Rajasthan highlighted prevalent health issues among salt workers, including eye and skin problems and a 12.0% hypertension rate (Sachdev *et al*., 2006; Chavan *et al*., 2019). The challenging salt farm conditions, marked by heat-related risks and physical demands, also contribute to musculoskeletal disorders (Shengli, 2010).

Salt production in Bangladesh primarily occurs along the coastal regions, notably in Cox's Bazar and Chittagong districts, where saline seawater is utilized. Recent data highlights a surge in salt production with increased land under salt cultivation. Reports from the Bangladesh Small and Cottage Industries Corporation (BSCIC) indicate that the country has witnessed historic highs in salt production, reaching around 2.233 million tonnes for 2022-2023 (BSCIC, 2023). During the season, salt cultivation expanded to cover 66,424 acres, marking a growth of 3,133 acres from the previous year. Despite this

achievement, challenges persist for marginal farmers. The production in Cox's Bazar alone saw a spike, with daily yields exceeding 36 thousand metric tons due to prevailing heat conditions (TBS, 2023). However, farmers face hurdles in direct sales to mill owners, often navigating through intermediaries who pocket the price difference.

Bangladesh introduced the National Salt Policy in 2022 with goals to boost salt production and establish a buffer stock of approximately 0.1 million metric tons. Additionally, the policy focuses on expanding the salt industry by designating new lands for cultivation and establishing Eco-friendly industrialized areas (MoI, 2022). So, it is expected that salt production in Bangladesh will increase in the coming years. However, little focus is given on the health of the salt pan workers, and this demands immediate scrutiny and intervention. Kutubdia and Maheshkhali Islands of Cox's Bazar district in Bangladesh have carved a distinctive identity as pivotal contributors to the nation's salt production sector. This study aims to shed light on the occupational health challenges faced by salt pan workers in Kutubdia and Maheshkhali Islands. The main objective of the study is to explore the occupational health hazards of salt farming and the treatment seeking behavior of the salt pan workers in Kutubdia and Maheshkhali Islands of Cox's Bazar of Bangladesh. The specific objectives of the study include:

- Identifying different types of health hazards commonly experienced by the salt pan workers of Kutubdia and Maheshkhali Islands of Cox's Bazar of Bangladesh and
- Exploring the treatment seeking behavior of the salt pan workers of Kutubdia and Maheshkhali Islands of Cox's Bazar of Bangladesh.

Materials and Methods

Study area: Kutubdia and Maheshkhali Islands of Cox's Bazar district are in the South-eastern part of Bangladesh (Fig. 1). There are eight Upazilas under the Cox's Bazar district, and Kutubdia and Maheshkhali are two of them. Kutubdia Island is created by tidal, supratidal and fluvial processes of river Ganges. The topography is particularly mudflat, sandy and gentle slope. Cyclone and storm surges are the most common and frequent disaster of Kutubdia Island which causes a lot of sufferings for the inhabitants. Kutubdia Island consists of six unions named- Ali Akbar Dail, North Dhurung, South Dhurung, Lemshikhali, Kaiarbil, Baraghope. It has 58,463 households and a total area of 215.8 square kilometers (83.3 sq mi). Kutubdia is rich in producing salt and dried fish. An Island off the coast of Cox's Bazar. It has an area of 268 square kilometers. Maheshkhali Island consists of eight unions named- Bara Maheshkhali, Chhota Maheshkhali, Dhalghata, Hoanak, Kalarmarchhara, Kutubjom, Matarbari, Saflapur.

Through the Centre of the Island and along the eastern coastline rises a range of low hills, 300 feet high.

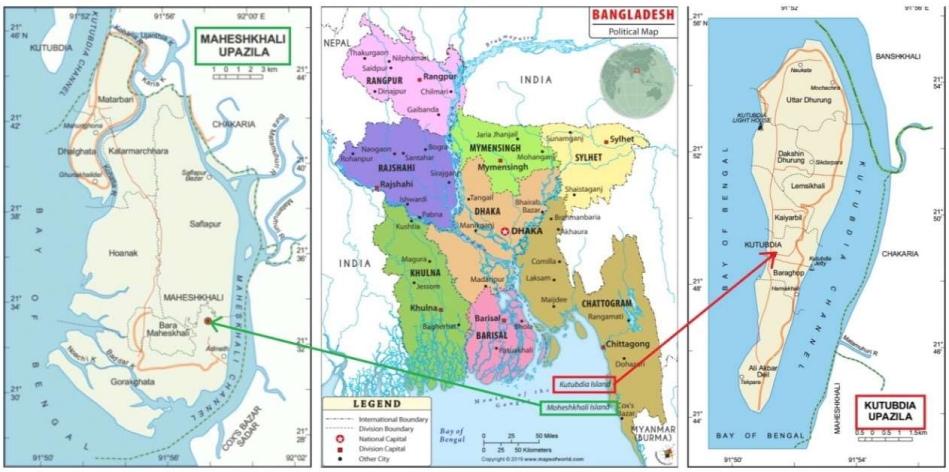

Fig. 1. Kutubdia and Maheshkhali Islands of Cox's Bazar, Bangladesh.

Research design: The research utilized qualitative research approach to gain insights into the experiences of salt pan workers. Qualitative approach provides no-numerical description of conditions with deeper comprehension. The approach is concerned with providing deeper insights into problems without quantification (Moser and Korstjens, 2017). Qualitative approach provides researcher clear and in-depth understandings of people experience in such analytical way that is easy and simple (Cleland, 2017). It is also useful for gathering perceptions, experience and behavior of the respondents (Moser and Korstjens, 2017). As this study is concerned with the experience of the salt pan workers and their behavior, qualitative is approach is chosen as an appropriate method of study. Qualitative research typically involves observation of characteristics, in-depth interview or focus group discussion (Cornel *et al*., 2019). This study involved individual interviews with the workers to delve deeper into their perspectives. Furthermore, the study organized focus group discussions (FGDs) to facilitate group interactions and gather collective viewpoints. Additionally, key informant interviews (KIIs) were undertaken with experts or community leaders to obtain specialized insights and expert opinions on the subject matter (Fig. 2).

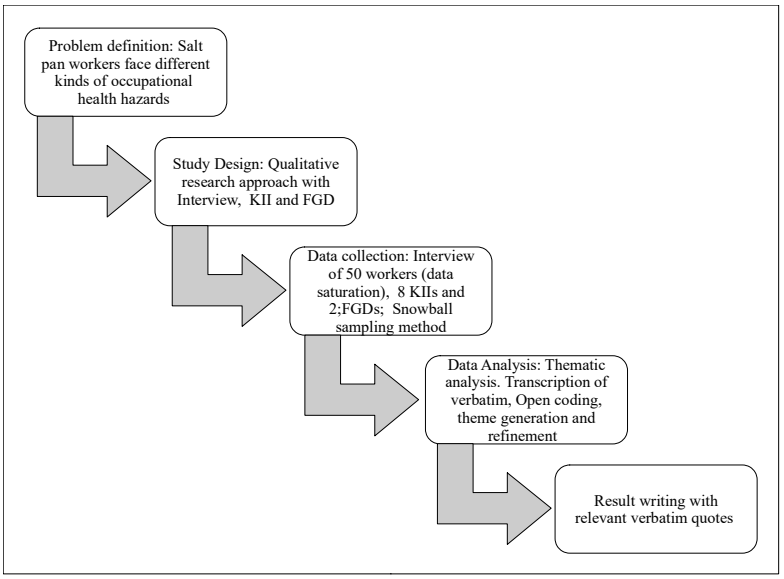

Fig. 2. Research process.

Sampling and Data collection: Qualitative interview generally involves open-ended and unstructured or semi-structure and guided questionnaire (Bryman, 2008; Bamberg, 2012). In this study, both semi-structured and unstructured interview were applied. Semi-structured questionnaire was used to collect data from salt pan workers and key informants while unstructured interviews were conducted in FGDs. A total 50 salt pan workers were interviewed to understand their experience with different health hazards due to their occupation and their preferences for seeking treatments. Each of the interviews lasted for around 30 minutes. The sample size is determined by theme (data) saturation method. Theme or data saturation method involves identification of a higher number of themes within a corpus of data (Wutich *et al*., 2024). When no new theme or information is produced from interviews, saturation point is achieved. Sample size in any qualitative and quantitative study is an important issue. The determination of sample size in qualitative research is rarely discussed and poorly understood (Wutich *et al*., 2024) with no clear rules (Lichtman, 2010; van Rijnsoever, 2017; Kindsiko and Poltimäe, 2019). But there is recent development in literature on minimum sample size also known as saturation (Wutich *et al*., 2024). Wutich *et al.* (2024) reviewed minimum sample size for saturation of data in different types of qualitative research. It is found that the minimum sample size required for theme saturation is nine for interview and four focus

groups (Guest *et al*., 2006; Hennink and Kaiser, 2022). These are minimum numbers among different theme saturation studies. So, the numbers of interview for saturation vary based on the context with recent web based work suggesting a number of 30-67 interviews for saturation (Squire *et al*., 2024). Thus, more case and context specific research is recommended for fully understanding the required interviews for saturation (Wutich *et al*., 2024). The saturation point sample size for the study was 24 and 26 for Kutubdia and Maheshkhali respectively. The result shows same patterns of health hazards and treatment seeking behavior for both the islands.

As the target population was salt pan workers of Kutubdia and Maheshkhali Islands, snowball sampling method was employed to identify relevant participants for the interview. In the method, participants were asked to assist in finding potential participants of the study interest.

Eight KIIs and two FGDs were also carried out. KIIs include Union Parishad Member, representative from Salt Farmers Association, Local administration- UNO, representative from BSIC and Local Medical Officer. FGDs were conducted with farmers, Salt Workers' Association and day labors involved in salt farming. In addition, published papers, reports of BSCIC, and newspapers have been consulted.

Data analysis and presentation: In qualitative research, analyzing and presenting qualitative data is one of the most confusing aspects (Burnard *et al*., 2008). Apart from that the process of analyzing data is also labor intensive and time consuming.

Kothari and Garg (2014) defined qualitative data analysis as the conversion to raw data to a form that is appropriate for researchers to make decisions. It is the process of ordering data and make sense out of it (Bryman, 2002). Data analysis is important in research so that both the readers and researchers can make sense out of it (Miles and Huberman, 1994). There are two fundamental approaches, namely deductive and inductive approach of qualitative data analysis (Spencer *et al*., 2004; Lathlean, 2006). While in deductive approach, a predetermined concepts, theories or research findings are used to set out expectations for data analysis and interpretations, actual data is used to derive the structure of analysis in inductive approach (Burnard *et al*., 2008). The later one is comprehensive and time-consuming (Burnard *et al*., 2008) and commonly used (Lathlean, 2006). In this study, inductive approach of data analysis is followed for analyzing data. Out of different inductive methods, thematic analysis was applied in this study to explore the qualitative dimensions of the workers' health status, challenges, and concerns in depth. It involved analyzing transcripts, identifying themes within data and gathering themes together.

Initially, workers' narratives about their health were transcribed, aiming to capture the authenticity and nuanced details of their experiences. Following this, a thorough immersion into the transcribed data allowed for the identification of preliminary patterns and potential themes. Through a methodical coding process, the data segments were systematically organized into coherent themes and sub-themes. Throughout the analysis, these themes were continually refined and elaborated upon, facilitating a collaborative approach to ensure they resonated with and accurately represented the workers' perspectives and lived experiences. The whole analysis has been performed in Microsoft Office.

In qualitative research, there are two main approaches to writing up the findings (Burnard, 2004). First approach, the traditional approach (Burnard, 2008) involves presenting the main findings under each major theme with relevant verbatim quotes to highlight the findings followed by separate discussion. The other approach combines the discussion with the findings integrating in the context of the research (Burnard, 2008). Here, findings and discussion are presented in different sections and the traditional approach is followed for presenting the findings.

Results and Discussion

Respondents details: A total of 50 salt pan workers from both Kutubdia and Maheshkhali Islands were interviewed using a semi-structured questionnaire. Table 1 shows the demographic characteristics of respondents and the duration of the working in the occupation. In Kutubdia, 6 respondents were under the age of 30, whereas 13 fall within the 30-40 age range, and the remaining 5 were above 40. Conversely, in Maheshkhali, 8 respondents are below 30, 12 fall within the 30-40 age range, and 6 are above 40. Thus, the majority of the respondents, accounting for around 50% of the total, are between 30 and 40 years old. Educationally, Kutubdia shows that 4 are illiterate, 11 have primary education, 7 possess secondary education, and a smaller 2 have higher secondary qualifications. On the other hand, in Maheshkhali, 4 are illiterate, 8 have primary education, a significant 13 have secondary education, and 1 holds higher secondary credentials. Majority of the workers were engaged in salt farming for 15-25 years and representing around 50% of the total respondents.

Health hazards

Dehydration and Heat-Related illnesses: The salt farmers emphasized the prevalence of dehydration, especially when they work during the blistering summer months. The period

of salt farming is from November to May which includes winter (November- February) and summer (Pre-monsoon) seasons of Bangladesh. The months of summer (pre-monsoon) have prevailing higher temperatures. The workers work around 10-12 hours under the sun which left them exposed to scorching sun. This leads to dehydration of the workers. One of the respondents illustrated the situation as:

One of the primary health problems we face during salt farming is dehydration, especially during the scorching summer months.

Table 1 Participant detail.

Characteristics	Category	Kutubdia	Maheshkhali	Total
Age	Less than 30	6	8	14
	30-40	13	12	25
	More than 40	5	6	11
Education	Illiterate	4	4	8
	Primary	11	8	19
	Secondary	7	13	20
	Higher Secondary	2	1	3
Duration of work	Less than 15	6	5	11
	15-25	12	13	25
	More than 25	6	8	14

Despite their efforts to stay hydrated, the intense heat often leads to fatigue, dizziness, and an overall sense of exhaustion. The environmental conditions amplify the challenge, with farmers continuously losing fluids and battling the unforgiving sun, which underscores the urgent need for effective preventive measures. One of them also added:

Summers are harsh here, and despite our efforts to stay hydrated, there are moments when dizziness and fatigue become overwhelming.

Respiratory health problems: The salt farmers frequently encounter symptoms such as persistent coughs, chest heaviness, and over time, the emergence of chronic respiratory conditions. One respondent has shared his view as:

A persistent cough is almost a given among us, and I've observed many of my colleagues developing chronic respiratory conditions over time.

Farmers perceive that they inhale a significant amount of salt and dust during their work. They believe that although they cannot see these particles with the bared eye, the particles exist in the air and enter their lungs during the inhalation process, thereby having a detrimental impact on their respiratory health. As one respondent reported:

Continuously breathing in the salty mist and dust really takes a toll on my respiratory health. Over time, I've noticed that this constant exposure leads to discomfort, breathing difficulties, and other related health issues. It's challenging, as I can feel the effects on my lungs, making it harder to breathe freely and comfortably.

Musculoskeletal issues: The physical demands inherent in salt farming manifest in various musculoskeletal issues among the community. Tasks such as lifting heavy salt bags and engaging in repetitive motions contribute to widespread backaches, joint pains, and muscle strains. These physical ailments not only affect individual farmers' mobility and productivity but also emphasize the need for ergonomic considerations and support mechanisms.

Lifting heavy salt bags and constantly bending over the pans has taken a toll on my back and joints. I have experienced persistent backaches and joint pains because of these repetitive tasks. It is not just me; many of us in the community feel the strain and discomfort from these physical demands.

Dermatological concerns: Among salt pan workers, there is a common occurrence of skin-related issues ranging from mild to severe. Most of the workers frequently experience skin dryness, which can be quite uncomfortable and often leads to irritation. Beyond the initial dryness and irritation, some workers face more severe dermatological conditions. These conditions include rashes, blistering, or other skin ailments that require medical attention.

I have observed that just months of working in the salt pan results in skin dryness, which can feel tight and uncomfortable. Beyond just dryness, I frequently experience irritation, making my skin feel sensitive and sometimes even painful to touch. Unfortunately, the challenges do not stop there. There have been occasions when persistent rashes and redness develops.

Vision and eye health: Many farmers report frequent eye irritations, increased sensitivity to light, and blurred vision, emphasizing the need for protective eyewear and interventions to mitigate long-term vision-related complications. The reflective nature of salt pans and the intense glare expose salt farmers to heightened risks related to vision and eye health. Following an illustration from a respondent:

I work for long hours in the salt pan. After just a few hours into my shift, I begin to experience issues related to vision glare. This glare not only makes it challenging to see clearly but also contributes to a range of other problems that persist even after I have completed my work for the day. Many of my colleagues and I frequently encounter symptoms such as eye irritations, episodes of blurred vision, and heightened sensitivity to light. It is concerning how this constant exposure affects our eyesight.

Exposure to injury and diseases: Salt farmers frequently operate without the benefit of essential protective measures. Despite the inherent risks associated with their occupation, such as direct exposure to salt, contaminants, and airborne particles, there is a notable absence of safeguards. This absence extends across various facets of their work, from the initial preparation of salt beds to the intensive processes of raking, harvesting, and subsequent packaging. One of the respondents revealed as follows:

We utilize basic tools necessary for tasks like preparing the pans and other activities in the salt-making process. However, we do not employ protective measures such as gloves, sunglasses, or masks. Instead, we rely on our hands and legs, directly exposing ourselves to the salts.

Farmers forgo protective measures due to longstanding familiarity with their challenging work environment. Years of exposure have made them accustomed to the risks of salt and contaminants. Moreover, traditional practices and a lack of awareness about modern safety protocols contribute to this mindset. As a result, while dangers persist, cultural norms and immediate productivity often overshadow the adoption of essential safety precautions. In response to the question why workers don’t use protective measures came as follows:

We work in this manner because we are accustomed to it, and it's a tradition that has been passed down through generations.

This quote certainly indicates their lack of awareness. Not only do they work without adequate protective measures due to tradition and familiarity with the environment, but they also grapple with financial constraints. Middlemen often dictate low prices for their produce, leaving farmers with limited resources to invest in safer production methods. This economic pressure further hampers their ability to prioritize safety over immediate financial concerns. The worker further added:

We also cannot invest more money since we don't receive a fair price for our produce, while middlemen reap significant profits.

Treatment seeking behavior: In both study regions, most respondents primarily rely on local pharmacies and nearby doctors for medical treatment. Surprisingly, less than 15% of participants from these areas utilize the upazila healthcare facilities. Few of them seek medical care outside their islands for better services. Furthermore, only a small fraction of respondents turns to Homeopathic treatments. The data underscores a notable trend: a predominant dependence on local pharmacies and individual practitioners, rather than more extensive healthcare facilities or alternative therapies. As respondents asserted:

Our local pharmacies and nearby doctors are our main sources for medical treatments.

While a few seek medical care outside our islands for better services, their number is too low.

Treatment cost: During the salt cultivation period, farmers typically incur expenses ranging between 6000 to 8000 Taka on medical treatment. Expenses include mainly cost of medicines. This specific financial commitment during this phase highlights the health challenges and risks associated with salt farming, necessitating significant expenditure on healthcare services to address related ailments and concerns.

The research provides an in-depth exploration of the working conditions, health challenges faced by salt pan workers in Kutubdia and Maheshkhali, Bangladesh. The findings illuminate critical areas of concern, shedding light on both the occupational hazards inherent to salt farming and the broader systemic challenges that these communities confront. One striking observation is the longevity of service among salt farmers in both regions. In Kutubdia, a majority (75%) of the respondents have been engaged in this labor-intensive occupation for over 15 years, with nearly a quarter dedicated for more than 25 years. Similarly, in Maheshkhali, half of the respondents have committed over a quarter-century to salt farming. Such extended tenures suggest a deep-rooted cultural and economic reliance on this traditional livelihood, underscoring the need for sustainable practices and welfare initiatives to support these seasoned workers.

Solar salt production process involves the physical demands and environmental exposures that farmers navigate daily. While the method is time-honored and central to the local economy, the absence of modern safety and sustainability measures poses significant risks to farmers' health and the ecosystem. As global conversations around sustainable agriculture gain momentum, integrating eco-friendly practices in salt farming could mitigate environmental degradation and enhance worker safety.

The health challenges articulated by respondents shows a concerning picture. From dehydration and heat-related illnesses during the grueling summer months to chronic

respiratory conditions due to salt and dust inhalation, farmers confront a myriad of health risks. Furthermore, musculoskeletal issues, dermatological concerns, and vision-related complications compound their vulnerabilities. These health implications not only impact individual well-being but also signify broader public health implications that warrant immediate attention (Fig. 3).

The revelation that farmers operate without essential protective measures is alarming. While cultural norms and economic constraints perpetuate this practice, the resultant health repercussions are undeniable. The absence of protective gear, coupled with direct exposure to salts, contaminants, and airborne particles, underscores the urgent need for awareness campaigns, training, and policy interventions to safeguard farmers' well-being.

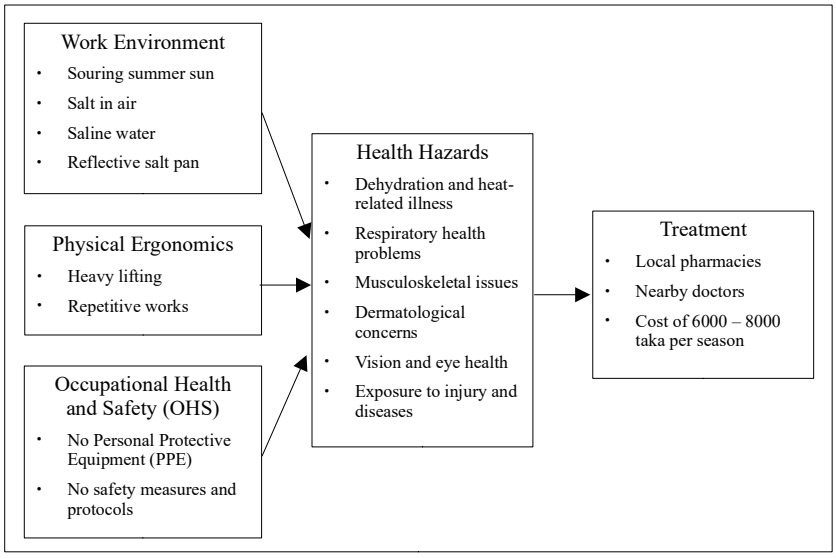

Fig. 3. Occupational health hazards and treatment seeking behavior of salt pan workers in Kutubdia and Maheshkhali Islands of Cox's Bazar, Bangladesh.

The predominant reliance on local pharmacies and nearby doctors highlights potential gaps in healthcare accessibility and quality. The limited utilization of centralized healthcare facilities suggests a need for infrastructure development, capacity building, and awareness initiatives to enhance medical service delivery. Additionally, the financial burden of medical treatment, with farmers incurring substantial expenses during the cultivation period, underscores the economic implications of health challenges and the imperative for comprehensive support mechanisms.

Conclusion

The present study found that salt pan workers in Kutubdia and Maheshkhali face different types of health hazards due to the working environment and lack of protective equipment in the process of salt farming. The environment poses significant health risk as the environment has great amount of salt in air and water which affects both inner and outer organs of the workers. Exposed to salt causes different health issues like chronic respiratory and dermatological conditions. The solar salt production method requires the workers to work under scouring heat conditions which causes dehydration and heat-related illnesses. Workers are also exposed to other health hazards like musculoskeletal problems, glare sensitivity, injury etc. Most of the people take medication from local pharmacies and thus local pharmacies and doctors play a crucial role in providing treatment to most of the people. This reflects their reliance on local medication than modern treatment facilities. In the face of current situation, priority must be given on the health and well-being of the salt pan workers. Several measures should be put in place to deal with the prevailing health and treatment facility issues. Implementing comprehensive health and safety programs, providing access to medical care, and ensuring proper use of protective equipment can help overcome health issues in salt farming. Apart from these, safety seminars, educational and awareness campaigns can also be recommended.

References

Agwa-Ejon, J. F. and A. Pradhan. 2018. Life cycle impact assessment of artisanal sandstone mining on the environment and health of mine workers. *Environ Impact Assess Rev*. **72**: 71-78.

Alapati, P. and K.S. Shaik. 2017. Indigenous method to combat environmental health hazards of agricultural workers while harvesting. *Int. J. Educ. Sci. Res*. **7**(5): 91-100

Alateeq, M.M., P.P. Fathimathul Rajeena and M.A.S. Ali. 2023. Construction site hazards identification using deep learning and computer vision. *Sustainability.* **15**(3): 2358.

Ayenew, E., W. Akafu and D. Wolde Daka. 2022. Prevalence of work-related health hazard and associated factors among health workers in Public Health Institutions of Gambella Town, Western Ethiopia : cross-sectional survey. *J. Environ. Public Health.* **2022**: 1-10.

Azad, S.U. 2017. Study of the health effects of coal mining on coal mine workers of Baluchistan. *Int. J. Occup. Saf. Health.* **5**(1): 7-10.

Bamberg, M. 2012. Narrative Analysis. In: *APA Handbook of Research Methods in Psychology* (ed. H. Cooper), 2nd ed., pp. 77-94. American Psychological Association.

Bryman, A. 2008. *Social Research Methods*, 3rd ed. Oxford University Press, Oxford.

BSCIC. 2023. *Annual Report 2022-2023*. Bangladesh Small and Cottage Industries Corporation (BSCIC), Dhaka, Bangladesh

Burnard, P. 2004. Writing a Qualitative Research Report. *Nurse Educ. Today* **24**: 174-179.

Burnard, P., P. Gill, K. Stewart, , *et al.* 2008. Analysing and Presenting Qualitative Data. *Br Dent J*, **204**: 429-432.

Chavan, S.J., P.S. Shelke, J.M. Tale and S. Prabhankar. 2019. Epidemiological study of ocular morbidities in saltpan worker in Mumbai. *Perspect. Med. Res*. **7**: 10-13.

Cherian, J., Z. Singh, J. Bazroy, A.J. Purty, M. Natesan and V.K. Chavada. 2015. Study of morbidity pattern among salt workers in Marakkanam, Tamil Nadu, India. *J. Clin. Diagn Res*, **9**(4): LC01-3.

Cleland, J.A. 2017. The Qualitative Orientation in Medical Education Research. *Korean J. Med. Educ*. 29: 61-71.

Corner, E.J., E.J. Murray and S.J. Brett. 2019. Qualitative, Grounded Theory Exploration of Patients' Experience of Early Mobilisation, Rehabilitation and Recovery after Critical Illness. *BMJ Open*, 9: e026348.

Dong, X. S., J.A. Largay, S.D. Choi, X. Wang, C.T. Cain and N. Romano. 2017. Fatal falls and PFAS use in the construction industry: Findings from the NIOSH FACE reports. *Accid. Anal. Prev.*. **102**: 136-143

Eom, R., and Y. Lee. 2020. Working environments and clothing conditions in the construction industry. *Fash. Text.* **7**(1): 1-14.

Gilson, N.D., N.W. Burton, J.G. van Uffelen and W.J. Brown. 2011. Occupational sitting time: employees' perceptions of health risks and intervention strategies. *Health Promot. J. Austr.* **22**(1): 38-43.

Glad Mohesh, M.I., and A. Sundaramurthy. 2016. Lung health and heart rate variability changes in salt workers. *Indian J. Tuberc.* **63**(2): 115-118.

Guest, G., A. Bunce and L. Johnson. 2006. How Many Interviews Are Enough? An Experiment with Data Saturation and Variability. *Field Methods* **18**(1): 59-82.

Guest, G., E. Namey and K. McKenna. 2017. How Many Focus Groups Are Enough? Building an Evidence Base for Non-Probability Sample Sizes. *Field Methods* **29**(1): 3-22.

Haldiya, K.R., M.L. Mathur, R. Sachdev, H.N. Saiyed. 2005. Risk of high blood pressure in salt workers working near salt milling plants: A cross-sectional and interventional study. *Environ Health* **4**: 13

Hennink, M.M., B.N. Kaiser and M.B. Weber. 2019. What Influences Saturation? Estimating Sample Sizes in Focus Group Research. *Qual. Health Res.* **29**(10): 1483-1496.

ILO. 1999. Report of the Director-General: Decent work. In: *Proceedings of the 87th International Labour Conference*, Geneva, Switzerland, 1-17 June 1999. Available at: https://www.ilo.org/public/english/standards/relm/ilc/ilc87/rep-i.htm.

Kindsiko, E. and H. Poltimäe. 2019. The Poor and Embarrassing Cousin to the Gentrified Quantitative Academics: What Determines the Sample Size in Qualitative Interview-Based Organization Studies? FQS Forum: *Qual. Soc. Res*. **20**(3): Art.1.

Kothari, C.R. and G. Grarg. 2014. *Research Methodology, 3rd ed*. New Age International Publishers.

Lathlean, J. 2006. Qualitative Analysis. In: *The Research Process in Nursing* (eds. K. Gerrish and A. Lacy), pp. 417-433. Blackwell Science, Oxford.

Lichtman, L. (ed.). 2010. *Qualitative Research in Education: A User's Guide*, 2nd ed. Sage Publications, Thousand Oaks.

Luangwilai, T., M.G. Robson and W. Siriwong. 2021. Effect of heat exposure on dehydration and kidney function among sea salt workers in Thailand. *Rocz Panstw Zakl Hig.* **72**(4): 435-442.

Luangwilai, T., M.G. Robson and w. Siriwong. 2022. Investigation of kidney function changes in sea salt workers during harvest season in Thailand. *Rocz Panstw Zakl Hig*, **73**: 121-130.

Manwani, V.K. and S. Pandey. 2016. An epidemiological study of mechanical health hazards amongst agricultural workers in rural India. *Int. J. Occup. Saf. Health.* **4**(2): 19-23.

McCulloch, J. and P. Miller. 2023. *Mining Gold and Manufacturing Ignorance Occupational Lung Disease and the Buying and Selling of Labour in Southern Africa* (1st ed.). Springer Nature, Singapore

Miles, M.B. and A.M. Huberman. 1994. *Qualitative Data Analysis: An Expanded Sourcebook*. Sage Publications.

MoI. 2022. *National Salt Policy 2022*. Ministry of Industries, Government of the People's Republic of Bangladesh, Dhaka, Bangladesh

Moser, A. and I. Korstjens. 2018. Series: Practical Guidance to Qualitative Research. Part 3: Sampling, Data Collection and Analysis. *Eur. J. Gen. Pract*. 24: 9-18.

Nguyen, T.H.Y., M. Bertin, J. Bodin, N. Fouquet, N. Bonvallot and Y. Roquelaure. 2018. Multiple exposures and coexposures to occupational hazards among agricultural workers: a systematic review of observational studies. *Saf. Health Work.* **9**(3): 239-248.

Sachdev, R., L.M. Mathur, K.R. Haldiya and H.N. Siyed. 2006. Work-related health related health problems in salt workers of Rajasthan, India of Rajasthan, India. *Indian J. Occup. Environ. Med.* **10**(2): 62-64.

Sanadhya, S., R. Nagarajappa, A.J. Sharda, K. Asawa, M. Tak, M. Batra and H. Daryani. 2013. The oral health status and the treatment needs of salt workers at Sambhar Lake, Jaipur, India. *J. Clin. Diagn Res.* **7**(8): 1782-1786.

Shengli, N. 2010. Ergonomics and occupational safety and health. An ILO Perspective. Appl. Ergon. **41**: 744-753.

Son, B., F. Wambalaba, M.K. Chakulya, and M. Simonian. 2020. What multi-level solutions can simultaneously promote zambian mine workers' health and benefits to mining companies? *Athens J. Health Med. Sci.* **7**(4): 217-234.

Spencer, L., J. Ritchie and W. O'Connor. 2004. Analysis: Practices, Principles and Processes. In: *Qualitative Research Practice* (eds. J. Ritchie and J. Lewis), pp. 199-218. Sage Publications, London.

Squire, C.M., K.C. Giombi, D.J. Rupert, J. Amoozegar and P. Williams. 2024. Determining an Appropriate Sample Size for Qualitative Interviews to Achieve True and Near Code Saturation: Secondary Analysis of Data. *J. Med. Internet Res*. 26: e52998.

TBS. 2023. April 20. *Record salt production, yet marginal farmers see little reward*. The Business Standard. https://www.tbsnews.net/economy/record-salt-production-yet-marginal-farmers-see-little-reward-619998

Tchir, D.R. and M.L. Szafron. 2020. Occupational health needs and predicted well-being in office workers undergoing web-based health promotion training: cross-sectional study. *J. Medical Internet Res.* **22**(5): e14093-e14093.

Thakur, R., P. Jumade, R. Waghmare, S. Joshi and A. Joshi. 2020. Perceptions, practices and health hazards of agricultural workers from rural central India with regard to pesticide use - a cross sectional study. *J. Evol. Med. Dent. Sci*. **9**(47): 3528-32.

United Nations. 2015 *Transforming Our World: The 2030 Agenda for Sustainable Development*. Resolution Adopted by General Assembly. United Nations: New York, NY, USA.

van Rijnsoever, F.J. 2017. (I Can't Get No) Saturation: A Simulation and Guidelines for Sample Sizes in Qualitative Research. *PLoS One* **12**(7): e0181689.

WHO. 1983. Recommended Health based occupational exposure limits for selected vegetable dusts (Report of a study group)'. *WHO Technical Report Series*, 684, pp. 35-49.

WHO/ILO. 2021 *WHO/ILO joint estimates of the work-related burden of disease and injury, 2000-2016: global monitoring report*. Geneva: World Health Organization and the International Labour Organization. Licence: CC BY-NC-SA 3.0 IGO.

Wutich, A., M. Beresford and H.R. Bernard. 2024. Sample Sizes for 10 Types of Qualitative Data Analysis: An Integrative Review, Empirical Guidance, and Next Steps. *Int. J. Qual. Methods* 23.

(Revised copy received on 03/03/2025)

J. Asiat. Soc. Bangladesh, Sci. **51**(1): 103-114, June 2025
DOI: http://doi.org/10:3329/jasbs.v51i1.82794

COMPARATIVE PERFORMANCE OF TWO DIFFERENT BIOFERTILIZERS IN ACIDIC AND ALKALINE SOILS ON OKRA GROWTH

AYSHA AKTER AND SONIA HOSSAIN
Department of Soil, Water and Environment, University of Dhaka, Dhaka-1000, Bangladesh

Abstract

The present study evaluates the effects of two different types of biofertilizers on the growth of okra (*Abelmoschus esculentus*) following completely randomized design with three treatments (control, vermicompost, trichocompost) and three replications using acid soil (pH 4.77) and alkaline soil (pH 7.87) The results showed partial (pH 5.9) and complete (pH 6.4) neutralization of soil acidity by trichocompost and vermicompost whereas pH increased in alkaline soil but EC decreased significantly by both treatments. Besides, total OC, total N, total P, total K, total S all increased significantly ($P < 0.05$) in both soils (except S in alkaline soil) by both biofertilizer application but total Ca, Mg, Fe, Mn decreased in acid soil while results were mixed in alkaline soil. Results of plant height and root length were increased significantly ($p < 0.01$) in both acidic and alkaline soil by vermicompost and trichocompost application. For nutrient uptake, Vermicompost appeared equally useful for acidic and alkaline soil and trichocompost appeared more useful in acidic soil than alkaline soil. The application of the two biofertilizers in both the soils had significant positive effects on the growth of okra.

Key words: Biofertilizers, Acidic soil, Alkaline soil, Okra growth.

Introduction

Biofertilizers are becoming increasingly popular in many countries and for many crops because of the adverse impacts of inorganic fertilizer on environment and plant growth. Biofertilizers are inputs containing microorganisms capable of mobilizing native elements from non-usable form to usable form through biological processes (Bahadur and Manohar, 2001). Vermicompost (vermi-compost, vermiculture) is the product of the decomposition process using various species of worms, usually red wigglers, white worms, and other earthworms, to create a mixture of decomposing vegetable or food waste, bedding materials, and vermicast (also called worm castings, worm humus, worm manure, or worm faeces). Vermicompost contains water-soluble nutrients and is an excellent, nutrient-rich organic fertilizer and soil conditioner (Kelly and Knutzen, 2008).

*Corresponding author: soniahossain_ng@yahoo.com

Vermicompost stimulates the microbial activity of soil, improves nutrient content and increase growth yield and quality of the plant (Arora *et al*., 2011). On the other hand, *Trichoderma* spp. is free living fungi that are common in soil and root systems and are well- known to solubilize phosphates and micronutrients. They can produce phosphates and several organic acids. Trichoderma spp. recently was suggested as a plant growth promoting fungi due to their ability to produce siderophores, phosphate solubilizing enzymes, and phytohormones (Haidar *et al*., 2018).

Vegetables are the integral part of the balanced diet of human since time immemorial. Globally, the role of vegetables has been recognized in solving the problem of food and nutritional security. Okra (*Abelmoschus esculentus L.*) is an important vegetable crop of Malvaceae family, which supplies higher nutrition (carbohydrates, fats, protein, minerals and vitamins) in our diet. Okra is tolerant of a wide range of soil pH but prefers neutral pH of 6.5 to 7.0. It is a fast growing annual which has captured a prominent position among the vegetables in Bangladesh. It is a multiple use crop. Dried seeds are nutritious food. It contains upto 20% protein and the fibre from okra canes is a possible paper pulp source, while the dried canes are a fuel source (Lyngdoh *et al*., 2013).

Materials and Methods

Soil sampling site: *Acid soil sample was collected from Kalapara, is an Upazila of* Patuakhali District in the Division of Barisal, Bangladesh. The sampling area belongs to the agro-ecological zone, AEZ-13. Alkaline soil sample was collected from Matuail Union, Jatrabari Thana of Dhaka metropolitan. The sampling area belongs to the agro-ecological zone, AEZ-19.

Processing of the sample: After collection the soil samples were divided into two parts- one was used for required background analysis of various parameters and the larger portion was kept separately for the development of pot experiment. The former part was air-dried for 4 days by spreading in a thin layer and then hammered to make the clods smaller. Visible roots and debris were discarded from the soil sample. For hastening the drying process, the soil sample exposed to sunlight. After that, larger and massive aggregates were broken down into smaller aggregates by gently crushing them using a wooden hammer. The ground samples were screened through a 2mm stainless steel sieve. The sieved sample was then stored into plastic containers and the mouth was well-capped. Then the container was kept in a cool dry place in the laboratory. The other part of the soil sample was dried in the sun and larger clods were crushed by hammer and roots were discarded. This sample was used for pot experiment. The initial soil sample

was analyzed before set up of the pot experiment. This pot experiment was conducted in the premises (net house) of the Department of Soil, Water & Environment, University of Dhaka. A total number of 18 pots were used for the analysis. Irrigation water quality and amount were carefully maintained. For the pot experiment, vegetable crop called okra (*Abelmoschus esculentus)*, in the family of Malvaceae was used.

Pot preparation and treatment: Five kilogram (5kg) of soil samples were taken in each seven kilogram (7kg) plastic pot for the culture of 4 okra seeds and growth of okra plants. In order to study the effect of biofertilizer, vermicompost and trichocompost were taken as treatments. Vermicopost was collected from Siddique bazar, Dhaka. Trichocompost was collected from online nurseries and gardening store. Collected biofertilizers were air dried, passed through a 2 mm stainless steel sieve and preserved in airtight plastic containers. For treatment each pot contains 27 g of biofertilizers. The experiment was laid out in a Completely Randomized Design (CRD) having three (3) replications. For each soil, three (3) treatments were distributed randomly.

Growth performance study: Plant height were measured using a meter scale from the ground level to the apex. From each pot two plants were measured and averaged (centimeter). Leaf number and pod number were also recorded. The leaf area has been calculated using the linear equation LA (leaf area) = 11.98 + (0.06×L×W) where L= length of leaf and W= width of leaf (Bhatt and Chanda, 2003).

Digesion of biofertilizer and soil: For digestion, 0.5 g of biofertilizer was taken. It was digested with aqua-regia (HCl: HNO3 =3:1). (Jackson, 1962). For digesion of soil, 2.5 g of sieved samples were weighed and digested with aqua-regia (HCL: HNO_3 =3:1). (Jackson, 1962).

Analysis of soil and biofertilizer: The pH of the samples were measured electrochemically by using a glass electrode pH meter as described by Jackson (1958). The ratio of sample to water was 1:2.5. The electrode was calibrated using standard buffer solutions at pH 4.0 and 7.0. Electrical conductivity was measured by an EC meter at a ratio soil samples to water as 1:5 as described by USSL staff (1954). Cation exchange capacity was measured by 1N ammonium acetate at pH 7.0 (Chapman and Pratt, 1965). Organic carbon was determined by wet oxidation of Walkley and Black (1934). In this method, the soil carbon was oxidized with chromic acid (derived from potassium dichromate). Then the excess chromic acid left after the oxidation of organic carbon was determined volumetrically with standard ferrous sulphate solution and the quantity of substance oxidized was calculated from the amount of chromic acid required. Organic matter was calculated by multiplying the percentage of organic carbon with

conventional Van- Bemmelen‘s factor of 1.724 (Piper, 1950). Total nitrogen was determined by Kjeldahl‘s digestion with concentrated sulfuric acid (H_2SO_4) as described by Jackson (1958). The distillation of the digest was done with 40% sodium hydro-oxide (NaOH) and the distillates were collected at 2% Boric acid mixed indicator. The distillates were titrated against sulfuric acid (H_2SO_4). Total phosphorus of the samples were determined colorimetrically using a spectrophotometer at 490 nm by developing yellow color with vandamolybdate after digesting the samples ((Jackson, 1973). Total potassium of the samples were determined from the digest by a flame photometer (Jackson, 1962). Total sulfur content of the samples were determined from digest by turbidity of suspended barium sulfate using Tween-80 stabilizer. The turbidity was measured by spectrophotometer at 420 nm as described by Page *et al*. (1989). Calcium, Magnesium, iron, manganese, zinc, chromium and sodium contents were determined by Atomic Absorption Spectrophotometer (AAS) as described in Jackson (1973).

Collection, digesion and analysis of plant samples: Collected plant samples were washed first with tap water and then with distilled water. The heights of the collected plants were noted down. The fresh weights of plants and pods were taken separately with an electric balance. The samples were kept one day for air dry. Then the samples were oven dried at 80 ±5°C for 48 hours. The oven dry weights of the samples were also taken. Then shoot and root were separated of each plant and grounded with mortar and pestle. The grounded samples were kept in envelops with proper labeling and sorted in dry place.

Grounded shoot and pod were weighted 0.5 g separately and taken into 100 ml Pyrex beaker. Then all the weighted samples were mixed with 15 ml of conc. Nitric acid (HNO_3) and left overnight for predigesting. The predigested samples were heated in a sand bath for about 15 minutes. Then the samples were cooled and 5 ml perchloric acid ($HCLO_4$) was added. Again samples were digested until the contents become colorless. The digests were cooled, filtered, diluted to 50 ml and transferred into dry plastic bottles (Jackson, 1973). This extract was used for further analysis.

Total nitrogen of the plant samples (shoot and pod) was determined by Kjeldahl‘s digestion with concentrated sulfuric acid (H_2SO_4) as described by Jackson (1958). The distillation of the digest was done with 40% sodium hydro-oxide (NaOH) and the distillates were collected at 2% Boric acid mixed indicator. The distillates were titrated against sulfuric acid (H_2SO_4). Total phosphorus of plant samples were determined colorimetrically using a spectrophotometer at 490 nm by developing yellow color with vandamolybdate after digesting the plant samples (Jackson, 1973). Total potassium of plant samples was determined from the digest by a flame photometer (Jackson,

1962).Total sulfur content of plant samples was determined from digest by turbidity of suspended barium sulfate using Tween-80 stabilizer. The turbidity was measured by spectrophotometer at 420 nm as described by Page *et al*. (1989). Total calcium, magnesium, iron, manganese, zinc, chromium and sodium contents of plant samples were determined following standard method. From the value of nutrient content, nutrient uptake was calculated as: Nutrient uptake ($kgha^{-1}$) = Nutrient content (%) × Dry weight ($kgha^{-1}$)/100 (Huq and Alam, 2005).

The data collected in the experiment were calculated and the calculated results were graphically evaluated by using Microsoft excel (version 2013). Calculated results were statistically analyzed in the form one way ANOVA, using Minitab 17.

Results and Discussion

The initial characteristics of the two types of soil samples and the two types of biofertilizer samples showed that, Acidic soil had a OC of 0.5 %, OM 0.95%, CEC 3.64 (cmol(+)/kg), EC 3.17 mS/m, total N 0.22 %, total P 0.04 %, total K 0.07%, total S 0.33%, total Ca 0.01%, total Mg 1.33 %, total Na 0.27 %, total Zn 0.004%, total Fe 2.52%, total Mn 0.02% and alkaline soil had a OC of 0.41 %, OM 0.71%, CEC 2.22 (cmol(+)/kg), EC 0.27 mS/m, total N 0.16 %, total P 0.07 %, total K 0.02%, total S 0.18 %, total Ca 0.02%, total Mg 0.13 %, total Na 0.05 %, total Zn 0.006%, total Fe 1.98 %, total Mn 0.1% (Table 1). Initial pH value revealed that vermicompost was acidic and trichocompost was alkaline in nature. Vermicompost had a OC of 3.86%, OM 6.64%, CEC 4.73 (cmol(+)/kg), EC 2.76 mS/m, total N 1.03 %, total P 0.14%, total K 0.93%, total S 0.78 %, total Ca 0.87%, total Mg 0.55%, total Na 0.02%, total Zn 0.03%, total Fe 1.04%, total Mn 0.04%. Trichocompost had a OC of 4.08%, OM 7.01%, CEC 5.97 (cmol(+)/kg), EC 2.96 mS/m, total N 0.76%, total P 0.12%, total K 0.72%, total S 0.62%, total Ca 2.69%, total Mg 0.46%, total Na 0.07%, total Zn 0.02%, total Fe 1.21%, total Mn 0.07%.

The result showed that, treatment with both biofertilizers in both acidic and alkaline soil took higher time duration to reach the maturity stage over the control (Table 2). This might be due to the initial pH value of vermicompost (6.58) and trichocompost (7.70) optimized the pH of both soils and made soils more suitable to grow with proper time duration. Similar results were reported by Hamidi *et al.,* 2009. Prolonged phonological stages due to biofertilizers application in present study was an indication of suitable condition and time available for plant growth and development. Comparing the results of both soil it can be said that, for vegetative growth stages both the biofertilizers showed almost similar results.

Table 1. Initial properties of two types of soils and two types of biofertilizers.

Properties	Acidic soil	Alkaline soil	Vermi-compost	Tricho-compost
pH	4.77	7.87	6.58	7.70
CEC (cmol(+)/kg)	3.68	2.22	4.37	5.97
EC (mS/m)	3.17	0.27	2.76	2.96
Organic carbon (%)	0.55	0.41	3.86	4.08
Organic matter (%)	0.95	0.71	6.64	7.01
Total Nitrogen (%)	0.22	0.16	1.03	0.76
Total Phosphorus (%)	0.04	0.07	0.14	0.12
Total Potassium (%)	0.07	0.02	0.93	0.72
Total Sulfur (%)	0.33	0.18	0.78	0.62
Total Calcium (%)	0.01	0.02	0.87	2.69
Total Magnesium (%)	1.33	0.13	0.55	0.46
Total Sodium (%)	0.27	0.05	0.02	0.07
Total Zinc (%)	0.004	0.006	0.03	0.02
Total Iron (%)	2.52	1.98	1.04	1.21
Total Manganese (%)	0.02	0.10	0.04	0.07

Table 2. The effect of vermicompost and tricho-compost on phenology of okra.

Growth stages	Code	Days after sowing (DAS)					
		Acidic soil			Alkaline soil		
		Control	Vermi	Tricho	Control	Vermi	Tricho
Germination	V0	0-6	0-10	0-10	0-5	0-9	0-8
Emergence	V1	6	10	10	5	9	8
Primary leaves	V2	9	14	13	8	13	11
First trifoliate leaf	V3	17	31	29	17	25	24
Fifth trifoliate leaf	V4	28	42	38	26	36	34
Pre-flowering	R5	44	52	49	41	54	49
Flowering	R6	48	58	55	47	61	56
Pod formation	R7	No pod	64	61	56	69	63
Pod filling	R8	No pod	73	67	64	76	71
Maturity	R9	No pod	85	83	82	88	86

Post-harvest soil samples were analyzed to evaluate the changes occurred in the physicochemical properties in different treatments (Table 3). In acidic soil, highest pH value was 6.40, total N 0.28%, total P 0.06%, total 0.28%, total Na 1375.20 ppm recorded in vermicompost applied soil, highest EC value was 1.70 mS/m, OC 0.67%, OM 1.15%, total Mg 1.44%, total Mn 294.49 ppm, total Zn 75.21 ppm recorded in trichocompost applied soil, highest total K was 2.01%, total Ca 0.03%, total Fe 2.57% recorded in control. In acid soil pH, EC, OC, OM total S, total Fe, total Mn, total Zn, total Na were differed statistically ($p < 0.01$ and $p < 0.05$). In alkaline soil, highest pH value was 8.12, CEC 5.17 was cmol (+)/kg, OC 0.65%, OM 1.22%, total K 1.78%, total S 0.26%, total Mg 1.35%, total Fe 2.19%, total Na 1269.68 ppm recorded in vermicompost applied soil, highest EC value was 0.24 mS/m, total N 0.29 %, total P 0.08 %, total Ca 0.06 %, total Zn 76.86 ppm recorded in trichocompost applied soil. Highest total Mn 228.50 ppm was recorded in control. In alkaline soil, OC, OM, total N, total P, total S, total Mg, total Fe, total Mn, total Zn, total Na differed statistically ($p < 0.01$ and $p < 0.05$). The present study indicates that in both acidic and alkaline soil, vermicompost and trichocompost applied soil showed increased values of pH, OC, OM, total N and almost all nutrients over the control. This might be due to the initial properties of both vermicompost and trichocompost added with soil. Similar results found by Azarmi *et al*., 2008; Tharmaraj *et al*., 2011.

The result revealed that, for both soils, significantly ($p < 0.01$) higher plant height and root length were recorded with biofertilizers treated soils over the control soils (Table 4). The increased in plant height and root length in response to applied vermicompost and trichocompost may be due to release of nutrients, biological fixed nitrogen and also by excreting auxin, kinetins, vitamins. Similar results were found by Malik *et al.* (2005); Nuruzzaman *et al.* (2003); Prabhu *et al.* (2003).

The data presented in Table 5 revealed that, In alkaline soil, the values of total N, P, K, S, Ca, Mg uptake in shoot and pod were significantly ($p < 0.0\%$ and $p < 0.05\%$) higher in vermicompost and trichocompost treated soils than control. This might be due to the application of different biofertilizers which enhanced the CEC of soil and established better root system. In acidic soil, similar results found except for total N uptake in shoot and total Mg in pod, they showed higher values in trichocompost treated soil. Similar results were reported by Tanwar *et al*. (2003); Thenua and Sharma (2011).

The data presented in Table 6 revealed that, for both soils, the values of total Na and Zn uptake in shoot and pod were significantly ($p < 0.01\%$ and $p < 0.05$) higher in biofertilizers treated soils. This might be due to favorable soil condition and pH condition

Table 3. Chemical properties of post-harvest soil under different treatments.

Soil used	Treatment	pH	CEC (cmol (+)/kg)	EC (mS/m)	OC (%)	OM (%)	Total N (%)	Total P (%)	Total K (%)	Total S (%)	Total Ca (%)	Total Mg (%)	Total Fe (%)	Total Mn (ppm)	Total Zn (ppm)	Total Na (ppm)
Acidic soil	Control	5.57	5.44	0.53	0.51	0.87	0.25	0.05	2.01	0.25	0.03	1.40	2.57	204.50	66.80	1046.40
	Vermi-compost	6.40	4.86	0.89	0.66	1.13	0.28	0.06	1.69	0.28	0.02	1.15	2.28	178.43	56.47	1375.20
	Tricho-compost	5.90	5.44	1.70	0.67	1.15	0.27	0.05	1.98	0.27	0.02	1.44	2.41	294.49	75.21	1175.20
	P-value	<0.05	>0.05	<0.01	<0.01	<0.05	>0.05	>0.05	>0.05	<0.01	>0.05	>0.05	<0.01	<0.01	<0.01	<0.01
Alkaline soil	Control	7.82	3.29	0.20	0.51	0.90	0.24	0.07	1.14	0.16	0.05	0.10	1.73	228.50	74.81	359.60
	Vermi-compost	8.12	5.17	0.19	0.65	1.22	0.21	0.05	1.78	0.26	0.04	1.35	2.19	212.20	74.12	1269.68
	Tricho-compost	8.10	3.18	0.24	0.59	1.02	0.29	0.08	1.01	0.14	0.06	0.11	1.52	223.34	76.86	407.00
	P-value	>0.05	<0.05	>0.05	<0.01	<0.05	<0.05	<0.05	>0.05	<0.01	>0.05	<0.01	<0.01	<0.01	<0.01	<0.01

*** <0.01 = significant at 1 %, **<0.05 = significant at 5 %, *>0.05= not significant

Table 4. Growth performance of *Abelmoschus esculentus* in response to different treatments.

Soil used for growing plant	Treatment	Plant height (cm)	Root length (cm)	Leaf number per plant	Leaf area (cm2)	Pod number per plant
Alkaline soil	Control	28.30	8.50	4.00	18.02	3.00
	Vermicompost	35.70	12.20	6.00	18.92	4.00
	Trichocompost	30.60	11.80	5.00	18.12	4.00
P-value		<0.01	<0.01	>0.05	>0.05	>0.05
Acidic soil	Control	19.30	8.70	4.00	17.02	No pod
	Vermicompost	23.60	10.20	5.00	17.98	3.00
	Trichocompost	23.10	9.20	5.00	17.12	1.00
P-value		<0.01	<0.01	>0.05	>0.05	>0.05

*** <0.01 = significant at 1%, **<0.05 =significant at 5%, * >0.05 =not significant.

Table 5. Macronutrients uptake by *Abelmoschus esculentus* under various treatments.

Soil used	Treat-ment	Total N (kg/ha)		Total P (kg/ha)		Total K (kg/ha)		Total S (kg/ha)		Total Ca (kg/ha)		Total Mg (kg/ha)	
		Shoot	Pod	Shoot	Pod	Shoot	Pod	Shoot	Pod	Shoot	Pod	Shoot	Pod
Alkaline soil	Control	17.32	9.75	1.11	0.39	10.28	2.86	1.94	0.80	8.42	3.49	4.07	1.27
	Vermi	40.55	16.5	2.40	0.78	18.92	3.87	5.11	1.34	20.57	5.06	7.06	1.70
	Tricho	21.15	12.4	1.42	0.61	12.27	3.24	1.75	0.67	10.63	6.45	5.25	1.57
P-value		<0.01	<0.01	<0.01	<0.01	<0.01	<0.01	<0.01	<0.01	<0.01	<0.01	<0.01	<0.05
Acidic soil	Control	9.88	No pod	0.42	No pod	4.52	No pod	0.53	No pod	2.62	No pod	9.63	No pod
	Vermi	15.60	9.82	0.90	0.43	7.23	3.07	1.39	2.62	4.84	2.43	4.84	1.11
	Tricho	28.34	3.14	0.76	0.23	7.31	1.59	0.60	1.59	4.31	0.93	4.31	1.29
P-value		<0.01	<0.01	<0.05	<0.01	<0.01	<0.01	<0.01	<0.01	<0.01	<0.01	<0.01	<0.01

*** <0.01 = significant at 1%, **<0.05 =significant at 5%, * >0.05 =not significant.

after treated with biofertilizers which enhanced nutrient availability and nutrient uptake as well as a better growth and activity of roots. In alkaline soil, there is no significant difference in Fe uptake in pods and Mn upatake in both shoot and pod. In acidic soil, there is no significant difference in Fe and Mn uptake in shoot. These might be due to lower Fe, Mn content of both biofertilizers and soils. Similar findings were observed by Idries and Snadhu (1979); Jagdale *et al.* (1980); Bera *et al*. (2013).

Table 6. Micronutrient uptake by *Abelmoschus esculentus* under various treatments.

Soil used	Treatment	Total Na (kg/ha)		Total Fe (kg/ha)		Total Mn (kg/ha)		Total Zn (kg/ha)	
		Shoot	Pod	Shoot	Pod	Shoot	Pod	Shoot	Pod
Alkaline soil	Control	0.25	0.07	0.48	0.05	0.02	0.006	0.26	0.08
	Vermi	0.41	0.11	0.34	0.05	0.04	0.009	0.35	0.10
	Tricho	0.19	0.08	0.07	0.01	0.02	0.02	0.15	0.07
P-value		<0.01	>0.05	<0.01	>0.05	>0.05	>0.05	<0.01	>0.05
Acidic soil	Control	0.09	No pod	0.17	No pod	0.02	No pod	0.09	No pod
	Vermi	0.25	0.06	0.17	0.05	0.03	0.007	0.16	0.06
	Tricho	0.23	0.03	0.14	0.03	0.02	0.003	0.11	0.02
P-value		<0.01	<0.05	>0.05	<0.05	>0.05	<0.05	<0.05	<0.05

*** <0.01 = significant at 1%, **<0.05 =significant at 5%, * >0.05 =not significant.

From the study, it can be stated that, the application of vermicompost appeared equally effective in both acidic and alkaline soil over the control on the growth of *Abelmoschus esculentus*. On the other hand, Application of trichocompost appeared more effective in acidic soil than alkaline soil.

References

Arora, V. K., C.B. Singh, A. S. Sidhu and S. S. Thind, 2011. Irrigation, tillage and mulching effects on soybean yield and water productivity in relation to soil texture. *Agric. Water. Manag.* **98**(4): 563-568.

Azarmi, R., T.G. Mousa and D.T. Rahim, 2008. Influence of vermicompost on soil chemical and physical properties in tomato (*Lycopersicum esculentum*) field. *African j. biotech.* **7**(14): 2397-2401.

Bahadur, A. and R. Manohar, 2001. Response of okra to biofertilizers. *J. Veg. Sci.* **28**(2): 197-198.

Bera, A. K., K. Pramanik and D. Panda, 2013. Response of biofertilizers and homobrassinoloids on growth, relative water content and yield of lentil. *J. Crop. Weed*. **9**: 84-90

Bhatt, M. and S. V. Chanda, 2003. Prediction of leaf area in (*Phaseolus vulgaris L.*) by non-destructive method. *J. Plant Physiol*. **29**: 96-100.

Chapman, H. D. and P. E. Pratt. 1965. Methods of analysis for soils, plants and waters. Univ. of Calif., *Div. of Agric. Sci*. pp. 309.

Haidar, B., M. Ferdous, B. Fatema, S. H. Ferdous, M. H. Islam and H. Khan, 2018. Population Diversity of Bacterial Endophytes from Jute and Evaluation of Their Potential Role as Bioinoculant. *Microbial. R*es. **208**: 43-53.

Hamidi, A., R. Chaokan, A. Asgarjadeh, M. Dehghanshoar, A. Gahlavand and M.J. Malakouti, 2009. Effect of plant growth promoting rhizobacteria (PGPR) on phenology of late maturity maize (*Zea mays* L.) hybrids. *Ira. J. crop. Sci*. **11**(3): 249-270.

Huq, S.M.I. and M.D. Alam, 2005. *A handbook on analysis of soil, plant and water*. BACER-DU, University of Dhaka, Bangladesh, xxii+ pp. 1-246.

Idries, M. and G.R. Sandhu, 1979. *Rhizobium* inoculation in the mungbean cultivation. *J. Sci*. **31**(3-4): 165-173.

Jackson, M.L. 1958. Soil Chemical Analysis. Prentice Hall Inc., Englewood Cliffs. New Jersy, USA. **85**.

Jackson, M.L. 1962. Soil chemical analysis. Prentice Hall of India Pvt. Ltd., New Delhi. pp. 215-224.

Jackson, M.L. 1973. Soil Chemical Analysis. Prentice Hall Inc., Englewood Cliffs. New Jersy, USA. pp. 1-498.

Jagdale, N.G., B.B. More, B.K. Kove and P.L.L. Patil, 1980. Effect of different dose of *rhizobium* inoculation on nodulation, dry matter weight, nitrogen content and yield of bangal gram. *Fill. Pnn. Agric.* **19**(1): 216-162.

Kelly, C. and K. Knutzen, 2008. The Urban Homestead: your guide to self-sufficient living in the heart of the city. Port Townsend: Process Self Reliance Series.

Lyngdoh, Y.A., R. Mulge and A. Shadap, 2013. Heterosis and combining ability studies in near homozygous lines of okra [*Abelmoschus esculentus* (L.) Monech] for growth parameters. *The Bioscan.* **8**(4): 1275-1279.

Malik, B.S., S. Paul, R.K. Sharma, A.P. Seth and O.P. Verma, 2005. Effect of Azotobacter chrocochum on wheat (Triticum aestivum L.) yield and its attributing components. *Ind. J. agri. Sci.* **75** (9): 600-602.

Nuruzzaman, M., M. Ashrafuzzaman, M.Z. Islam and M. R. Islam, 2013. Effect of biofertilizers on vegetative growth of okra. *Korean. J. Crop. Sci*. **48** (2): 73-80.

Page, A.L., R.H. Miller and D.R. Keeney, 1989**.** Method of soil analysis, part-2, 2nd ed. *American Soc. Agnon. Inc. Pub*. Madison, Wisconsin, USA.

Piper, C.G. 1950. Soil and plant Analysis. Hans Publishers, Bombay, India.

Prabhu, T., S. Ismail, A.K. Sannindranath and M. Rofi, 2003. Effect of integrated nutrient management on growth and yield of okra (*Abelmoschus esculentus* (L.) Monech) cv Parvani Kranti. Orissa J. Hort. **31**: 17-21.

Tanwar, S.P.S., G.L. Sharma and M.S. Chahar, 2003. Effect of P and biofertilizers on yield, nutrient content and uptake by blackgram (*Vigna mungo*). *Legume. Res*. 26(1): 39-49.

Tharmaraj, K., P. Ganesh, K. Kolanjinathan, R. Suresh Kumar and A. Anandan, 2011. Influence of vermicompost and vermiwash on physicochemical properties of rice cultivated soil. *Curr. Bot.* **2**(3): 18-21.

Thenua, O.V.S. and R.K. Sharma, 2011. Effect of phosphorus, sulphur and phosphate solubilizing bacteria on productivity and nutrient uptake of cheakpea. *Annuals. Agri. Res*. **32**(3-4): 116-119.

USSLS (United State Salinity Laboratory staff). 1954. Diagonostic and Improvement of Saline and Alkali soils. Agricultural Handbook No. 60. United states Department of Agriculture, USA. pp. 160-170.

Walkey, A. and I.A. Black, 1934. An examination of Degtjareff methods for determining soil organic matter and proposed modification of the chronic acid titration method. *Soil Sci*. **37**: 29-38

(Revised copy received on 13/03/2025)

J. Asiat. Soc. Bangladesh, Sci. **51**(1): 115-122, June 2025
DOI: http://doi.org/10:3329/jasbs.v51i1.82795

DESCRIPTION OF A NEW SPECIES OF ORB-WEAVING SPIDER OF THE GENUS *CYRTARACHNE* THORELL, 1868 FROM BANGLADESH (ARANEAE : ARANEIDAE : CYRTARACHNINAE)

V. BISWAS[1]* AND D. RAYCHAUDHURI[2]
[1]*Department of Zoology, Khulna Government Womens' College Khulna-9000, Bangladesh*
[2]*Entomology Laboratory, Department of Zoology, University of Calcutta, Kolkata-700 019, India*

Abstract

Taxonomic description of a new species of orb-weaving spider of genus *Cyrtarachne* Thorell is provided herewith. In this study, species *Cyrtarachne kaikobadi* n. sp. was identified as new to science. The paper presents an illustrated description of the new species together with brief generic diagnosis and distribution.

Key words: Taxonomy, Orb-weaving spider, *Cyrtarachne,* Araneae, Araneidae, Cyrtarachninae, Bangladesh.

Introduction

Spiders of the genus *Cyrtarachne* Thorell are common orb-weaving spiders in the garden and forests of Bangladesh. They belong to the family Araneidae and make typical webs within plant leaves on which they stay for the preys. Their preys are composed of many small pest insects those are injurious to economic plants. Members of the genus *Cyrtarachne* are colourful, small to medium in size and are typical in shape. They are very slow in nature and some times stay whole day on the webs in the same position for the preys. They are one of the common biological control agents of insect pests in the gardens and forests.

The genus *Cyrtarachne* was first erected by Thorell in 1868 with the type-species *C. grubei* (Keyserling, 1864). At present, it is composed of 55 species in the world fauna and 12 species in the Indian Sub-continent but only 3 species are described in Bangladesh (World Spider Catalog, 2024; Tikader, 1960, 1962; Caleb and Sankaran, 2024; Biswas and Raychaudhuri, 2019; Chowdhury and Nagari, 1981; Okuma *et al.*, 1993). A good number of species are also described in other different countries of the world (Yin and Zhao, 1994; Barrion and Litsinger, 1995; Yin *et al.*, 1997; Song *et al.*, 1999; Tanikawa, 2007, 2013; Kim and Lee, 2012). The present paper contains illustrated description of a new species *C. kaikobadi* n. sp. with its generic diagnosis and distribution.

*Corresponding author: E-mail: vivekarach@gmail.com

Materials and Methods

Collection and Preservation: The specimens were collected from different gardens of southwestern coastal areas of districts Bagerhat and Khulna of Bangladesh during April to May. Collections were made by jarking the branches of trees and shrubs on an inverted umbrella placed underneath the plants. The specimens after collection were placed to a large glass jar containing wade of cotton with chloroform for anesthesizing the specimens. These were then transferred to a petridish filled with 70% ethyl alcohol for sorting. After sorting, the specimens were then placed to separate glass vials with 70% alcohol for future identification and study.

The collected specimens were primarily put in 70% alcohol and after identification, these were preserved permanently in Audmans' Preservatives (90 parts ethyl alcohol + 5 parts glycerine + 5 parts glacial acetic acid) following Lincoln and Sheals (1985) and Tikader (1987).

Identification and study: The specimens were identified by the study of various important taxonomic characters viz. - body shape, size, colour, eye pattern, decoration, structure of legs, chelicerae, pediplps, epigynum etc. The female epigynum was dissected out by the help of fine blade and the put it in clove oil for 10 to 12 hours (over night) following Levi (1965) and Tikader (1987). All other characters were studied following the description and keys made by different authors like - Davies (1988), Tikader (1982, 1987), Yaginuma (1986), Chen and Zhang (1991), Barrion and Litsinger (1995), Yin *et al.* (1997), Tanikawa (2007), Biswas (2009) and Kim and Lee (2012).

After identification, the species was later confirmed from the Arachnida section, Zoological Survey of India, Kolkata. The specimens are now preserved with the collection of the Department of Zoology, Khulna Government Womens' College, Khulna and later it will be deposited permanently to the Museum of the Department of Zoology, University of Dhaka, Bangladesh, in due course of time.

Illustration and photograph: Whole body and different body-parts of spiders were illustrated by a Camera Lucida fitted with Stereozoom Binocular Microscope. Leg and palpal measurements were taken under the same condition in the following sequences : femur, patella, tibia, metatarsus, tarsus and total length and all these measurements are taken in millimeters (mm).

The Photographs of the identified specimens were taken in natural condition (in the field by DSLR Camera) and in the laboratory by Camera fitted microscope (model SV8, Zeiss).

Results and Discussion

Systematics

Family: ARANEIDAE Clerck, 1757; Subfamily: Araneinae O.P. Cambridge, 1871
Tribe: Araneini O.P. Cambridge, 1871; Genus: *Cyrtarachne* Thorell, 1868

Type species: *C. grubei* (Keyserling, 1864) 1868. *Cyrtarachne* Thorell, *Eng. Resa. Arachn.* : 10. *Dema* : Karsch, 1878 : 801; *Cyrtarachne*: Simon, 1895 : 880; Pocock, 1900 : 228; Yaginuma , 1960 : 61 ; Tikader, 1960 : 547; Barrion and Litsinger, 1995: 581; Platnick, 1997 : 498; Yin *et al*. : 267; Majumder, 2005 : 9; Biswas, 2009: 149; World Spider Catalog, 2024 , Version 24.5, Nat. Hist. Mus. Bern, http ://wsc.nmbe.ch

Diagnosis: Spiders of the genus *Cyrtarachne* Thorell are small to medium in size with body rounded to nearly rounded. Cephalothorax dorsally strongly convex and wider than long. Eyes small; lateral eyes large and contiguous. Chelicerae small, thick ; inner and outer margins with small teeth. Maxillae and labium leathery and scopulate. Legs long and slender ; tibiae I with strong spines.

Abdomen triangular or rhomboid or elongately oval, with or without humps ; leathery and with or without sigilla. Epigyne variable.

Biological note: These spiders build specialized geometrical webs within plant leaves in the garden and forests. They stay there long time for the preys and consume small pest insects from the webs. For this reason, they are considered as one of the important biological control agents of insect pests of economic plants.

Distribution: Asia, Australia, Africa.

Description of new species

***Cyrtarachne kaikobadi* n. sp.** (**Figs.1a - 1e; Plate 1**)

Material examined: Holotype : 1 female, Harinkhana , Bagerhat, 07. IV. 1997 & 18. V. 1997 , Coll. V. Biswas; Paratype: 1 female, ADI, Daulatpur , Khulna, 12. VII. 1998, Coll. V. Biswas; Allotype: Nil.

Designation of the types

Holotype: This is a single female specimen preserved permanently in Audmans' preservatives. It was collected from the web of a shrub of village Harinkhana, district Bagerhat on 7th April, 1997 and the whole illustrated description of the species is made on the basis of its taxonomic characters.

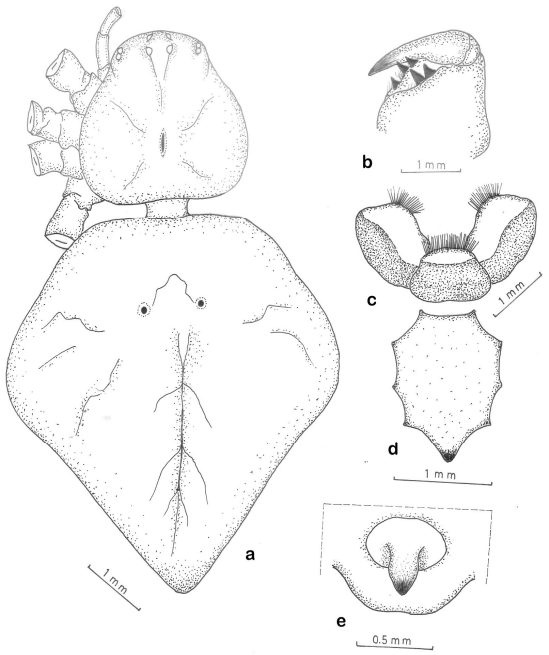

Fig. 1(a-e). *Cyrtarachne kaikobadi* n. sp. a. Whole body (dorsal view); b. Chelicerae; c. Maxillae & Labium; d. Sternum; e. Epigynum

Plate 1. *Cyrtarachne kaikobadi* n. sp. (dorsal view)

Paratypes: This is also a single female specimen collected from Agricultural Diploma Institute (ADI), Daulatpur, district Khulna. It is also preserved in Audmans' preservative on 12th July 1998.

General: Body small, brown, robust, nearly rhomboid. Cephalothorax and legs brown ; abdomen yellow-brown with white dorsal reticulate markings. Total body length 10 mm. carapace 4 mm long, 4.10 mm wide ; abdomen 6 mm long and 5.10 mm wide.

Cephalothorax: longer than wide, medially wide, anteriorly narrowing with 2 lateral and 1 median tubercles ; medially with a distinct transverse furrow ; cervical furrows weakly distinct (Fig. 1a). Eyes pearly white, similar; anterior row recurved and posterior row faintly so ; lateral eyes close and situated on tubercles ; median eyes marginal and placed lateral to the median tubercle ; ocular quad squarish. Chelicerae brown, small, strong, each of inner and outer margins with 2 and 3 teeth (Fig. 1b). Maxillae brown-black, longer than wide, anteromedially broad and scopulate (Fig. 1c). Labium brown-black, wider than long, anteriorly scopulate (Fig. 1c). Sternum dark brown, nearly heart-shaped, posteriorly bluntly pointed, anterior margin concave (Fig. 1d). Legs long and slender, clothed with spines and hairs; leg formula 2143 and the measurements (in mm) of leg segments are shown in Table 1.

Table 1. Measurements (mm) of leg segments of *C. kaikobadi* n. sp.

Leg	Femur	Patella	Tibia	Metatarsus	Tarsus	Total
I	2.10/2.10	1.00/1.00	2.00/2.00	2.10/2.10	0.60/0.60	7.80/7.80
II	2.80/2.80	1.00/1.00	2.00/2.00	1.80/1.80	0.60/0.60	8.20/8.20
III	1.80/1.80	0.60/0.60	1.20/1.20	1.00/1.00	0.50/0.50	5.10/5.10
IV	2.50/2.50	1.00/1.00	2.00/2.00	1.00/1.00	0.50/0.50	7.10/7.10

Abdomen : Rhomboid, medially wide, posteriorly narrowed and bluntly pointed ; dorsum anteromedially with 2 sigilla and decorated with white reticulate markings ; epigyne tongue-like (Fig. 1e).

Male unknown, it will be described when available in the collection.

Etymology: The species is named after Professor Muhammad Kaikobad of Govt. P.C. College, Bagerhat to whom I am greatly indebted in this research.

Distribution : Bangladesh : Gardens of village Harinkhana, district Bagerhat and Agricultural Diploma Institute (ADI) garden, Daulatpur, district Khulna (type-localities).

Remarks: The species is nearly related to *C. biswajiti* Biswas & Raychaudhuri, 2019 in having the rhomboid structure of both the species. But none of its congeneric species (Tikder, 1982 ; Yaginuma, 1986 ; Koh, 1989 ; Shinkai & Takano, 1988 ; Namkung & Kim, 1985 ; Barrion & Litsinger, 1995 ; Yin *et al.* 1997 ; Kim & Lee, 2012) are known have abdomen posteriorly nearly tail-like. The present species also possesses the following diagonostic characters -

1. Structure of female genitalia (or epigynum) is quite different and it is tongue-like (Fig. 1e).
2. Cheliceral inner and outer margins with 3 and 2 teeth respectively (Fig. 1b).
3. Maxillae and labium broad, scopulate and without any spine (Fig. 1c).
4. Structure of sternum elongate (Fig. 1d).

The species, is therefore, decribed as new to science.

Discussion

The new species *Cyrtarachne kaikobadi* n. sp. is a small, rhomboid, brownish coloured orb-weaving spider. Members of this spiders are available on the webs made by their own within gardens plants. It has some specialized diagnostic characters of like - chelicerae, maxillae, labium and also female genitalia on the basis of which it is established as a new species. So, from this study, it may be assumed that there are more numbers of endemic fauna (species) present in different areas of the country.

Taxonomic study on the orb-weaving spider genus *Cyrtarachne* Thorell of Bangladesh is scarce, except Okuma *et al.* (1993), Biswas (2009) and Biswas and Raychaudhuri (2019). Therefore, a detailed taxonomic study on this genus may discover several new species in future.

As the new species *C. kaikobadi* n. sp. is an inhabitant of the gardens and forests, so, it may expect that it must have a predatory role in controlling pest insects of those ecosystems.

Acknowledgements

The authors are grateful to late Dr. S. C. Majumder, Scientist – SD, Arachnida section, Zoological Survey of India, Kolkata, for the confirmation of species identification and also to the Head, University of Calcutta, for kind permission to allow the laboratory during the study (during 1993-95).

References

Barrion, A.T. and J.A. Litsinger, 1995. *Riceland spiders of South and Southeast Asia.* CAB International, Wallingford, U.K. ; International Rice Research Institute (IRRI), Philippines, 700 p. + 16 plates.

Biswas, V. 2009. *Encyclopedia of flora and fauna of Bangladesh. Vol. 18, Part - I, Arthropoda, Arachnida*, (Ahmed, Z. ed.). Asiatic Society of Bangladesh, Dhaka, 437 p.

Biswas, V. and D. Raychaudhuri, 2019. Taxonomic account of orb-weaving spider genus Cyrtarachne Thorell, 1868 (Araneae : Araneidae) of Bangladesh. *J. biodiverse. Conserve. bioresour. manag.*, **5**(2): 75-82.

Caleb, J.T.D. and P.M. Sankaran, 2024. *Araneae of India – Spider diversity of India,* Version 2023. Available from http ://www.indianspiders.in [accessed on 21st November, 2024].

Chen, Z.F. and Z.H. Zhang, 1991. *Fauna of Zhejiang, Araneida.* Zhejiang Science and Technology Publishing House, 356 p.

Chowdhury, S.H. and S. Nagari, 1981. Rice-field spiders from Chittagong. *Proc. Zool. Soc. Bangladesh:* 53-72.

Davies, V.T. 1988. Illustrated guide to the genera of orb-weaving spiders of Australia. *Mem. Qld. Mus.*, **25**: 273-332.

Kim, S.T. and S.Y. Lee, 2012. Invertebrate fauna of Korea : Araneid spiders. *Natl. Inst. Biol. Resour.*, **21**(16): 1- 146.

Koh, J.K.H. 1989. *A guide to common Singapore spiders*. Singapore Science Centre, 160p.

Levi, H. W. 1965. Techniques for the study of spider genitalia. *Psyche,* **72**(2): 152-158.

Lincoln, R. J. and J. G. Sheals, 1985. *Invertebrate Animals : Collection and Preservation.* British Museum (Natural History), London, 150 p.

Okuma, C., N.Q. Kamal, Y. Hirashima, Z. Alam and T. Ogata, 1993. *Illustrated Monograph on the rice-field spiders of Bangladesh.* IPSA - JICA, Salna, Gazipur, 93 p.

Shinkai, E. and H. Takano, 1984. *A field- guide to the spiders of Japan.* Tokai University Press, 204 p.

Song, D.X., M.S. Zhu and J. Che, 1999. *The Spiders of China.* Hebei Science and Technology Publishing House, 640 p.

Tanikawa, A. 2007. *An Identification Guide to the Japanese Spiders of the families Araneidae, Nephilidae and Tetragnathidae.* Arachnological Socielty of Japan, Osaka, Japan, 121 p.

Tanikawa, A. 2013. Two new species of genus *Cyrtarachne* (Araneae : Araneidae) from Japan hitherto identified as *C. inaequalis*. *Acta Arachnologica*, **62**(2): 95-101.

Tikader, B.K. 1960. Revision of Indian spiders of the genus Cyrtarachne (Argiopidae : Arachnida). *J. Bombay Nat. Hist. Soc.*, **57**(3): 547-556.

Tikader, B.K. 1962. Further studies on Indian spiders of the genus *Cyrtarachne* (Family Argiopidae). *J. Bombay Nat. Hist. Soc*., **60**(1): 268-276.

Tikader, B.K. 1982. *Fauna of India, Spiders (Araneae : Araneidae),* Vol. 2(1), Zoological Survey of India, Kolkata. 293 p.

Tikader, B.K. 1987. *Handbook on Indian Spiders*. Director, Zoological Survey of India, Kolkata. 251 p.

World Spider Catalog, 2024. *World Spider Catalog*, Version 24.5, Natural History Museum, Berlin, Online at – http :// www.wsc.nmbe.ch (accessed on 14th November, 2024).

Yaginuma, T. 1986. *Spiders of Japan in colour*. Hoikusha publishing Company Limited, Osaka, Japan, 305 p.

Yin, C.M. and J.Z. Zhao, 1994. Some species of the family Araneidae from China (Arachnida : Araneae). *Acta Arachnologica Sinica*, **3**(1): 1 - 7.

Yin, C.M., J.F. Wang, M.S. Zhu, L.P. Xie, X.J. Peng and Y.H. Bao, 1997. *Fauna Sinica : Arachnida : Araneae : Araneidae*. Science Press, Beijing, China, 460 p.

(Revised copy received on 24/03/2025)

J. Asiat. Soc. Bangladesh, Sci. **51**(1): 123-150, June 2025
DOI: http://doi.org/10:3329/jasbs.v51i1.82796

A TRUST-BASED MALICIOUS RSU DETECTION MECHANISM IN EDGE-ENABLED VEHICULAR AD HOC NETWORKS

FARHANA SIDDIQUA AND MOSARRAT JAHAN*
Department of Computer Science and Engineering, University of Dhaka, Dhaka-1000, Bangladesh

Abstract

Edge-enabled Vehicular Ad Hoc Networks (VANETs) provision real-time services, storage, computation, and communication facilities to vehicles through Roadside Units (RSUs). Nevertheless, RSUs are often easy targets for security assaults due to their resource-constrained nature and placement in an open, unprotected environment. The compromised RSUs impede the VANET operations, causing traffic mismanagement and threats to human safety. Hence, an effective malicious RSU detection mechanism is crucial for VANETs. More specifically, a mechanism to detect the misbehavior of RSUs on RSU-to-RSU (R2R) communications, essential for message forwarding, beacon message sharing, and traffic alert sharing among RSUs, needs to be included. Besides, current works use only vehicle speed and density in beacon messages to assess trust without considering the sensor-detected data in the same messages. Nonetheless, sensor data is useful for traffic management, and neglecting them creates inaccuracy in trust estimation. This paper addresses these limitations and proposes a trust-based scheme to detect malicious RSUs that uses R2R interaction to analyze an RSU's behavior. We also offer a mechanism to detect alteration of sensor-detected data in beacon content and incorporate this scheme in the trust calculation of RSUs. The experimental results show that the proposed solution effectively detects approximately 92% malicious RSUs, even in the presence of hostile vehicles. Moreover, integrating the proposed solution with the VANET routing protocols improves routing efficiency.

Key words: Vehicular Ad Hoc Networks, VANET, Roadside Unit (RSU), Trust Management, Security, Beacon Message

I. Introduction

Vehicular Ad Hoc Network (VANET) is a leading-edge technology enabling systematic management of vehicles running on roads and highways. It models the transportation system as an ad hoc network and facilitates information exchange among the moving vehicles (Onieva *et al.*, 2019). It improves human safety, reduces road accidents and traffic jams, and creates provisions for smart travel planning (Sheikh *et al.*, 2019). Due to the highly dynamic environment of VANET, the availability of correct information at the right moment is a prime requirement for its proper operation. In this regard, Roadside

*Corresponding author: mosarratjahan@cse.du.ac.bd

Units (RSUs) play a vital role in accelerating information processing and providing services at low latency. However, the advantage of minimum latency comes with the cost of numerous security and privacy issues introduced by RSUs, affecting information accuracy (Abhishek *et al.*, 2019).

RSUs are edge devices usually deployed along the roadside on traffic lights, bus stops, road signs, etc., to provide various services to the vehicles (Onieva *et al.*, 2019) They can be installed anywhere but are cost-effective to deploy in areas where traffic volume is high, and placement of expensive general-purpose edge devices with higher computing facilities is not feasible (Onieva *et al*., 2019). In VANETs, RSUs are trusted with several important responsibilities such as vehicle authentication (Yao *et al.*, 2019), rogue vehicle detection (Al-Otaibi *et al.*, 2019), and revocation (Malik *et al.*, 2018). However, RSUs fall short of serving their purposes competently for two reasons. Firstly, they are typically resource-constrained compared to the general-purpose edge devices, although they have enough resources to serve the vehicles in their coverage area (Onieva *et al.*, 2019). Due to their resource-constrained nature, they cannot support computation-intensive security mechanisms, making them easy victims of various security attacks. Secondly, due to the outdoor placement without tight protections from network operators, RSUs are vulnerable to intrusions, physical attacks, malfunctions, node compromise, sensor tampering attacks, etc. (Van der Heijden *et al.*, 2018). Therefore, RSUs compromised by security attacks severely affect the correct functioning of the entire system, leading to severe consequences threatening human safety. Hence, accurate identification of malicious RSUs and avoiding them from the VANET operation is essential to ensure safe, secure and time-sensitive operation of VANETs.

Traditional cryptography-based security mechanisms are not suitable for dynamic-nature VANET due to their time-consuming and intensive computations and the inability to address some security attacks such as false data injection and internal attacks (Zaidi *et al*., 2014). Hence, trust-based schemes have been considered as an alternative to identify malicious entities in VANET at a low-cost (Hussain *et al.*, 2020). At present, very few research works focus on identifying the malicious behavior of RSUs, an indispensable part of VANETs (Abhishek *et al.*, 2019; Lu *et al.*, 2018; Alnasser and Sun, 2021). Among them, (Abhishek *et al.*, 2019) detects malicious RSUs based on vehicles' feedback (vehicle-to-RSU (V2R) communication), (Lu *et al.*, 2018) based on Received Signal Strength Indicator (RSSI), and (Alnasser and Sun, 2021) based on the discrepancy of an RSU's decision with other RSUs. However, none of them consider the behavior of an RSU on R2R communication. Besides providing services to vehicles and other road entities, RSUs also interact with their one-hop neighbor RSUs for message routing

(Mershad *et al.*, 2012), periodic beacon message broadcasting (Maglaras *et al.*, 2013), and traffic alert sharing (Jindal and Bedi, 2017). They use message routing to forward vehicles' data packets (Mershad *et al.*, 2012) and utilize beacon messages to share traffic information with other RSUs and vehicles (Maglaras *et al.*, 2013). Besides, RSUs share traffic alerts to avoid unwanted situations such as accidents and bad road conditions (Jindal and Bedi, 2017). This indicates that R2R transmissions occupy a significant portion of the communications that an RSU uses to contact the VANET entities. Hence, the trustworthiness of an RSU should also reflect its reliable behavior in all these aspects, which is missing in the existing literature. In contrast to V2R communication, R2R communications are stable as the positions of RSUs are static, and they frequently interact with their one-hop neighbor RSUs, enabling precise and error-free trust calculations.

Besides, existing works verify vehicle speed and density to determine the legitimate beacon content, and these parameters are used in the trust calculation based on beacon messages (Arshad *et al.*, 2018; Zaidi *et al.*, 2015). Apart from vehicle speed and density, an RSU also shares sensor-detected data such as humidity (Jindal and Bedi, 2017), temperature (Jindal and Bedi, 2017), and carbon emission level (Maglaras *et al.*, 2013) in beacon messages. The correctness of these sensor-detected data is also crucial as they directly impact traffic management; for example, vehicles usually try to avoid industrial areas prone to excessive carbon emissions. Hence, ignoring sensor-detected data to verify the validity of beacon content can create difficulty in traffic management. Therefore, trust calculation based on the beacon content should also reflect the correctness of sensor data, which is not considered in the literature.

In this paper, we address the shortcomings mentioned above and propose a malicious RSU detection mechanism based on trust calculations that evaluates an RSU's behavior depending on its interaction with other RSUs in the VANET. In particular, we make the following contributions:

- We propose a trust-based mechanism to assess an RSU for its behavior in all the R2R communications. We incorporate an equation to compute an aggregated trust score of an RSU that uniquely combines its score in individual R2R communication.
- We offer a robust mechanism to detect the correctness of sensor-identified data in a beacon message and assign a weight to each beacon message based on the validity of its sensor data. Finally, sensor data verification is combined with the verification of vehicle speed and density in the same beacon message to compute trust based on beacon content.
- We implement the proposed scheme and evaluate the performance through extensive

experiments. The results demonstrate the effectiveness of the proposed solution in detecting malicious RSUs, which is approximately 92% in the presence of rogue vehicles. The experimental results also show that the proposed scheme improves the routing efficiency of the existing VANET routing protocols when incorporated with them. Besides, we observe that sensor data verification in beacon messages moderately improves the decision accuracy of the proposed scheme.

II. Related Work

Trust-based mechanisms are cost-effective solutions to detect malicious entities in VANETs. They assign trust scores to VANET entities based on their behavior to measure their credibility (Hussain *et al.*, 2020; Soleymani *et al.*, 2015). Although there are numerous works on the trust mechanisms for detecting malicious vehicles (Hussain *et al.*, 2020; Soleymani *et al.*, 2015; Tripathi and Sharma, 2019), very few papers consider the issue of identifying rogue RSUs.

(Abhishek *et al.*, 2019) proposed a trust-based mechanism where every vehicle sends feedback about the RSU it has interacted with to a central trusted server. In this regard, a vehicle evaluates an RSU based on the channel quality and the total number of packets received from or transmitted to the RSU. The central trusted server calculates an aggregated trust value for every RSU based on the received feedback that is later compared with a threshold value to classify the RSU as malicious or authentic. They also employed a Gaussian kernel-based similarity metric mechanism to handle the impact of false feedback from misbehaving vehicles. This work only considered downlink packet drops; therefore, the authors proposed an updated version in (Abhishek and Lim, 2022) that defends uplink attacks and downlink attacks. However, this model only handles selective packet modification attacks performed by RSUs during V2R communication, which partly reflects the behavior of an RSU. Besides, (Lu *et al.*, 2018) used the physical (PHY)-layer properties such as RSSI of the ambient radio signal to detect rogue edge nodes. In this scheme, resource-limited smartwatches and smartphones inside a car outsource heavy computation to an edge node located inside the vehicle. In this case, an outside malicious edge node situated in the VANET environment can launch a man-in-the-middle attack by sending messages to the mobile devices requesting services. The mobile device uses the physical layer properties to distinguish ambient radio signal traces of an outside edge node from an inside legitimate edge node. However, this solution cannot ensure the content accuracy shared by the edge devices, which is crucial for the reliable operation of the VANET. Moreover, (Hao *et al.*, 2008) proposed a distributed key

management scheme where a trusted authority plays the role of the key generator and an RSU as a key distributor. An RSU forms a group with the vehicles within its transmission range and provides them the group key after confirming vehicles' authenticity. After receiving any complaints about other misbehaving vehicles, the trusted authority takes help from the RSU to recover the malicious vehicle's real identity. In this case, a compromised RSU might provide the signature of a legitimate vehicle instead of the malicious one to the authority. The proposed scheme prevents this issue by not providing RSU any access to vehicles' private keys. The main goal of this work is to ensure that an RSU performs its duty accurately as a key distributor not to identify the rogue RSUs. (Alnasser and Sun, 2021) proposed a trust model to prevent malicious RSUs that conduct recommendation attacks while detecting rogue road entities such as vehicles, cycles, motorcycles, and pedestrians. In this model, every VANET entity observes their one-hop neighbors' behavior and sends their observations to the nearest RSUs. The responsible RSU analyzes the received behavioral information and decides on an entity's trustworthiness. Besides, it sends the final list to the central cloud server, which monitors RSUs' behavior and makes the final decisions regarding malicious road entity detection. In contrast to the previous works, our proposed solution analyzes the behavior of an RSU in all the means it can communicate with other RSUs in the VANET and produces an aggregated trust value reflecting realistic conjecture on the reliability of an RSU for R2R communications.

Existing research works that explore false data detection mechanisms in VANETs mainly consider vehicles' speed and density shared in beacon messages. For example, (Arshad *et al.*, 2018) proposed a trust management system and fake data detection scheme that utilizes vehicle speed and density shared in beacon messages to measure the trustworthiness of a vehicle. This scheme also uses beacon and safety messages to filter out incorrect messages and gets facts from data to assess traffic data reliability. Besides, (Zaidi *et al.*, 2015) proposed an Intrusion Detection System (IDS) that also uses speed and density collected from neighbor vehicles' beacon messages to identify rogue vehicles. The proposed IDS analyzes the collected data statistically to detect false information attacks. In another work, (Al-Otaibi *et al.*, 2019) classified traffic data using vehicle speed to identify rogue vehicles. In this work, an RSU analyzes traffic data provided by vehicles within its transmission area to calculate an estimated speed range. A vehicle is rogue if its speed does not belong to the calculated speed range. Similarly, (Paranjothi *et al.*, 2020) also utilized vehicles' speed to detect rogue vehicles. This scheme chooses vehicles with a more significant number of neighboring nodes as guard vehicles. These vehicles perform a hypothesis test on the neighbor vehicles' speed to

identify malicious vehicles. Moreover, (Liu *et al.*, 2020) proposed a false message detection scheme that uses a traffic flow model to analyze the actual behavior of a vehicular environment by utilizing vehicle speed and density collected from neighbor vehicles' beacon messages. (Jalooli *et al.*, 2024) utilized Blockchain to store trust scores of vehicles. This scheme validates sensor data to determine message authenticity. It further allows vehicles to query RSUs to get information on the trustworthiness of message sender vehicles. Besides, (Zhang *et al.*, 2024) used both vehicle consensus and Gradient Boosting Decision Tree (GBDT) to detect false messages where vehicle densities are processed as time series data. (Lone and Verma, 2025) proposed a mechanism to detect misbehavior in VANETs based on multidimensional plausibility and consistency checks on beacon data, focusing on position and speed information.

In contrast to prior works, our scheme considers sensor-detected data as well as speed and density information in the beacon messages to verify the validity of traffic data and incorporates both types of data to evaluate trust based on beacon content.

III. Proposed Scheme

In this section, we present a trust-based solution to detect malicious RSUs in the VANET. We first discuss the system model for the proposed scheme, followed by a detailed description of the working principle of the proposed scheme.

A. System Model

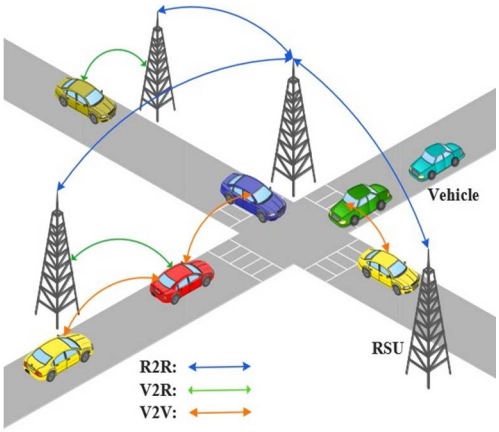

Fig. 1. System model of the proposed scheme.

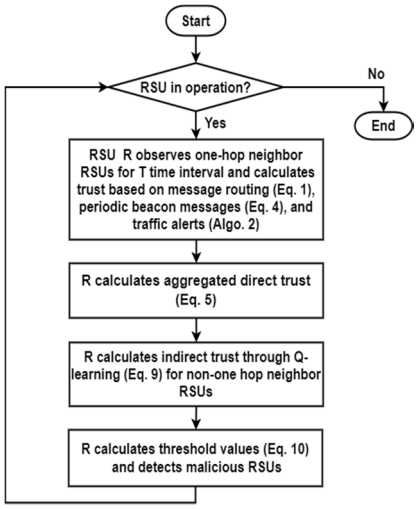

Fig. 2. Flow diagram of the proposed scheme for RSU *R*.

Figure 1 presents the system model of our proposed scheme. It comprises two entities, *vehicles* and *RSUs*. *Vehicles* are equipped with an Onboard Unit (OBU), a Global Positioning System (GPS), and different types of sensors to collect information from their surroundings (Onieva *et al.*, 2019). They exchange periodic beacon messages, which is also known as Basic Safety Message (BSM) (Van der Heijden *et al.*, 2018) and Cooperative Awareness Message (CAM) (Jin and Papadimitratos, 2018) to inform their existence and provide traffic information perceived through their sensors. They also share traffic alerts to notify emergency events to other vehicles and the nearest RSU. The communication among the vehicles known as Vehicle-to-Vehicle (V2V) communication ranges from 50 to 300 meters (Zhang and Chen, 2019). On the other hand, the communication between an RSU and vehicles is known as V2R communication. *RSUs* are local cloud servers placed at less than the one-kilometer distance in an area where traffic volume is usually high (Zhang and Chen, 2019). They are equipped with a network device supporting IEEE 802.11p protocol, devices to communicate with the infrastructure network, a GPS, and sensors (Van der Heijden *et al.*, 2018). They provide real-time services to vehicles and process the data collected from vehicles through V2R communications (Al-Otaibi *et al.*, 2019). Besides, RSUs generate beacon messages periodically (Maglaras *et al.*, 2013) and share alert messages when emergency events occur (Jindal and Bedi, 2017). They also work as a relay node to propagate messages generated by vehicles and RSUs (Mershad *et al.*, 2012). An RSU communicates with other RSUs via R2R communication, and the communication range is limited to 1000 meters (Zhang and Chen, 2019). We consider a hop count of 6 to transmit messages generated by RSUs as traffic data can be relevant up to $5km$ (Lee *et al.*, 2014) and the maximum distance between two RSUs is $1km$.

B. ***Overview of the Proposed Scheme***

Each RSU R monitors its one-hop neighbor RSUs for a pre-defined time duration T shown in Fig. 2. During this time, R observes the behavior of its one-hop neighbor RSUs for routing messages, broadcasting beacon messages, and transferring traffic alerts. When T expires, R assigns trust scores to its neighbors in each of the above-mentioned communication scenarios based on their behavior and eventually combines all the trust scores to calculate the direct trust of the one-hop neighbor RSUs. For non-one hop RSUs, R uses the Q-learning mechanism (Guleng *et al*., 2019) to determine their trust values. R also decides a threshold value for every other RSUs in the network and compares it with the corresponding trust value to identify an RSU as *legitimate* or *compromised* node.

*C. **Trust Calculation based on Message Routing***

The proposed scheme observes the behavior of an RSU for dropping packets and altering packet content while it acts as a relay node to route messages from a source vehicle to a destination vehicle (Mershad *et al.*, 2012), or forward packets from remote RSUs to a central RSU (Huang *et al.* 2017). Each RSU R_1 forwards packets to its one-hop neighbor RSU R_2 and monitors the behavior of R_2 on forwarding these packets for a fixed time interval *T*. R_1 counts the number of forwarded and dropped packets by R_2 and checks whether the forwarded messages are maliciously modified. Based on the observation, R_1 calculates the trust value, $Trust_{routing}$ of R_2 as follows:

$$Trust_{routing} = \frac{P_{forward}}{P_{forward} + P_{drop}} \times P_{modify} \quad (1)$$

where $P_{forward}$ is the number of packets forwarded, P_{drop} is the number of packets dropped, and P_{modify} is the packet modification parameter. Eq. 1 indicates that $Trust_{routing}$ is computed based on packet forwarding ratio ($P_{forward}/P_{forward} + P_{drop}$) and packet modification parameter (P_{modify}). Here, P_{modify} is a binary variable where $P_{modify} = 0$ when an RSU is maliciously altering packet content and $P_{modify} = 1$ for an honest RSU not changing packet content. The multiplication operation in Eq. 1 puts higher priority on P_{modify} as $P_{modify} = 0$ makes $Trust_{routing} = 0$. This argument is justified as the trust value of a malicious RSU modifying packet content should be 0 even though it is forwarding some data packets. $Trust_{routing}$ varies in the range [0, 1].

Each RSU R_1 uses a Watchdog module (Marti *et al.*, 2000) that overhears the incoming and outgoing traffic of other entities within R_1's transmission range. Hence, a watchdog module of R_1 can detect whether R_2 forwards a packet towards the next node. This module stores the recently sent packets by R_1 and removes a packet from the buffer when it overhears the same packet being forwarded by the next-hop RSU R_2. In this case, R_1 increments $P_{forward}$. If a packet remains in the buffer for more than the expected time $t_{expected(R_1, R_2)}$, R_1 considers R_2 has dropped that packet and increments P_{drop}. R_1 calculates $t_{expected(R_1, R_2)}$ as follows (Bhoi, and Khilar, 2014):

$$t_{expected(R_1, R_2)} = \frac{L}{r_{(R_1, R_2)}} + \frac{d_{(R_1, R_2)}}{V_{propagation}} + t_{other} \quad (2)$$

where *L* is the length of message, $r_{(R_1, R_2)}$ is the data transmission rate, $d_{(R_1, R_2)}$ is the distance between R_1 and R_2, $V_{propagation}$ is the propagation speed, and t_{other} represents the queuing and processing delay. The watchdog module in R_1 estimates t_{other} from the packet forwarding tendency of R_2 that can be computed by taking the

difference of packet reception time and packet forwarding time in R_2. Besides, R_1 adjusts the link data rate based on the value in the *window* field of the TCP header in acknowledgement packets.

The watchdog mechanism also compares the hash value of a packet on the incoming interface of the observed RSU with the hash value of the same packet on the outgoing interface (Patil and Tahiliani, 2014). The hash values are computed on the packet fields that are not supposed to change during routing (Patil and Tahiliani, 2014). If both hash values are the same, then no packet modification is performed by next-hop RSU. If the watchdog module detects a packet modification then R_1 sets P_{modify} = 0, otherwise P_{modify} = 1.

D. ***Trust Calculation based on Beacon Messages***

Each RSU periodically transmits *hello* messages that are beacon messages to its one-hop neighbor RSUs and vehicles to inform its existence and traffic-related information (Maglaras *et al.*, 2013). The proposed scheme considers the beacon message generation rate and the accuracy of beacon message content to detect malicious behavior of RSUs. An RSU is trustworthy only when it does not cause flooding attacks and propagate false information using beacon messages. Hence, the proposed scheme first examines whether any flooding attack occurs. If a flood attack is not detected, trust value for beacon messages is computed by analyzing the correctness of beacon content.

1) ***Trust Calculation based on Beacon Message Generation Rate:*** A malicious RSU prevents the message propagation by other entities of the VANET by flooding the communication channel with beacon messages. We use the flooding attack detection mechanism proposed in (Sajjad *et al.*, 2015) to detect RSU's misbehavior. An RSU R_1 observes its one-hop RSU R_2 in a time slot i of length T and counts $B_i(R_2)$, the number of beacon messages generated by R_2 during this interval. R_1 also keeps track of the beacon message rate of R_2 for the latest Z time slots and calculates the weighted average of beacon message generation rate as $B_{avg}(R_2) = \sum_{t=1}^{Z}(t/Z) \times B_t(R_2)$. If $B_i(R_2) > B_{avg}(R_2)$ in a time slot *i*, then flooding attack is detected, and R_1 sets $Trust_{beacon}$ to 0; Otherwise $Trust_{beacon}=1$.

Sender ID	Position	Timestamp	Event Type	Event Value	Location

Fig. 3. Vehicle and RSU traffic alert format.

2) ***Verification of Beacon's Content****:* Each RSU periodically shares beacon messages with its adjacent RSUs and vehicles within its transmission range to notify its existence, traffic condition, weather forecast, etc. (Jindal and Bedi, 2017). Besides, vehicles also

share beacon messages with their neighbor vehicles and the nearest RSU. Alongside, an RSU collects data about traffic situations, weather, etc. through its sensors (Sheikh *et al.*, 2019). Thus, an RSU receives huge volume of data from the beacon messages provided by both vehicles and neighbor RSUs and from its sensors (Hussain *et al.*, 2020). The RSU analyzes those data, generates aggregated results for different purposes, and includes the analyzed result in the beacon messages to provide a traffic overview to the vehicles and one-hop neighbor RSUs. An RSU usually shares speed (Al-Otaibi *et al.*,

Algorithm 1. Content verification of the *i*-th beacon message.

Input:
$TH_{speed\_density}$: threshold to verify speed and density
TH_{time}: threshold to verify timestamp
n: number of beacon messages received in T
Speed: estimated average speed by R_1
Density: estimated vehicle density by R_1
$B[i].Speed$: speed in R_2's i-th beacon
$B[i].Density$: vehicle density in R_2's i-th beacon
M_V: traffic alert received from a vehicle
$X[n]$: list of vehicle count reporting *IGNORE_RSU*
$Beacon[n]$: list of beacon message status

```
1:  function VERIFY_BEACON_CONTENT(R2, B[i])
2:      Y = N = 0
3:      if |B[i].Speed − Speed| ≥ TH_speed_density then
4:      Beacon[i] = 0
5:      else if |B[i].Density − Density| ≥
        TH_speed_density then
6:      Beacon[i] = 0
7:      else
8:      Beacon[i] = 1
9:      end if
10:     if Beacon[i] = = 1 then
11:     while M_V ! = NULL do
12:     if M_V.Event_Type = =' IGNORE_RSU'
13:     and M_V.Event_Value = = 0 and
14:     B[i].Timestamp − M_V.Timestamp ≤ TH_time
15:     and M_V.Location == R2.Position then
16:         Y + +
17:     else
18:         N + +
19:     end if
20:     end while
21:     end if
22:     if Y > N then
23:         Beacon[i] = 0
24:         X[i] = Y
25:     else if Y = = 0 then
26:     Total ← count_adjacent_vehicle()
27:     X[i] = Total
28:     else
29:         X[i] = Y
30:     end if
31: end function
```

2019), density (Arshad *et al.*, 2018), temperature (Jindal and Bedi, 2017), humidity (Jindal and Bedi, 2017), and carbon emission level (Maglaras *et al.*, 2013) in beacon messages. If flooding attack is not detected (discussed in Section III-D1), R_1 verifies the content of the i-th beacon message received from R_2 in two ways as described in Algo. 1. They are:

- R_1 estimates the speed and density of vehicles coming from the area of R_2 (Al-Otaibi *et al.*, 2019; Arshad *et al.*, 2018) and matches them with the same information in R_2's beacon message. If they vary by a certain threshold value, $TH_{speed\_density}$, R_1 sets the i-th beacon message, $Beacon_i = 1$; Otherwise, R_1 sets $Beacon_i = 0$ shown in lines 3∼9 of Algo. 1.
- In line 10, if $Beacon_i = 1$ (i.e, the speed and density information are correct) R_1 counts the feedback of intermediate vehicles to verify the remaining data in R_2's i-th beacon message. A vehicle V in the transmission range of R_2 verifies temperature, humidity, and carbon emission level shared in R_2's beacon message through its sensors. If the discrepancy of information in R_2's beacon message and V's sensor data exceeds a threshold value, TH_{sensor_data}, V generates an *IGNORE_RSU* traffic alert indicating invalid content. The neighbor vehicles of V verify the generated alert as they have also received the same beacon message from R_2. They share V's alert with their neighbor vehicles if the alert is correct. Otherwise, they discard the traffic alert. Thus, the alert propagates through the VANET and ultimately reaches the one- hop neighbor RSU R_1. R_1 receives alerts from multiple adjacent vehicles and counts those IGNORE_RSU alerts M_V whose timestamp difference with R_2's i-th beacon is less than or equal to a pre-defined threshold value TH_{time} in lines 10∼21. If the majority of neighbor vehicles ($Y > N$ in line 22) agree that R_2's beacon content is inaccurate, R_1 sets $Beacon_i = 0$, otherwise $Beacon_i = 1$. Here, $X[i]$ keeps a record of the number of adjacent vehicles of R_1 reporting IGNORE_RSU for the i-th beacon and used to calculate a weight w_i in Eq. 3. If R_1 does not receive any alert, $X[i]$ is set to the number of adjacent vehicles in lines 26∼27 in Algo. 1. Note that in Algo. 1, R_1 verifies speed, density, and sensor data one by one and considers neighbor RSU R_2 legal ($Beacon_i = 1$) if all of these parameters are accurate. However, R_2's beacon content is considered invalid if R_1 finds modification in any of these parameters and does not proceed to check another one.

In our scheme, both vehicles and RSUs generate traffic alerts following the format shown

in Fig. 3 (Arshad *et al.*, 2018). Here, *Sender ID* is a unique ID of a vehicle or RSU, *Position* is the current position of a vehicle or RSU, *Timestamp* is the traffic alert creation time, *Event Type* indicates traffic event, *Event Value* contains a binary value to indicate the presence and absence of the event and *Location* denotes the event place. We define a new event type *IGNORE_RSU* to detect invalid data. A vehicle assigns *Event Value* = 0 for *IGNORE_RSU* to indicate an RSU at *Location* is a malicious RSU generating false data and 1 to confirm it as an honest RSU.

3) ***Trust Calculation based on Beacon Content:*** Suppose R_1 receives *n* beacon messages from R_2 during *T*. R_1 receives *IGNORE_RSU* alerts from adjacent vehicles and determines $Beacon_i$ based on majority vehicles' opinion or the result of its verification of speed and density as shown in Algo. 1. R_1 assigns a weight w_i to each beacon message *i* as follows:

$$w_i = \frac{X_i}{\sum_{i=1}^{n} X_i} \tag{3}$$

where X_i is the total number of one-hop neighbor vehicles of R_1 reporting *IGNORE_RSU* alert for the *i*-th beacon message. w_i actually indicates the proportionality of adjacent vehicles of R_1 reporting IGNORE_RSU alerts for the *i*-th beacon to the total number of adjacent vehicles generating IGNORE_RSU alerts for *n* beacon messages in *T*. If $Beacon_i$ = 1 (i.e, the speed and density information are correct) and no alert is received for the *i*-th beacon message in sensor data verification phase (line 25 of Algo. 1), X_i is set to the total number of vehicles adjacent to R_1 to prevent w_i setting to 0 and assign highest possible trust score to an RSU not altering beacon content. The trust value based on beacon content is calculated as the weighted average of $Beacon_i$ generated during *T* as $\sum_{i=1}^{n}(w_i \times Beacon_i)$. Here, w_i is multiplied with $Beacon_i$ to assign a score on R_1's belief on the correctness of the *i*-th beacon message. Finally, the trust based on beacon message is computed as follows:

$$Trust_{beacon} = \begin{cases} 1/0, for\ flooding\ attack \\ \sum_{i=1}^{n}(w_i \times Beacon_i), \quad otherwise \end{cases} \tag{4}$$

E. ***Trust Calculation based on Traffic Alerts***

Traffic alerts are time-sensitive, and erroneous traffic alerts can cause serious problems such as difficulties in managing traffic and creates threats to human safety (Zaidi *et al.*, 2014). When an emergency event occurs, vehicles observing that event generate and broadcast traffic alerts to the vehicles within their transmission range and the nearest RSU (Arshad *et al.*, 2018). Similarly, RSUs noticing the same event also generate and broadcast the traffic alerts to the one-hop neighbor RSUs and vehicles under their coverage (Ahmed *et al.*, 2018). A malicious RSU can modify the traffic alert with

malicious intent. Thus, the trust of an RSU should also reflect the degree of RSU's capability of transmitting authentic traffic signals.

Figure 4 presents a scenario of how traffic alert is verified in the proposed scheme. Here, RSU R_2 monitors the area where an accident took place and RSU R_1 is a one-hop neighbor of R_2 observing the behavior of R_2 for T time duration. Vehicles observing the accident notify R_2 about the event and broadcast the traffic alert to vehicles within their transmission range. Besides, R_2 also broadcasts a traffic alert for the same accident to R_1

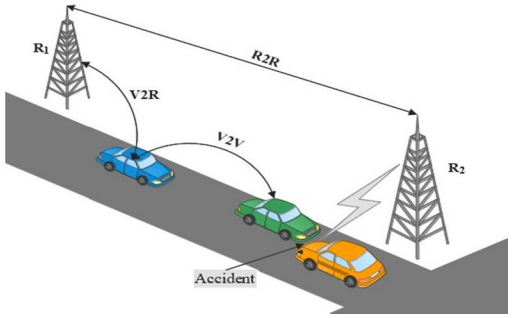

Fig. 4. R2R false alert detection.

Algorithm 2. Trust calculation of R_2 based on traffic alerts.

Input:
M_{R_2}: traffic alert received from one-hop RSU R_2
$M_V[n]$: traffic alert received from n adjacent vehicles
TH_{time}: threshold value for timestamp differences

1: $i = 0$
2: $Y = N = 0$
3: **while** $i < n$ **do**
4: **if** $M_{R_2}.Event\_Type == M_V[i].Event\_Type$ and $M_{R_2}.Event\_Value == M_V[i].Event\_Value$ and $M_{R_2}.Location == M_V[i].Location$ and $M_{R_2}.Timestamp - M_V[i].Timestamp \leq TH_{time}$ **then**
5: $Y++$
6: **else**
7: $N++$
8: **end if**
9: $i++$
10: **end while**
11: **if** $Y > N$ **then**
12: $Trust_{alert}=1$
13: **else**
14: $Trust_{alert}=0$
15: **end if**

and vehicles under its transmission range. Thus, a vehicle receives traffic alerts on the same event from neighbor vehicles and RSUs. It verifies the authenticity of the received traffic alerts using the information sensed by itself or the same traffic alerts received from other neighbor vehicles (Guleng *et al*., 2019) and RSUs. A nonsource vehicle considers the content of the maximum number of received alerts on the same event as valid and shares that message with its neighbors. Thus, the alert message propagates from one vehicle to another and ultimately reaches R_1. RSU R_1 receives traffic alerts on an event from R_2 and multiple adjacent vehicles V. It calculates the trust value of R_2 following Algorithm 2. For each received traffic alert $M_V[i]$ from an adjacent vehicle, R_1 compares it with the traffic alert M_{R_2} received from R_2. If both messages match on (1) Event Type, (2) Event Value, (3) Location (as shown in Fig. 3) and the difference of timestamps is less than or equal to a pre-defined threshold TH_{time}, R_1 considers them as a match and increments Y. Otherwise, N is updated. If the number of match, Y is greater than the number of nonmatch, N, then R_1 sets the trust of R_2 based on traffic alert, $Trust_{alert}$ to 1; Otherwise $Trust_{alert} = 0$, indicating R_2 as a malicious RSU. We can accomplish the same traffic alert verification process using the Decentralized Environmental Notification Message (DENM) (Santa *et al*., 2014) in Intelligent Transportation System (ITS).

*F. **Aggregated Direct Trust Calculation***

R_1 calculates the direct trust, $Trust_{direct}$ of R_2 as follows:

$$Trust_{direct} = (w_1 \times Trust_{routing} + w_2 \times Trust_{beacon}) \times Trust_{alert} \quad (5)$$

where $Trust_{routing}$, $Trust_{beacon}$, and $Trust_{alert}$ are trust values based on message routing, beacon message broadcasting, and traffic alert sharing, respectively. We multiply $Trust_{alert}$ with the weighted sum of $Trust_{routing}$ and $Trust_{beacon}$ to assign highest priority to traffic alerts. Among VANET applications, traffic alert-based services are of utmost importance, serving time-critical and emergency functions such as the notification of an accident, and bad road conditions (Zaidi *et al*., 2014). Improper timing of traffic alerts can cause severe consequences such as road accidents hampering human safety. VANET entities use periodic beacon messages to enhance traffic efficiency and collaboration (Al-Otaibi *et al*., 2019). Meanwhile, message routing mechanisms are used to provide other services like social networking and infotainment (Mershad *et al*., 2012). Here to note that $Trust_{alert}$ holds a binary value (1 or 0). Due to non-critical timing nature, we assign

weights to $Trust_{beacon}$ and $Trust_{routing}$ based on the frequency of respective messages. w_1 and w_2 are weights that sum to 1 and are defined as follows:

$$w_1 = \frac{F_{routing}}{F_{routing} + F_{beacon}} \quad (6) \qquad w_2 = \frac{F_{beacon}}{F_{routing} + F_{beacon}} \quad (7)$$

where $F_{routing}$ is the frequency of messages for routing, and F_{beacon} is the frequency of beacon messages.

We study all possible combinations of w_1, w_2, $Trust_{beacon}$, and $Trust_{routing}$ and observe that a trust factor with a greater weight can hide the malicious property presented by the other trust factor in the following two circumstances:

1) $Trust_{beacon} < 0.5$ and $w_1 \geq w_2$: The packet routing rate of one-hop RSU is greater than or equal to the beacon message generation rate, and the one-hop RSU behaves maliciously for beacon messages. In this case, $Trust_{routing}$ hides the effect of $Trust_{beacon}$.

2) $Trust_{routing} < 0.5$ and $w_2 \geq w_1$: $Trust_{routing}$ indicates that the one-hop RSU has dropped more than 50% (Xia *et al.*, 2018) of the packets or it has modified the messages before routing. $w_2 \geq w_1$ indicates that the beacon message generation rate of one-hop RSU is greater than or equal to the packet routing rate. Thus, $Trust_{beacon}$ hides the packet drop/modify attribute of one-hop RSU.

To handle the above-mentioned cases, we cut off the weight from a trust factor which hides the malicious activities displayed by other trust factor as follows (Wang *et al.*, 2020):

$$w = aTe^{-(bT)} \quad (8)$$

where T is the pre-defined time interval, $b = w_1$ if $w_1 \geq w_2$ else w_2, and $a = 1 - b$. We assign the new weight w to the trust factor that hides the malicious activities of another trust factor, and $1 - w$ is assigned to the remaining trust factor.

For the remaining combination of w_1, w_2, $Trust_{routing}$, and $Trust_{beacon}$, a trust factor with higher weight does not hide the malicious behavior presented by the other trust factor. Hence, w_1 (computed by Eq. 6) and w_2 (computed by Eq. 7) are not updated following Eq. 8 in these cases.

G. ***Indirect Trust Calculation***

We use the Q-learning method (Guleng *et al.*, 2019) to compute indirect trust. In this technique, every RSU maintains a Q-table containing an entry for every other RSUs and

broadcasts the table with *hello* messages. In the Q-table, each entry contains [$Q(m, n)$, X], where $Q(m, n)$ is the trust value of RSU_m determined by RSU_n, and X is a boolean variable which indicates whether RSU_m is a one-hop neighbor of RSU_n or not. The initial Q-value of each RSU is 0. Suppose RSU_p updates the Q-table and the Q-value of RSU_m at RSU_p is updated as follows:

$$Q_{new}(m, p) = \alpha \times Q_{old}(m, p) \times \{r + \gamma \times avg_{v \in NB_m} Q(m, v)\} + (1 - \alpha) \times Q_{old}(m, p) \quad (9)$$

where $Q_{new}(m, p)$ is the new trust value of RSU_m evaluated by RSU_p, $Q_{old}(m, p)$ is the previously assigned trust value, NB_m is the set of one-hop neighbor RSUs of RSU_m, α is the learning rate set to 0.7 (Guleng *et al*., 2019), $r = Trust_{direct}$ if RSU_m is a one-hop neighbor of RSU_p; otherwise, $r = 0$, and γ is the discount factor set to 0.9 (Guleng *et al*., 2019). Eq. 9 takes the average of trusts provided by the neighbor RSUs to handle the Q-table modification by malicious RSUs and it is denoted as $avg_{v \in NB_m} Q(m, v)$.

Significant communication overhead occurs due to huge message passing to update the entries of Q-table for each RSU in the network. To minimize this communication overhead, we limit both the Q-table size and the number of times the Q-table should be broadcasted to 6 following the hop count constraint discussed in section III-A.

H. Threshold Calculation and Malicious RSU Detection

Each RSU exhibits different behavior from the others. Therefore, it is crucial to maintain an individual threshold value for every RSU. The proposed scheme uses the threshold adjustment mechanism (Kerrache *et al.*, 2018) to identify malicious RSUs where the initial trust value and threshold value for each RSU are set to 0.5. The threshold value varies in the range of [0.5, 1], and the trust value varies in the range of [0, 1]. The threshold value is adjusted according to the changes in trust value which reflects the behavior changes of an RSU. The new threshold value, TH_{new} is determined as follows:

$$TH_{new} = \begin{cases} \beta + 0.5 & if\ \beta > 0 \\ TH_{old} & if\ \beta = 0 \\ 0.5 & if\ \beta < 0 \end{cases} \quad (10)$$

where β is expressed as $\beta = Trust_{old} - Trust_{new}$.

Each RSU computes trust values of other RSUs in the network and compares the trust value with the corresponding threshold value to identify them as *legitimate* or *compromised* RSU. An RSU is classified as *legitimate* when trust value is higher than TH_{new}. Otherwise, it is a *compromised* RSU.

I. Handling Malicious Vehicles

The proposed scheme uses intermediary vehicles between the one-hop neighbor RSUs to verify beacon content and traffic alerts. Although it is not possible to completely overcome the impact of malicious vehicles, we incorporate a mechanism to minimize it. A malicious vehicle in the transmission path can create a false traffic alert or drop or modify the correct alert messages. In our scheme, nonmalicious neighbor vehicles observing the same event verify the traffic alert's authenticity and drop the message if it is incorrect. They share the message with the vehicles within their transmission range, only if it is valid. Vehicles not observing the event rely on the majority opinions of neighbor vehicles and source RSU and verify the alert accordingly. To reduce the effect of malicious vehicles further, the RSU prefers the opinion of the majority of its adjacent vehicles regarding any event message. Section III-D and III-E discuss the handling of rogue vehicles in details for verification of beacon messages and traffic alerts, respectively.

IV. Simulation Results

In this section, we present the results of different experiments conducted to evaluate the performance of the proposed scheme. Besides, the experimental outcomes showing the impact of the proposed method on the current VANET routing protocols are also presented in this section.

A. Experimental Setup

We used Network Simulator 3 (NS-3) (Riley and Henderson, 2010) to evaluate the performance of our proposed scheme. Besides, we used Simulation of Urban Mobility (SUMO) (Behrisch *et al.*, 2011) to construct a realistic vehicular mobility model. A visual network editor of SUMO known as NetEdit (Behrisch *et al,*, 2011) was used to insert and manually position static RSU nodes at every intersection in the traffic environment. After that, vehicles were loaded into this network model. SUMO configuration files were used to generate trace files containing the information of vehicle movements, and they were fed into the NS-3 simulation. The ns2-mobility-helper (ns-3 documentation, 2025) tool in NS-3 was then used to parse this trace file and get the coordinates and velocity of the vehicles. It then assigned the corresponding mobility patterns to network nodes by maintaining temporal and spatial alignment with communication layers. Figure 5 presents our simulation model generated by SUMO.

For simulation, we considered an area of $14km \times 14km$ where 25 RSUs were serving 500 vehicles running with an average speed of $20m/s$. NS-3 uses IEEE 802.11p

communication protocol, which sets the transmission range of vehicles and RSUs to 250m and 900m, respectively. A summary of the simulation parameters is presented in Table I.

We considered the impact of both malicious vehicles and malicious RSUs to evaluate the performance, as the verification of both beacon messages and traffic alerts involves vehicles running on the road. Experiments were conducted with an increasing percentage of malicious RSUs, MR (20%, 40%, and 60%) and an increasing percentage of malicious

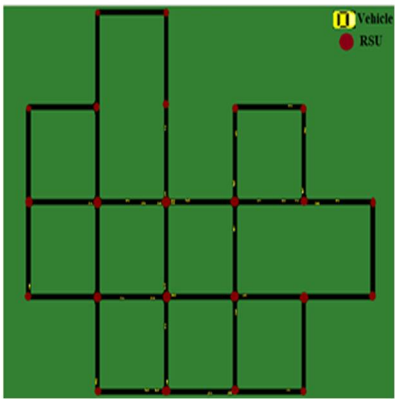

Fig. 5. Simulation traffic model.

Table 1. Parameters used in simulation.

Parameter	Value
Simulation area	14 km × 14 km (Mershad *et al.*, 2012)
Number of vehicles	500 (Jindal and Bedi, 2017)
Transmission range of vehicle	250m (Kerrache *et al.*, 2018)
Vehicle speed	20m/s (Mershad *et al.*, 2012)
Number of RSUs	25 (Mershad *et al.*, 2012)
Distance between RSUs	900m (Bhoi, and Khilar, 2014)
Transmission range of RSU	900m (Bhoi, and Khilar, 2014)
Simulation time	20m

vehicles, MV (5%, 10%, 15%, and 20%). Each experiment ran the simulation for 20 minutes and the results were averaged over 10 iterations with error bars indicate 95% confidence intervals (Guleng *et al.*, 2019). We follow (Guleng *et al.*, 2019; Xia *et al.*, 2019) to adopt an attack model for our proposed scheme. In our experiments, malicious RSUs dropped and forwarded packets with a probability of 0.5. During packet transmission, they modified packets with a probability of 0.5. Rogue RSUs also created flooding attacks and altered information in beacon messages with a probability of 0.5. Further, they altered traffic alerts with a probability of 0.5. On the other hand, malicious vehicles generated *IGNORE_RSU* alert for an accurate beacon message with a probability of 0.5. They dropped *IGNORE_RSU* event or modified the event value with a probability of 0.5. Besides, they modified the traffic alerts with a probability of 0.5.

In our simulation, Q-learning was employed to compute indirect trust of nonneighbor RSUs. The state represents the current trust knowledge an RSU has about nonneighbor RSUs, incorporating Q-value and the trust feedback received from the neighbor RSUs. The action is the periodic update of the Q-value using the defined update formula in Section III-G. The reward was set to zero for nonneighbors due to the absence of direct

trust information. We used a fixed learning rate (α = 0.7) and a discount factor (γ = 0.9) (Guleng *et al.*, 2019).

B. Performance Metrics

We evaluated the performance of the proposed scheme using five performance metrics. Table II enlists the parameters used to define these performance metrics.

Table 2. Parameters used in performance metrics.

Parameter	Description
True Positive (TP)	No. of malicious RSUs identified correctly.
False Positive (FP)	No. of legitimate RSUs identified as malicious RSUs.
True Negative (TN)	No. of legitimate RSUs identified correctly.
False Negative (FN)	No. of malicious RSUs identified as legitimate RSUs.

1) False Positive Rate (FPR): It shows the probability of legitimate RSUs to be identified as malicious RSUs as $False\ Positive\ Rate = \frac{FP}{FP + TN}$ (11)

2) False Negative Rate (FNR): It shows the probability of malicious RSUs to be identified as legitimate RSUs as $False\ Negative\ Rate = \frac{FN}{FN + TP}$ (12)

3) Precision: It is the ratio of correctly detected malicious RSUs to the total number of RSUs that are identified as malicious and defined as $Precision = \frac{TP}{TP + FP}$ (13)

4)Recall: It is the ratio of correctly identified malicious RSUs to the total number of actual malicious RSUs and defined as $Recall = \frac{TP}{TP + FN}$ (14)

5)Accuracy: It is the ratio of correctly identified malicious RSUs and legal RSUs to the total number of RSUs and defined as $Accuracy = \frac{TP + TN}{TP + FP + FN + TN}$ (15)

C. Performance Analysis

In this section, we present our findings on the performance of the proposed scheme derived from the analysis of different experiments. Although the work of (Abhishek *et al.*, 2019) calculates the trust of RSUs, it is not possible to compare this scheme with our proposed method in a meaningful way as each scheme calculates the trust values of RSUs considering the behavior of RSUs in diverse communication scenarios. Hence, we present the results for the proposed system only.

1) ***False Positive Rate (FPR):*** Figure 6a shows that FPR increases with MV and MR and

it reaches to approximately 30% when *MR*=60% and *MV* =20%. Two reasons are mainly working behind the generation of FPR in our scheme. If *MR* increases significantly, all the adjacent RSUs of a legal RSU may behave maliciously, and they can bound the legitimate RSU to drop packets by creating beacon flooding attacks. Thus, a legal RSU is identified as a malicious RSU. Besides, vehicles propagate traffic alerts to help verification of beacon content and alert messages. Rogue vehicles may generate *IGNORE _RSU* alerts for an honest RSU to prove it malicious. Similarly, when an honest RSU reports an event, hostile vehicles can drop or alter the traffic alerts generated by the honest vehicles for the same event and establish the RSU as a malicious one.

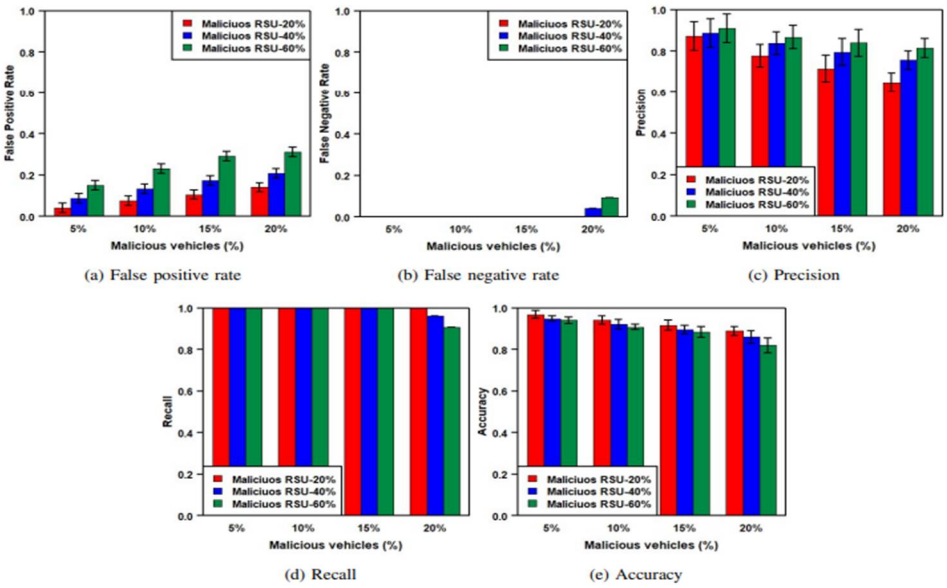

Fig. 6. Performance analysis of the proposed scheme.

2) False Negative Rate (FNR): As shown in Fig. 6b, malicious vehicles have very little influence on the FNR. When a malicious RSU generates a false beacon message, the rogue vehicles can either stop propagating *IGNORE_RSU* or modify the event value. Hence, the malicious attributes of an RSU remain unknown, and it is considered a legitimate RSU. When *MV* is relatively low, the nonmalicious vehicles suppress malicious vehicles' effect by verifying the same beacon messages. Therefore, FNR is not visible up to *MV* =15% in Fig. 6b. In our simulation, a situation where modified traffic alerts by malicious RSUs match with the rogue vehicles' opinion does not occur because of the low frequency of traffic alerts and independent decision-making of malicious vehicles without considering the action of malicious RSUs. Therefore, FNR is not

generated for traffic alerts. Malicious RSUs have no impact on the FNR. The proposed scheme generates maximum 8% FNR for *MR*=60% and *MV* =20% shown in Fig. 6b.

3) Precision: Figure 6c shows that the precision decreases with the rising values of *MV*. As we described in Section IV-C1, the impact of *MV* increases FPR. Thus, the precision decreases with the increasing values of *MV*. For a fixed *MV*, higher values of *MR* increase both TP and FP. Hence, precision increases with *MR* for a fixed *MV*. The precision reaches almost 81% when *MR*=60% and *MV* =20% shown in Fig. 6c. When *MR*=60%, the precision drops approximately 10% at *MV* =20% compared with *MV* =5%. Similarly, the precision drops approximately 26% at *MV* =20% compared with *MV* =5% when *MR*=20%. These results indicate that when *MR* is higher, precision mainly depends on the activities of rogue RSUs. On the other hand, for lower values of *MR*, the precision values are dominated by rogue vehicles' malicious activities.

4) ***Recall:*** The proposed solution identifies nearly all the malicious RSUs shown in Fig. 6d. The recall value is around 92% at *MV* =20%, and *MR*=60%. The recall ratio also indicates that the proposed solution is sensitive to the increasing *MV*. The higher values of *MV* enable the rogue RSUs to hide their malicious properties, as discussed in Section IV-C2. Fig. 6b shows that FNR is visible for higher values of *MV*. Therefore, slight increase of FNR at *MV* =20% in Fig. 6b reduces the recall values at *MV* =20% for *MR*=40%, and *MR*=60% shown in Fig. 6d.

5) ***Accuracy:*** Figure 6e shows the accuracy of the proposed scheme. If *MV* is fixed, accuracy decreases with increasing *MR*. As FP is nearly the same, and FN is rarely visible for fixed *MV*, accuracy depends on TP and TN. Higher values of *MR* increase both TP and FP, reducing FN and TN, respectively. As a consequence, accuracy decreases with higher values of *MR* for a specific *MV*. On the other hand, for fixed *MR*, with higher *MV*, both FP and FN increase, decreasing TN and TP, respectively. Hence, the accuracy decreases gradually with increasing *MV* for a particular *MR*. The proposed scheme achieves an accuracy of approximately 86% when *MR*=60% and *MV* =20%.

D. Impact of Beacon Sensor Data Verification

The proposed scheme considers an RSU's tendency to cause flooding attacks and alter beacon content in computing $Trust_{beacon}$. It incorporates a mechanism to check the correctness of sensor data in beacon messages (Section III-D2) in addition to checking the correctness of speed and density information found in existing literature (Al-Otaibi *et al.*, 2019; Arshad *et al.*, 2018). We conducted a simulation study to evaluate the effect of the sensor data verification mechanism. Experiments were conducted for a fixed number

of malicious vehicles *MV* = 20% and varying numbers of malicious RSUs, *MR*=20%, 40%, and 60%. We collected experimental results for the proposed scheme with (scenario 1) and without (scenario 2) the sensor data verification mechanism and compared the performance in both scenarios. Figure 7 shows the result of comparison which demonstrates a visible reduction in accuracy for both scenarios with the increasing number of malicious RSUs. However, integration of the sensor data verification mechanism improves accuracy, and the highest improvement is observed when *MR* = 60%, yielding an approximate 8% increase in accuracy.

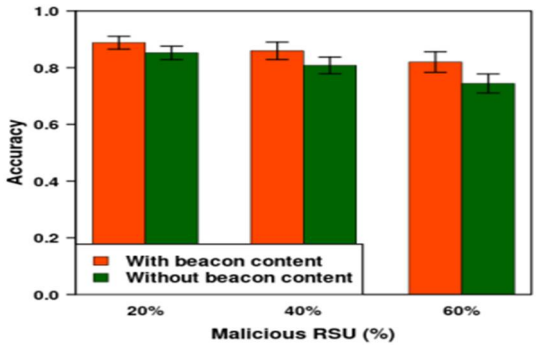

Fig. 7. Impact of sensor data verification in decision accuracy for *MV* =20%.

E. Network Performance Analysis

We incorporated our proposed scheme with several VANET routing protocols such as *Ad Hoc On-Demand Distance Vector (AODV) (*Sallam and Mahmoud, 2015), *Optimized Link State Routing (OLSR)* (Chouhan and Deshmukh, 2015), and *Destination Sequenced Distance Vector (DSDV)* (Rani *et al.*, 2011) to analyze the network performance. As an entity of VANET, RSU also uses these protocols for *R2R* and *V2R* communication (Chouhan and Deshmukh, 2015). We used the same simulation traffic model and parameters as discussed in Section IV-A. To generate data packets, we used 50 vehicles and all of the 25 RSUs as source nodes and considered all entities in the traffic model as receiver nodes. The simulation was performed for varying numbers of malicious RSUs, *MR* (20%, 40% and 60%) and a fixed number of malicious vehicles, *MV* =20%.

1) ***Network Performance Metrics:*** To analyze the network performance we used the following metrics:

1) *Packet Delivery Ratio (PDR):* It is the ratio of the total number of data packets received by destination nodes to the total number of packets sent from source nodes.

$$PDR = \frac{Total\ no.of\ packets\ received}{Total\ no.of\ packets\ sent} \quad (16)$$

2) *Throughput (Tp):* It is the number of data packets transmitted successfully at a given time.

$$T_p = \frac{Total\ no.\ of\ packets\ transmitted\ successfully}{Total\ time} \quad (17)$$

3) *Average End-to-End (AE2E) Delay:* It is the ratio of the time required to send data packets from source to destination to the total number of packets received.

$$AE2E\ Delay = \frac{\sum(Time\ to\ receive\ -\ Time\ to\ send)}{Total\ no.of\ packets\ received} \quad (18)$$

In the subsequent sections, we analyzed the performance of the network considering the presence and absence of the proposed trust model in all the routing protocols mentioned in Section IV-E.

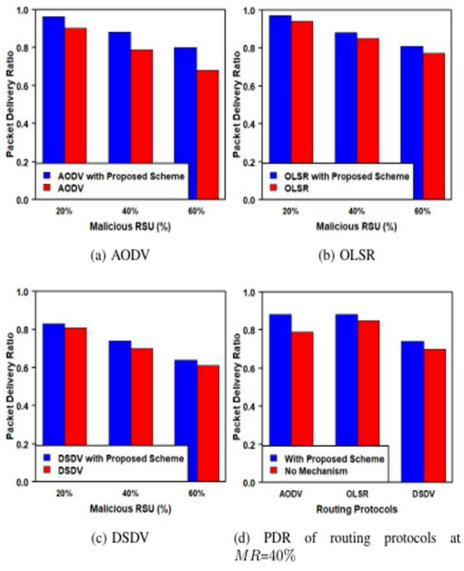

(a) AODV (b) OLSR

(c) DSDV (d) PDR of routing protocols at MR=40%

Fig. 8. Packet delivery ratio on various values of *MR* for *MV* =20%.

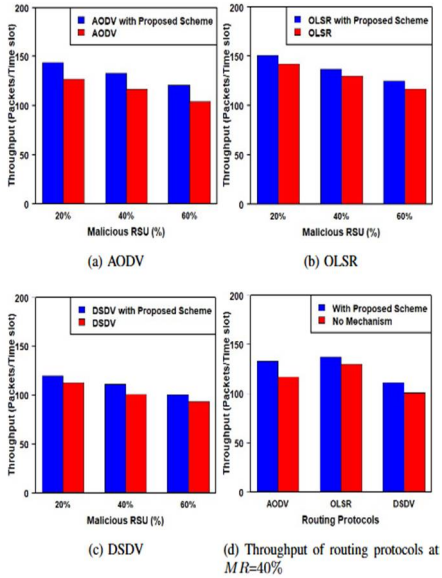

(a) AODV (b) OLSR

(c) DSDV (d) Throughput of routing protocols at MR=40%

Fig. 9. Throughput on various values of *MR* for *MV* =20%.

2) ***Packet Delivery Ratio (PDR):*** In the fundamental AODV, OLSR and DSDV protocols where the malicious RSU detection mechanism is missing, an RSU forwards packets to next-hop RSU without considering the malicious behavior of that RSU. If the next-hop RSU is malicious, it can drop packets, resulting in low PDR. In case of packet drops, packet retransmissions take place in each protocol. However, integration of the proposed trust model improves the PDR in all the protocols as an RSU can decide to exclude one-hop malicious RSUs from packet forwarding. As shown in Fig. 8a, 8b and 8c, the average improvement for AODV, OLSR, and DSDV is approximately 12%, 4% and 4%, respectively. Nevertheless, PDR decreases with the increasing number of malicious RSUs as they can jam the network through excessive beacon broadcasting or increase packet drop. From Fig. 8d it is clear that the basic OLSR protocol performs better than the other fundamental protocols. If any disconnection occurs, OLSR finds a new route faster than other protocols using routing tables. In contrast, DSDV takes a longer time to find a new route and, therefore, results in low PDR. In case of AODV, it is not facilitated like OLSR to get route information from some selected nodes known as MultiPoint Relay (MPR). Hence, AODV has lower PDR compared to OLSR. On the other hand, incorporation of the proposed trust model results in similar PDR for both AODV and OLSR as AODV usually creates a route immediately if needed, whereas OLSR updates the routing table periodically. During route discovery, AODV also takes the advantages of the trust model to avoid malicious RSUs. Hence, PDR increases significantly for AODV.

3) ***Throughput (Tp):*** Figure 9 presents the throughput of each routing protocol with/without the proposed trust model. As discussed earlier, each routing protocol with the trust model improves the packet delivery ratio and as a result the throughput increases. As shown in Fig. 9a, 9b and 9c, the average improvement for *AODV*, *OLSR*, and *DSDV* is approximately 14%, 6%, and, 8%, respectively. Similar to the *PDR*, we observe from Fig. 9d that the *OLSR* protocol exhibits best throughput, which is followed by the performance of *AODV* and *DSDV* protocols, respectively due to their underlying mechanism as mentioned in Section IV-E2.

4) ***Average End-to-End (AE2E) Delay:*** When the proposed trust model merges with the routing protocols, they select honest next-hop RSU to propagate messages. Hence, packet drops are reduced for each protocol which ultimately reduces packet retransmissions. As a consequence, end-to-end delay decreases as shown in Fig. 10. However, it is observed that the improvement in the end-to-end delay is minimal. Our proposed model only detects the malicious RSUs and does not exclude them from the network. Therefore, malicious impact such as beacon flooding remains in the network that can cause

congestion. Though end-to-end delay for both *OLSR* and *AODV* is nearly same as shown in Fig. 10d, *OLSR* shows slightly better performance due to the routing efficiency. Once again, *DSDV* shows the worst end-to-end delay performance.

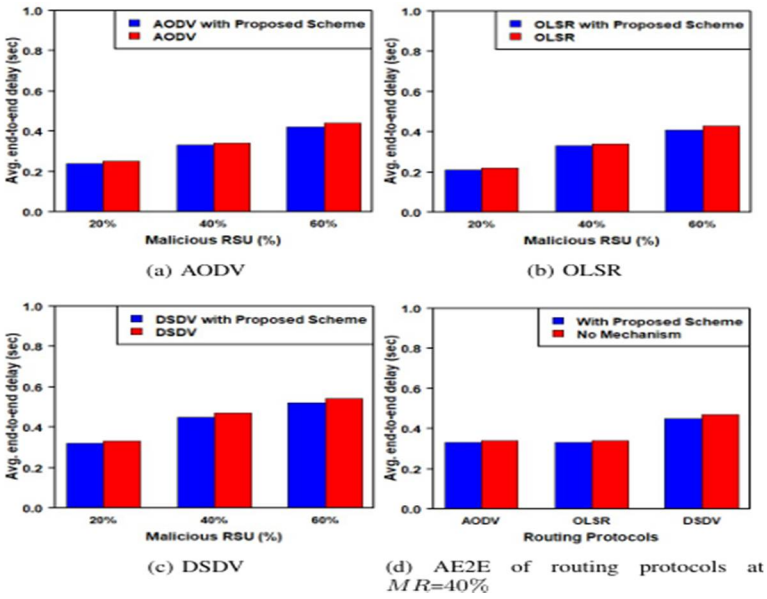

Fig. 10. Average end-to-end delay on various values of *MR* for *MV* =20%.

V. Conclusion and Future Work

In this paper, we proposed a trust-based malicious RSU detection mechanism for an edge-enabled VANET. Our proposed scheme analyzes R2R communication patterns to find the deviation in RSUs' behavior and assigns trust scores accordingly to distinguish malicious RSUs from nonmalicious ones. Besides, we proposed a mechanism to evaluate trust values based on the correctness of the beacon content provided by an RSU. The simulation results reveal that our scheme detects approximately 92% malicious RSUs and decides the type of RSUs with an accuracy of nearly 86% in the presence of rogue vehicles. Besides, the proposed scheme contributes a moderate network performance improvement of 14% when incorporated with the *AODV* routing protocol. In the future, we aim to include a sophisticated mechanism to minimize the impact of malicious vehicles. We also plan to utilize different machine learning mechanisms to identify malicious RSUs and want to study the performance of the proposed scheme using real-world data sets.

References

Abhishek, N. V., T. J. Lim, B. Sikdar and B. Liang. 2019. Detecting RSU misbehavior in vehicular edge computing. In: *Proc. IEEE/CIC Int. Conf. Commun.* pp. 42-47.

Abhishek, N. V. and T. J. Lim. 2022. Trust-based adversary detection in edge computing assisted vehicular networks. *J. Commun. Netw.* **24**(4): 451-462.

Ahmed, S., M. U. Rehman, A. Ishtiaq, S. Khan, A. Ali, and S. Begum. 2018. VANSec: Attack-resistant VANET security algorithm in terms of trust computation error and normalized routing overhead. *J. Sens.* **2018**(1): 6576841.

Alnasser, A., and H. Sun. 2021. Trust-based model for securing vehicular networks against RSU attacks, in *Proc. IEEE INFOCOM Conf. Comput. Commun. Workshops*. IEEE, pp. 1-6.

Al-Otaibi, B., N. Al-Nabhan, and Y. Tian. 2019. Privacy-preserving vehicular rogue node detection scheme for fog computing. *Sensors*, **19**(4): 965.

Arshad, M., Z. Ullah, M. Khalid, N. Ahmad, W. Khalid, D. Shahwar and Y. Cao. 2018. Beacon trust management system and fake data detection in vehicular ad-hoc networks. *IET Intell. Transport Syst.*, **13**(5): 780-788.

Behrisch, M., L. Bieker, J. Erdmann, and D. Krajzewicz. 2011. SUMO–simulation of urban mobility: An overview. In: *Proc. 3rd Int. Conf. Adv. Syst. Simul.*

Bhoi, S. K. and P. M. Khilar. 2014. IJS: An intelligent junction selection based routing protocol for VANET to support ITS services. *Int. Scholarly Res. Notices.* **2014**: 1-15.

Chouhan, T.S. and R.S. Deshmukh. 2015. Analysis of DSDV, OLSR and AODV routing protocols in VANETS scenario: using NS3. In: *Proc. Int. Conf. Comput. Intell. Commun. Netw.* IEEE, pp. 85-89.

Guleng, S., C. Wu, X. Chen, X. Wang, T. Yoshinaga and Y. Ji. 2019. Decentralized trust evaluation in vehicular internet of things. *IEEE Access*. **7**: 15980-15988.

Hao, Y., Y. Cheng and K. Ren. 2008. Distributed key management with protection against RSU compromise in group signature based VANETs. in *Proc. IEEE Globecom*, pp. 1-5.

Huang, L., H. Jiang, Z. Zhang, Z. Yan and H. Guo. 2017. Efficient data traffic forwarding for infrastructure-to-infrastructure communications in VANETs. *IEEE Trans. Intell. Transp. Syst.* **19**(3): 839-853.

Hussain, R., J. Lee and S. Zeadally. 2020. Trust in VANET: A survey of current solutions and future research opportunities. *IEEE Trans. Intell. Transp. Syst.* **22**(5): 2553-2571.

Jalooli, A., H. Khan and L. Purohit. 2024. Blockchain-enabled collaborative forged message detection in RSU-based VANETs. In *Proc. 8th Cyber Sec. Netw. Conf. (CSNet)*, pp. 60-67.

Jin, H., and P. Papadimitratos. 2018. Expedited beacon verification for VANET. In: *Proc. 11th ACM Conf. Secur. Privacy Wirel. Mob. Netw.* pp. 283-284.

Jindal, V., and P. Bedi. 2017. Reducing waiting time with parallel preemptive algorithm in VANETs. *Veh. Commun.* 7: 58-65.

Kerrache, C.A., A. Lakas, N. Lagraa and E. Barka.2018. UAV-assisted technique for the detection of malicious and selfish nodes in VANETs. *Veh. Commun.* **11**: 1-11.

Lee, E., E.-K. Lee, M. Gerla and S. Y. Oh. 2014. Vehicular cloud networking: architecture and design principles. *IEEE Commun. Mag.* **52**(2): 148-155.

Liu, J., W. Yang, J. Zhang and C. Yang. 2020. “Detecting false messages in vehicular ad hoc networks based on a traffic flow model. *Int. J. Distrib. Sens. Netw.* **16**(2): 1-12.

Lone, F.R. and H.K. Verma. 2025. MP-TMD: A multidimensional plausibility-driven cooperative trust model for multiple misbehaviour detection in intelligent transportation systems. *Cluster Computing*, **28**(3): 181.

Lu, X., X. Wan, L. Xiao, Y. Tang and W. Zhuang. 2018. Learning-based rogue edge detection in VANETs with ambient radio signals. In: *Proc. IEEE Int. Conf. Commun.*, pp. 1-6.

Maglaras, L. A., P. Basaras, and D. Katsaros. 2013. Exploiting vehicular communications for reducing CO_2 emissions in urban environments. In: *Proc. Int. Conf. Connected Veh. Expo (ICCVE).*, pp. 32-37.

Malik, N., P. Nanda, A. Arora, X. He and D. Puthal. 2018. Blockchain based secured identity authentication and expeditious revocation framework for vehicular networks. In: *Proc. 17th Int. Conf. Trust, Secur. Privacy Comput. Commun. (TrustCom)*. IEEE, pp. 674-679.

Marti, S., T. J. Giuli, K. Lai and M. Baker.2000. Mitigating routing misbehavior in mobile ad hoc networks. In: *Proc. 6th Annu. Int. Conf. Mob. Comput. Netw.* pp. 255-265.

Mershad, K., H. Artail and M. Gerla. 2012. ROAMER: Roadside units as message routers in VANETs. *Ad Hoc Netw.* **10**(3): 479-496.

ns-3 documentation. 2025. ns3::Ns2MobilityHelper Class Reference. Accessed June 6, 2022. [Online]. Available: https://www.nsnam.org/docs/release/3.19/doxygen/classns3_1_1_ns2_mobility_helper.html

Onieva, J.A., R. Rios, R. Roman and J. Lopez. 2019. "Edge-assisted vehicular networks security," *IEEE Internet Things J.* **6**(5): 8038-8045.

Paranjothi, A., M. Atiquzzaman and M.S. Khan. 2020. F-RouND: Fog-based rogue nodes detection in vehicular ad hoc networks. In: *Proc. IEEE Globecom*, pp. 1-6.

Patil, R., and M. P. Tahiliani. 2014. Detecting packet modification attack by misbehaving router. In: *Proc. 1st Int. Conf. Netw. Soft Comput.* pp. 113-118.

Qu, F., Z. Wu, F.-Y. Wang and W. Cho. 2015. A security and privacy review of VANETs. *IEEE Trans. Intell. Transp. Syst.* **16**(6): 2985-2996.

Rani, P., N. Sharma and P.K. Singh. 2011. Performance comparison of VANET routing protocols. In *Proc. 7th Int. Conf. Wirel. Commun. Netw. Mob. Comput.* IEEE, pp. 1-4.

Riley, G.F. and T. R. Henderson. 2010. The ns-3 network simulator. In: *Model. Tools Netw. Simul.* Berlin, Heidelberg: Springer, pp. 15-34.

Santa, J., F. Pereñíguez, A. Moragón and A. F. Skarmeta. 2014. Experimental evaluation of CAM and DENM messaging services in vehicular communications. *Transp. Res. Part C: Emerg. Technol.* **46**: 98-120.

Sajjad, S.M., S.H. Bouk and M. Yousaf. 2015. Neighbor node trust based intrusion detection system for WSN. *Procedia Comput. Sci.* **63**: 183-188.

Sallam, G. and A. Mahmoud. 2015. Performance evaluation of OLSR and AODV in VANET cloud computing using fading model with SUMO and NS3. In: *Proc. Int. Conf. Cloud Comput.* IEEE, pp. 1-5.

Sheikh, M.S., J. Liang and W. Wang. 2019. A survey of security services, attacks, and applications for vehicular ad hoc networks (VANETs). *Sensors* **19**(16): 3589.

Soleymani, S.A., A.H. Abdullah, W.H. Hassan, M.H. Anisi, S. Goudarzi, M.A.R. Baee and S. Mandala.2015. Trust management in vehicular ad hoc network: a systematic review. *EURASIP J. Wirel. Commun. Netw.* **2015**(1): 1-22.

Tripathi, K.N. and S. Sharma. 2019. A trust based model (TBM) to detect rogue nodes in vehicular ad-hoc networks (VANETS). *Int. J. Syst. Assur. Eng. Manag.* pp. 1-15.

Van der Heijden, R.W., S. Dietzel, T. Leinmüller and F. Kargl. 2018. Survey on misbehavior detection in cooperative intelligent transportation systems. *IEEE Commun. Surveys Tuts.* **21**(1): 779-811.

Wang, T., G. Zhang, M.Z.A. Bhuiyan, A. Liu, W. Jia and M. Xie. 2020. A novel trust mechanism based on fog computing in sensor–cloud system. *Future Gener. Comput. Syst.* **109**: 573-582.

Xia, H., S.-s. Zhang, B.-x. Li, L. Li and X.-g. Cheng. 2018. Towards a novel trust-based multicast routing for VANETs. *Secur. Commun. Netw.* **2018**(1): 7608198.

Xia, H., S.-s. Zhang, Y. Li, Z.-k. Pan, X. Peng and X.-z. Cheng. 2019. An attack-resistant trust inference model for securing routing in vehicular ad hoc networks. *IEEE Trans. Veh. Technol.* **68**(7): 7108-7120.

Yao, Y., X. Chang, J. Mišic´, V. B. Mišic´ and L. Li. 2019. BLA: Blockchain-assisted lightweight anonymous authentication for distributed vehicular fog services. *IEEE Internet Things J.* **6**(2): 3775-3784.

Zaidi, K., M. Milojevic, V. Rakocevic, and M. Rajarajan. 2014. Data-centric rogue node detection in VANETs. In: *Proc. IEEE 13th Int. Conf. Trust, Secur. Privacy Comput. Commun.* pp. 398-405.

Zaidi, K., M.B. Milojevic, V. Rakocevic, A. Nallanathan and M. Rajarajan. 2015. Host-based intrusion detection for VANETs: A statistical approach to rogue node detection. *IEEE Trans. Veh. Technol.* **65**(8): 6703-6714.

Zhang, X. and X. Chen. 2019. Data security sharing and storage based on a consortium blockchain in a vehicular ad-hoc network. *IEEE Access*. 7: 58241-58254.

Zhang, Y., C. Cheong, S. Li, Y. Cao, X. Zhang and D. Liu. 2024. False message detection in Internet of Vehicle through machine learning and vehicle consensus. *Inf. Process. Manage.* **61**(6): 103827.

(Revised copy received on 24/06/2025)